

**STABILIZATION CONTROL OF DOUBLE ROTARY
INVERTED PENDULUM USING HYBRID FUZZY/LQR
CONTROLLER**

JAMILU KAMILU ADAMU

SPS/15/MEE/00030

**DEPARTMENT OF ELECTRICAL ENGINEERING
FACULTY OF ENGINEERING
BAYERO UNIVERSITY KANO**

SUPERVISOR: ENGR. DR. HABIBU RABIU

JANUARY, 2020

**STABILIZATION CONTROL OF DOUBLE ROTARY
INVERTED PENDULUM USING HYBRID FUZZY/LQR
CONTROLLER**

JAMILU KAMILU ADAMU

SPS/15/MEE/00030

**THESIS SUBMITTED IN PARTIAL FULFILMENT OF THE
REQUIREMENTS FOR MASTERS DEGREE OF ELECTRICAL
ENGINEERING**

**DEPARTMENT OF ELECTRICAL ENGINEERING,
FACULTY OF ENGINEERING,
BAYERO UNIVERSITY KANO**

SUPERVISOR: ENGR. DR. HABIBU RABIU

JANUARY, 2020

DECLARATION

I hereby declare that I carried out the work reported in this dissertation in the department of Electrical Engineering, Bayero University, Kano, under the supervision of Engr. Dr. Habibu Rabi'u. I also solemnly declare that to the best of my knowledge, no part of this dissertation has been submitted here or elsewhere in a previous application for award of a degree. All sources of knowledge used have been duly acknowledged.

Engr. Jamilu Kamilu Adamu

SPS/15/MEE/00030

CERTIFICATION

This is to certify that the research work for this dissertation and the subsequent write up by Jamilu Kamilu Adamu (**SPS/15/MEE/00030**) were carried out under my supervision.,

Signature and Date-----
Supervisor: Engr. Dr. Habibu Rabi'u

Signature and Date-----
Head of Department (H.O.D).

APPROVAL PAGE

This dissertation has been examined and approved for the award of the degree of Master in Engineering (Electrical Control and Instrumentation).

Signature and Date -----
External Examiner: Prof. M. B Mu'azu

Signature and Date -----
Internal Examiner: Dr. Auwal Muhammad Abdullahi

Signature and Date -----
Supervisor: Engr. Dr. Habibu Rabi'u

Signature and Date -----
Head of department (H.O.D): Engr. Prof. Nuraddeen Magaji

Signature and Date -----
Representative of the Board of the school of post graduate studies.

ACKNOWLEDGEMENTS

First of all, I would like to express my highest appreciation to Allah S.W.T the Almighty and Merciful for given me life, strength, health, and opportunity to complete this thesis.

I would like to express my appreciations to my supervisor Dr. HabibuRabiu for the excellent guidance throughout the execution of this work. I also wish to express my profound gratitude to my internal and external supervisors; Dr. Auwal MuhammadAbdullahi and Prof. M.B Mu'azu respectively. Worthy of appreciation as well goes to my outstanding philosophers; Prof. NuraddeenMagaji, Dr. MukhtarFatihuHamza, Prof. Dahiru Sani Shu'aibu Dr. AmiruBature, Dr. Hasan Bashir, Dr. Mustapha Muhammad and Engr.AbdulbasidIsma'il Isa for their tremendous help. My vote of thanks also goes to my parents and my wife and rest of my family members for their prayers and for always being there for me, and motivation.

DEDICATION

This Research work is dedicated to my family members

TABLE OF CONTENTS

Declaration	-	-	-	-	-	-	-	-	-	-	i
Certification	-	-	-	-	-	-	-	-	-	-	ii
Approval	-	-	-	-	-	-	-	-	-	-	iii
Acknowledgements	-	-	-	-	-	-	-	-	-	-	iv
Dedication	-	-	-	-	-	-	-	-	-	v	
Table of contents	-	-	-	-	-	-	-	-	-	-	vi
List Abbreviations	-	-	-	-	-	-	-	-	-	-	xii
Abstract	-	-	-	-	-	-	-	-	-	-	xiii

CHAPTER ONE: Introduction

1.1 Background	-	-	-	-	-	-	-	-	-	-	1
1.2 Problem statement	-	-	-	-	-	-	-	-	-	-	4
1.3 Scope of the research	-	-	-	-	-	-	-	-	-	-	4
1.4 Aim of the Objectives	-	-	-	-	-	-	-	-	-	-	4

CHAPTER TWO: Literature Review

2.1 Introduction	-	-	-	-	-	-	-	-	-	-	6
2.2 Double rotary inverted pendulum (DRIP)	-	-	-	-	-	-	-	-	-	-	6
2.3 Intelligent control	-	-	-	-	-	-	-	-	-	-	7
2.4 Review of the fundamental concept	-	-	-	-	-	-	-	-	-	-	11
2.5 Classical control	-	-	-	-	-	-	-	-	-	-	11
2.6 Optimum control	-	-	-	-	-	-	-	-	-	-	13
2.6.1 Linear quadratic regulator (LQR)	-	-	-	-	-	-	-	-	-	-	14
2.7 Robust control	-	-	-	-	-	-	-	-	-	-	16
2.8 Research gap	-	-	-	-	-	-	-	-	-	-	18
2.9 General Fuzzy Systems	-	-	-	-	-	-	-	-	-	-	20
2.10 Crisp set	-	-	-	-	-	-	-	-	-	-	20
2.11 Fuzzy set	-	-	-	-	-	-	-	-	-	-	20
2.12 Propositional logic	-	-	-	-	-	-	-	-	-	-	22
2.13 Fuzzy logic	-	-	-	-	-	-	-	-	-	-	22
2.14 Fuzzy logic control	-	-	-	-	-	-	-	-	-	-	22
2.15 component of fuzzy logic controller	-	-	-	-	-	-	-	-	-	-	24
2.16 Fuzzy rule base (FRBS)	-	-	-	-	-	-	-	-	-	-	24
2.17 Inference mechanism	-	-	-	-	-	-	-	-	-	-	25
2.18 Fuzzification	-	-	-	-	-	-	-	-	-	-	26

2.19 Defuzzification	-	-	-	-	-	-	-	-	26
2.19.1 Means of maximum method (MOM)	-	-	-	-	-	-	-	-	26
2.19.2 Center of gravity method (COG)	-	-	-	-	-	-	-	-	27
2.19.3 Bisector of Area (BOA)	-	-	-	-	-	-	-	-	28
2.19.4 The Height Method (HM)	-	-	-	-	-	-	-	-	29
2.20 Membership functions (MFs)	-	-	-	-	-	-	-	-	29
2.20.1 Triangular membership function	-	-	-	-	-	-	-	-	30
2.20.2 Trapezoidal membership function	-	-	-	-	-	-	-	-	30
2.20.3 Gaussian membership function	-	-	-	-	-	-	-	-	31
2.20.4 Universe of discourse	-	-	-	-	-	-	-	-	31
2.20.5 Membership function selection	-	-	-	-	-	-	-	-	31
2.21 Setting up the control knowledge base	-	-	-	-	-	-	-	-	32
2.22 Linguistic descriptions	-	-	-	-	-	-	-	-	32
2.23 Linguistic value	-	-	-	-	-	-	-	-	33
2.24 Overlapping membership functions	-	-	-	-	-	-	-	-	34
2.25 Fuzzy-PID controller structure (FPID)	-	-	-	-	-	-	-	-	34
2.26 Double input FPID controllers	-	-	-	-	-	-	-	-	34
2.27 Hybrid FPID controller	-	-	-	-	-	-	-	-	36
2.28 Cascade control method	-	-	-	-	-	-	-	-	37
2.29 Controllability	-	-	-	-	-	-	-	-	38
2.3 Observability	-	-	-	-	-	-	-	-	39

CHAPTER THREE: Methodology

3.1 Introduction	-	-	-	-	-	-	-	-	40
3.2 System specifications	-	-	-	-	-	-	-	-	43
3.3 Torque (τ)	-	-	-	-	-	-	-	-	44
3.4 Matlab modeling	-	-	-	-	-	-	-	-	45
3.5 Model validation	-	-	-	-	-	-	-	-	46
3.6 Tests for controllability and observability	-	-	-	-	-	-	-	-	47
3.7 Controllability matrix	-	-	-	-	-	-	-	-	50
3.8 Observability matrix	-	-	-	-	-	-	-	-	51
3.9 Test for stability	-	-	-	-	-	-	-	-	52
3.10 Hybrid PID/LQR controller design	-	-	-	-	-	-	-	-	53
3.11 PID controller design	-	-	-	-	-	-	-	-	54

3.12 LQR controller design	-	-	-	-	-	-	-	-	55
3.13 Cascade control structure for DRIP	-	-	-	-	-	-	-	-	56
3.14 Hybrid FPID /LQR controller design	-	-	-	-	-	-	-	-	57
3.15 Design of fuzzy control rules	-	-	-	-	-	-	-	-	57
3.16 FPID structure	-	-	-	-	-	-	-	-	58
CHAPTER FOUR: Results and Discussion									
4.1 Introduction	-	-	-	-	-	-	-	-	60
4.2 Open loop responses	-	-	-	-	-	-	-	-	60
4.3 Stabilization control using cascade FPID and LQR	-	-	-	-	-	-	-	-	62
4.4 Performance indices ---	-	-	-	-	-	-	-	-	66
4.5 Stabilization control using cascade hybrid PID and hybrid FPID	-	-	-	-	-	-	-	-	67
4.6 System output characteristics	-	-	-	-	-	-	-	-	72
4.7 Test for robustness	-	-	-	-	-	-	-	-	74
4.8 Validation of Results	-	-	-	-	-	-	-	-	83
CHAPTER FIVE: Conclusion									
5.1 Introduction	-	-	-	-	-	-	-	-	85
5.2 Contribution of the Research	-	-	-	-	-	-	-	-	85
References	-	-	-	-	-	-	-	-	86

Table of Figures

Figure 1.1 Quansar DRIP	2
Figure 2.2 MOM Method	277
Figure 2.3 COG Method.....	288
Figure 2.4 BOA Method.....	288
Figure 2.5 Triangular Membership Function	30
Figure 2.6 Trapezoidal Membership Function	30
Figure 2.7 Gaussian Membership Function.....	31
Figure 2.8 Input Membership Function.....	32
Figure 2.9 Output Membership Function	32
Figure 2.10 Double Input Direct Action Type FPID Controller Structure	355
Figure 2.11 Hybrid FPID controller.....	366
Figure 2.12 General Cascade Control Structure	388
Figure 3.1 Schematic Diagram of DRIP	40
Figure 3.2 Simulink Model of DRIP.....	46
Figure 3.3 Hybrid Cascade PID/LQR Controller Structure for Double Rotary Inverted Pendulum.....	56
Figure 3.4 Internal Structure of FPID Controller	58
Figure 3.5 Hybrid Cascade PID-Fuzzy/LQR Controllers for Double Rotary Inverted Pendulum.....	59
Figure 4.1 Rotary arm open loop response.....	61
Figure 4.2 Lower pendulum open loop response.....	62
Figure 4.3 Upper pendulum open loop response	62
Figure 4.4 Arm Angular Position	63

Figure 4.5 Lower pendulum angular position.....	64
Figure 4.6 Upper pendulum angular position	65
Figure 4.7 Fuzzy controller output.....	65
Figure 4.8 LQR controller output signer	66
Figure 4.9 Hybrid controlled arm angle.....	68
Figure 4.10 Hybrid controlled lower pendulum angle.....	69
Figure 4.11 Hybrid controlled upper pendulum angle.....	69
Figure 4.12 Output of the first controller.....	70
Figure 4.13 Output of the second controller	71
Figure 4.14 Output of the third controller	71
Figure 4.15 Output of the hybrid controller	72
Figure 4.16 Hybrid FPID test for robustness: Arm response	74
Figure 4.17 Hybrid FPID test for robustness: Lower pendulum	75
Figure 4.18 Hybrid FPID test for robustness: Upper pendulum	75
Figure 4.19 Hybrid PID test for robustness: Arm angle.....	76
Figure 4.20 Hybrid PID test for robustness: lower pendulum	76
Figure 4.21 Hybrid PID test for robustness: upper pendulum.....	77

Figure 4.22 Output of the hybrid fuzzy controller under the disturbance	78
Figure 4.23 Output of the first fuzzy controller under the disturbance.....	79
Figure 4.24 Output of the second fuzzy controller under the disturbance.....	79
Figure 4.25 Output of the third fuzzy controller under the disturbance.....	80
Figure 4.26 Output of the hybrid PID controller under the disturbance.....	81
Figure 4.27 Output of the first PID controller under the disturbance	81
Figure 4.28 Output of second controller under the disturbance.....	82
Figure 4.29 Output of the third controller under the disturbance.....	83

List of tables

Table 3.1 SRV02 DRIP Specifications	43
Table 3.2 Fuzzy Rules for DRIP.....	57
Table 4.1 Performance Indices for FPID and LQR controller	67
Table 4.2 Arm control performance indices.....	73
Table 4.3 Lower pendulum control performance indices.....	73
Table 4.4 Upper pendulum control performance indices	73
Table 4.5 result validation using performance indices	83

List Abbreviations

IP	Inverted Pendulum
DIP	Double Inverted Pendulum
RIP	Rotary Inverted Pendulum
DRIP	Double Rotary Inverted Pendulum
FLC	Fuzzy Logic Controller
LQR	Linear Quadratic Regulator
PID	Proportional Integral Derivative
PD	Proportional Derivative
3D	Three Dimensional
DOF	Three Degrees of Freedom
FPID	Fuzzy-PID
IT2FLS	Interval Type-2 Fuzzy Logic Controller
LPV	Linear Parameter Varying
K_p	Proportional Response
K_i	Integral Response
K_d	Derivative Response
ARE	Algebraic Riccati Equation
DRE	Differential Riccati Equation
FRBS	Fuzzy Rule Base
SMC	Sliding Mode Controller
MOM	Mean of Maximum Method
COG	Centre of Gravity Method
BOA	Bisector of Area
HM	Height Method
MFs	Membership Functions
SIRMs	Single Input Rule Modules
SIMO	Single Input Multiple Output

Abstract

Double Rotary Inverted Pendulum (DRIP) is an under-actuated mechanical system which is inherently nonlinear and unstable. For decades, it has been widely used as an experimental setup to explain and test different kinds of control algorithms. The main control objectives of DRIP are: Swing-up control, stabilization control, switching control and trajectory tracking control. This research presents the design and enactment of a hybrid controller for the stabilization control of DRIP system. The proposed hybrid controller encompasses of two controllers. One is based on mathematical model and other is model free, so mathematical inaccuracy in the modeling of the system can be handled by model free controller. PID Fuzzy logic controller (FPID) and Linear Quadratic Regulator (LQR) are used together in a hybrid style. LQR is designed for improving the performance using full state feedback control and FPID is designed for accommodating nonlinearity using IF-THEN rules. The proposed controller was compared with published work. This is to validate the performance of the proposed control algorithm. Simulation results indicates that, the proposed hybrid FPID/LQR controller demonstrate a better performance compared with the published work for over 150% based on the performance indices considered in this research especially in the presence of disturbances. Based on this research, it is expected that the proposed controller can be applied in controlling other nonlinear, unstable, under-actuated mechanical systems.

CHAPTER ONE: Introduction

1.1 Background

The study on the inverted pendulum was first motivated based on the need to design stabilizing controllers for the rockets during vertical take-off. The rocket is highly unstable at the instant of launching, thus, there is a need of a continuous adjustment mechanism to stay at upright position in the open loop configuration(John, Koteswara, and Sivakumaran, 2013; Yang and Zheng, 2018).

The inverted pendulum represents a device, which is excellent for study of feedback control of an unstable system with different types of control strategies. It has been pointed out in (Boubaker 2013, 2017; Hamza et al., 2019)that, the inverted pendulum system is a fundamental benchmark for research in control theory. Rotary inverted pendulum (RIP) is a new version of IP which was propose by Furuta(Furuta, Yamakita, and Kobayashi, 1992). RIP is an important member of under-actuated mechanical systems and it is highly nonlinear, unstable and non-minimum phase system (Fatihu et al., 2019).

The control of an inherently unstable system is by nature interesting field of research, and the resulting stable system is an exciting visual demonstration of the capabilities of feedback control (Barton, 2009). This study focuses on the controller design for the stabilization of Double Rotary Inverted Pendulum (DRIP).The DRIP is a well-known example of under actuated mechanical device with chaotic behavior (Awtar et al., 2002).

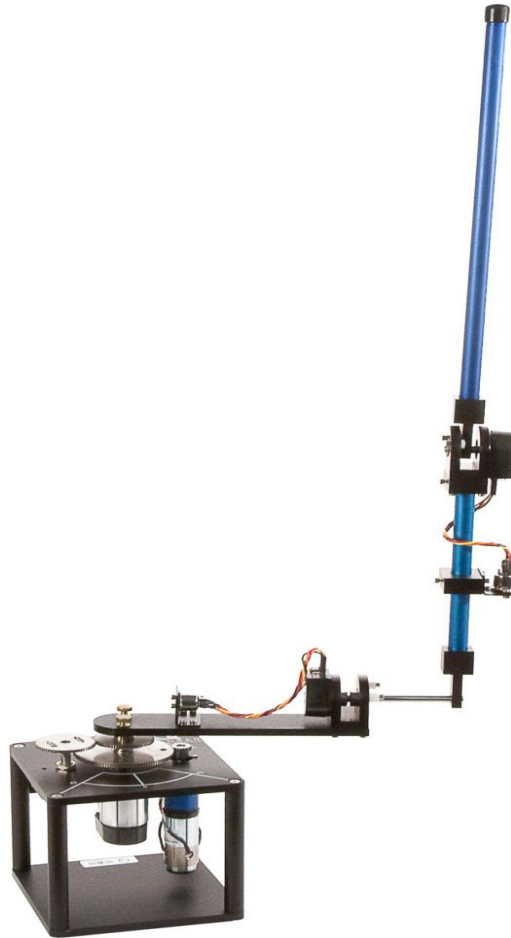


Figure 1.1 Quansar DRIP

The DRIP systems perform in an extensive range in real life applications such as aerospace systems, robotics, marine systems, mobile systems, flexible systems, pointing control, and locomotive systems (Kafetzis and Moysis, 2017). Moreover, when the pendulums of DRIP are at hanging position, it represents real model of the simplified industry crane application (Ghorbani, Shooredeli, and Teshnehlab, 2013).

The control objectives of the DRIP can be categorized into four categories (Hamza et al. 2019), (Hamza, Yap, and Choudhury, 2015), namely:

- I. Controlling the two pendulums from downward stable position to upward unstable position known as Swing-up control (John, Koteswara, and Sivakumaran, 2013; Mamma-Graham, 2014).

- II. Regulating the pendulums to remain at the unstable position known as stabilization control (Y. F. Chen, Huang, and Huang, 2014)
- III. The switching between swing-up control and stabilization control known as switching control (Nath and Mitra, 2014).
- IV. Controlling the DRIP in such a way that the arm tracks a desired time varying trajectory while the pendulum remains at unstable position known as trajectory tracking control (Aguilar-Avelar and Moreno-Valenzuela, 2015).

As mentioned earlier, this system is inherently unstable since even the slightest disturbance would cause the pendulum to start falling. Thus, some sophisticated control strategies is necessary to maintain a balanced pendulums.

Stabilization control of DRIP is not only a challenging problem but also a useful way to show the effectiveness of various control algorithms, such as; Proportional Integral Derivative (PID), Linear Quadratic Regulator (LQR), neural network, Fuzzy Logic Control (FLC) etc. (Singh and Yadav, 2012).

The LQR is an optimal control design method and is powerful technique for complex systems that have very strict performance requirements. It relates the state vector and control input vector. The cost function is parameterized by two matrices, Q and R, that weight the state vector and the system input respectively. LQR method is based on the state-space model and it tries to obtain the optimal control input by solving the algebraic Riccati equation (E and Jerome, 2013).

The FLC is the control technique that can deal with nonlinear systems (Kumbasar and Hagra, 2014). One special feature of FLC is that it utilizes the expertise of humans to control the physical system (Passino and Yurkovich, 1997), so that complex system can be controlled without precise knowledge of the plant. The designer can build up the controller based on

general idea of what it must accomplish. It is for this reason that FLC is particularly useful in instances where a human operator is being replaced, or where a human has an implicit model in mind of the input-output behavior of the system. Since the DRIP presents considerable control-design challenges, it is an attractive tool utilized by researchers for testing different control techniques and determining their performances (B. Li, 2013).

This study presents the investigation of performance of hybrid FPID/LQR controller for the stabilization of DRIP system with respect to the angular positions of the arm and the two pendulums in an inverted, unstable position.

1.2 Problem statement

This research is aimed at studying the techniques of stabilizing a DRIP comprehensively. DRIP is a control system that is inherently unstable, non-linear and non-minimum phase. Because of these inherent behaviors, keeping the DRIP's position in an upright and unstable position is a major challenge for the control engineering community. This research intends to use nonlinear control approach to solve these difficulties. It is suggested that a Hybrid FPID Controller can provide good control over the unstable balance position.

1.3 Scope of the research

This research will limit its scope to the DRIP's stabilization control.

1.4 Aim and objectives

This research aims to design new control algorithm which is the hybrid of Fuzzy-PID logic (FPID) and LQR controllers for the stabilization control of a DRIP system in the upright inverted position.

The objectives of this study are:

- I. To design a hybrid FPID/LQR based controllers in cascade topology for stabilization Double Rotary Inverted Pendulum over the unstable balance position.
- II. To design a hybrid PID/LQR based controllers in cascade topology for stabilization Double Rotary Inverted Pendulum over the unstable balance position.
- III. To simulate the controllers I and II, and compare their robustness.
- IV. To compare this work with work of Aranda-Escolástico *et. al*, (2016)

CHAPTER TWO: Literature Review

2.1 Introduction

This chapter provides an overview of the existing dynamic model and controllers for stabilization in an inverted and unstable upright position of different classes of Inverted Pendulum. Several research exists in literature that makes use of different control techniques for stabilising inverted pendulum. The research opportunities and challenges of the previous approaches in this area of research are presented.

2.2 Double rotary inverted pendulum (DRIP)

The rotation of the arm produces the primary distinction between the rotary inverted pendulum and other inverted pendulum constructions. Therefore, in the form of Coriolis forces and centrifugal torques, extra complexities are introduced. This not only offers a more engaged mathematical model but also interesting behaviors to study (Aranda-Escolástico et al., 2016).

A DRIP has two inverted pendulums connected with each other and finally attached to a rotating arm. The plane of the two pendulums on the radial arm is orthogonal (Hassanzadeh and Mobayen, 2011). This rotary arm is actuated with a controlling torque with the objective of balancing the two pendulums in the inverted position. Therefore, it has three DOF to be controlled with single actuator input and is thus termed as an under-actuated mechanical system. The actuated joint angle has a complete range of azimuths to stabilize the double inverted pendulum (Jabbar, Malik, and Sheikh, 2016).

The DRIP is an important member of nonlinear, unstable, non-minimum phase, and under-actuated mechanical systems. Underactuated mechanical systems are systems with fewer

independent control than degrees of freedom to be controlled (Choukchou-Braham et al., 2014; Fantoni and Lozano, 2002; Moreno-Valenzuela and Aguilar-Avelar, 2018).

Different researchers performed dynamic model of inverted pendulum with different approaches. Among which (Zhong and Helmut, 2001) derived the dynamic equations describing the model of double inverted pendulum (DIP) using Newtonian methods.

A nonlinear dynamical equation of the RIP system was developed using Kane's method in (Hamza, Yap, and Choudhury, 2016). The Matlab/Simulink model of RIP was developed based on the derived equations. Simulation study was carried out and the result shows that, for the Kane's based model, the pendulum falls in about 1.4 second while for Lagrange based model the pendulum falls in more than 1.75 second. This demonstrates that the Lagrange based model is more stable compared to the Kane's model.

Different control algorithms had been tested for different categories of inverted pendulum as describe below.

2.3 Intelligent control

The notion of intelligent control systems is based on a joint understanding of the notions of "control systems" and "intelligent systems" (Yu, 2009). Intelligent control refers to approaches to control system design, modeling, identification, and operation that use artificial intelligence techniques, such as fuzzy logic, neural networks, machine learning, evolutionary computation, and genetic algorithms. Intelligent control techniques are often capable of controlling dynamical systems that, because of their complexity, are very difficult to control by other techniques. Intelligent control systems are characterized by attempts to emulate important aspects of biological intelligence (Andújar et al., 2018).

During the past few years, significant research efforts have been devoted to the stability analysis and control of highly nonlinear and unstable system using intelligent systems.

There are groups of control method in FPID controller for IP, which had been implemented. However, much has not been done on DRIP in the literature due to the increase in complexity, nonlinearity, instability and complicated equations of motion that govern them.

The design of an intelligent controller based on a Takagi-Sugeno fuzzy model, which enlarges the region of attraction of the stabilization control of the chain pendulum was considered in (Aranda-Escolástico et al., 2016). This design was applied to the rotary inverted pendulum and to the double rotary inverted pendulum, and compared to other feedback control strategies such as Full State Feedback (FSF) and LQR. The results present a great applicability if applied to non-linear systems, where the region of attraction of classical controllers is not enough. However, it is suggested that, future works include the design of membership functions to maximize the region of attraction.

Interval type-2 fuzzy logic (IT2FL) controller in cascade form was designed in (Hamza et al., 2016) for stability control of Furuta pendulum. The paper, described the development of nonlinear dynamical equations of the RIP system using Kane's method. The Simulink model of RIP was developed based on the derived equations. The simulation result shows that the proposed controller is effective based on the four performance indexes (i.e. settling time, overshoot, undershoot and steady state error). However, despite the pendulum being single, the performance indices need to be improved.

A new fuzzy-evidential controller based on fuzzy inference and evidential reasoning is proposed for the stability control of the planar inverted pendulum system in (Tang, Zhou, and Jiang, 2016). In this new fuzzy-evidential controller, the empirical knowledge for

stabilization of the planar inverted pendulum system is expressed by fuzzy rules, while the coordinator of different control variables in each axis is built incorporated with the dynamic basic probability assignment (BPA) in the frame of fuzzy inference. The experimental result shows the effectiveness of the proposed method, as well as the merit that the new controller can force the system into its stable state faster than the method without evidential reasoning or based on LQR in the references.

In this study (Kharola, Patil, and Gupta, 2014) control of DIP was obtained using FPID having different membership functions (MFs) i.e. triangular, trapezoidal and gbell. The effects of shape of MF's on various controlling parameters i.e. stabilization time, maximum degree of overshoot and steady state error is also illustrated.

A swing-up control for rotary inverted pendulum using a cascade control scheme with two conventional proportional derivative (PD) controllers was presented in (Stelian-Emilian Oltean, 2014). The inner loop has a PD position controller of the pivot arm, while on the outer loop is the swing-up controller, the balance/stabilizing control is made by the use of fuzzy-PD controller. The system was modeled in Matlab/Simulink and the task was achieved in 4.5 second.

Additionally, (B. Li, 2013) deals with the stabilization control of DRIP System. Mathematical model is built for the RDIP with the Euler-Lagrange (E-L) equation. An LQR controller is designed for this system and its stability analysis is presented in the Lyapunov method. They re-develop the Direct Adaptive Fuzzy Control (DAFC) method for the purpose of exploring the possibility to improve the performance of the LQR control of the system. The simulation results of these two control schemes with their comparative analysis show that the DAFC is able to enhance the LQR controller by increasing its robustness in the DRIP control.

In (Bhangal, 2013) LQR based fuzzy controller was designed and its performance was compared with LQR controller for controlling DIP in a Matlab/Simulink environment. The simulation result shows that LQR based fuzzy controller has a better performance based on settling time, peak overshoot and steady state error as compared to the LQR controller in controlling the double inverted pendulum system.

A complex behavior of double inverted pendulum (DIP) with a vertically oscillating suspension point was presented in (Nikolov, 2012). The equations representing this model are nonlinear ordinary differential equations and were treated as nonlinear dynamical system. The result shows that stability of inverted state depends upon amplitudes of oscillation of suspended point. The numerical calculations show that dynamical bifurcation behavior of the system depends on parameter space of the system.

Additionally, (Sukontanakarn and Parnichkun, 2011) proposed a control algorithm which is the hybrid of neural network predictive control (NNPC) and LQR controller for control of a RDIP system. The NNPC is optimized directly to stabilize the DRIP at minimum cost. The neural network predictive control was proposed to improve control performance of the conventional LQR controller. At the training stage, the LQR controller was applied as reference input to the NNPC. Results from computer simulation shows that the proposed controller was able to guarantee stability of DRIP system.

An IT2FL and PID controller was designed for swing-up position control of DIP system in (Tinkir et al., 2010). Performances of these controllers are compared according to performance criterions. The performance of the IT2FL controller is compared with PID controller; the result shows that, IT2FL controller is better for control of the system. However, type-2 fuzzy sets membership functions are themselves fuzzy, which results in that the antecedents and the consequents of the rules are uncertain.

In (Arini, Nazaruddin, and Rohmanuddin, 2007), a controller based on FLC by observing input and output DRIP system when it was controlled by LQR controller was developed to control DRIP system. This method can only stabilize the pendulum system for 1.5 second.

A controller based on FLC has been developed to control Dual Rotary Inverted Pendulum system (Arini, Nazaruddin, and Rohmanuddin, 2007). The method that was used to design FLC is by observing input and output DRIP system when LQR controller controlled it. However, the simulation result using FLC shows that the system can only be stable for 1.5 seconds.

A new fuzzy controller for stabilization control of inverted pendulum systems is presented based on the Single Input Rule Modules (SIRMs) dynamically connected fuzzy inference model in (Yi and Yubazaki, 2000). It is made clear that the fuzzy controller performs the pendulum angular control and the cart position control in parallel, and switching between the two controls is realized by automatically tuning the dynamic importance degrees according to control situations. The simulation results show that the proposed fuzzy controller was able to stabilize the inverted pendulum systems within 9.0 s for an initial angle up to 30.08. However, it is known that the SIRMs model does not always achieve good performance in non-linear problems.

2.4 Review of the fundamental concept

An overview of control strategies related to the present study would be outline in the subsequent sections of this chapter.

2.5 Classical control

Classical control theory (also called conventional control theory) is a branch of control theory that deals with the behavior of dynamical systems with inputs, and how their behavior

is modified by feedback. It deals with linear time-invariant single-input single-output systems (W.-X. Zhong, 2004).

The Conventional PID controllers have been the most preferred controllers among others due to the simplicity of design and efficiency in the industrial applications and mechanical systems (Cetin and Iplikci 2015).

The PID controller shows an excellent performance for the linear system of classes of IP. The PID controller alone, or in hybrid form with other controller, or PI controller (when the derivative gain is zero), or PD controller (when the integral gain is zero) have been widely applied to different control objectives of RIP in literature as will be describe in the next paragraphs.

A research by(Paliwal 2017), designed a two-loop PID controller for linear model of an inverted cart– pendulum system via pole placement technique, where the (dominant) closed-loop poles to be placed at the desired locations are obtained from an LQR design. Simulation results show effective stabilization of IP system with low rise time and overshoot in both position and angle curves.

A triple PID controllers in parallel mode was used by (Krishna et al. 2016) to stabilize the linearized model of a parallel (dual) rotary inverted pendulum. The dynamic performance of which is compared with that of LQR and proved that, the later can guarantee the rotary dual inverted pendulum a faster and smoother stabilizing process.

Reference (Kharola et al. 2016), considers stabilization control of inverted pendulum on cart moving on an inclined surface. An offline control of the proposed system was achieved using PID and FLC controllers. A Matlab-Simulink model of the proposed system has been built using mathematical equations derived from Newton’s second law. The study compares

the proposed techniques in terms of settling time, overshoot, undershoot and steady state error. The simulation results confirm the validity of the proposed techniques.

An optimal PID controller is designed for a classical inverted pendulum (Pole-p and Reddy 2016) adopting a hybrid control structure. The design technique combines the traditional techniques in control theory and evolutionary algorithm to stabilize a cart-inverted pendulum dynamic. The result obtained for the system is convincing using the proposed hybrid control law for a preliminary robustness study. However, as indicated by the authors, the control algorithm must be modified to develop a robust PID controller capable to tackle parametric uncertainties and inclusion of delay in the system.

A PID controller is used to stabilize classical inverted pendulum such that the position of the carriage on the track is controlled quickly and accurately in (Jose et al. 2015).PID controller tuning for the proposed system model is showing only a very narrow region of stability. When the gains are increased, the system is settled fast but the overshoot is very high. When the overshoot is decrease by reducing the gain, the settling time has to pay the price.

2.6 Optimum control

The main objective of optimal control is to determine control signals that will cause a process (plant) to satisfy some physical constraints and at the same time extremize (maximize or minimize) a chosen performance criterion (performance index or cost function) (Naidu, 2003). The theory of optimal control is concerned with operating a dynamic system at minimum cost. One of the main results in the theory is that the LQR provides the solution.

2.6.1 Linear quadratic regulator (LQR)

The LQR controller is an optimal state feedback controller used to obtain the optimal performance of the system by minimizing the cost function, which relates the state vector, and control input vector. The LQR method is a powerful technique for designing controllers for complex systems that have stringent performance requirements and it seeks to find the optimal controller that minimizes a given cost function, which relates the state vector, and control input vector.

Consider an LTI system

$$\dot{x}(t) = Ax(t) + Bu(t), \quad t \geq 0, \quad x(0) = 0, \quad (2.1)$$

$$y(t) = Cx(t), \quad t \geq 0, \quad (2.2)$$

where, $A \in R^{n \times n}$, $B \in R^{n \times m}$, $C \in R^{p \times n}$, $D \in R^{p \times m}$ are system matrix, input matrix, output matrix and feed forward matrix, respectively. X is the state vector, u is the control input vector, and y is the output vector.

The conventional LQR problem is to obtain the control input

$$u(t) = -kx(t) \quad (2.3)$$

Where

$$K = R^{-1}B^T P(t) \quad (2.4)$$

which minimizes the following cost function (Kumare and Jerome 2016).

$$J(u) = \int_0^{t_f} (x^T(t)Qx(t) + u^T(t)Ru(t))dt \quad (2.5)$$

The cost function is parameterized by two matrices, Q and R , that weight the state vector and the system input respectively (E and Jerome 2013). Where $Q = Q^T$ is a positive semidefinite matrix that penalizes the departure of system states from the equilibrium, and $R = R^T$ is a positive definite matrix that penalizes the control input (Naidu 2003).

The major concern is to develop a stable linear feedback control law defined in (2.4) that can minimize the performance index J . With the aid Algebraic Riccati Equation (ARE) (2.6) which is solved to obtain the transformation matrix (P).

$$PA + A^T P - PBR^{-1}B^T P + Q = 0 \quad (2.6)$$

Then the transformation matrix P is used to determine the state feedback control gain matrix K . When the feedback gain K is obtained, the LQR controller can be easily designed to make the states approach zeros optimally (Ajami and Taheri 2012).

LQR optimal control problems have been widely investigated in the literature for control of different categories of IP.

A cart DIP is linearized around its equilibrium and then is kept in an upright position using two different methods in (Report and Moysis, 2016). First through LQR control and secondly using Laguerre functions.

In (Babu and Varghese, 2015) state feedback and LQR control methods are discussed for the stabilization of Rotary arm Inverted pendulum system. From the simulation results, it is found that both pole placement technique and LQR method are efficient in satisfying the design requirements and are robust to the parameter variations. The LQR control shows better results in minimizing the steady state value when compared to state feedback control method while pole placement method is better to improve the transient response of the system. Both

pole placement and LQR controllers are capable of maintaining the pendulum in its upright position.

(Sooraj, 2014), deals with the comparative study between linear and nonlinear control strategies applied on a RIP system, to stabilize its position on an unstable equilibrium point. The linear control technique such as LQR along with nonlinear control technique, sliding mode controller (SMC) were implemented and compared on the linearized and nonlinear model of the system respectively. As the LQR technique was used over a linearized model, it might lose some of the best properties of the system while linearizing.

In (John, Koteswara, and Sivakumaran, 2013), a SMC is designed to stabilize the RIP and then a state feedback controller is designed that would maintain the pendulum upright and handle disturbances up to a certain point. The state feedback controller is designed using the LQR. The Lagrangian method is used to obtain the equations of motion of the RIP system. According to the result obtained, for stabilization, the LQR produces smoother control signal. However, sliding mode control provides more robustness against parameter uncertainties.

The design and performance analysis of the cart DIP and simulation of LQR controller was considered in (Yadav, Sharma, and Singh, 2012). Matlab simulations were used to show the efficiency and feasibility of proposed approach. Euler Lagrange equation was used to derive the dynamic model of the system. However, linearized model of the system was used.

2.7 Robust control

In reality, any model of a plant we want to control will include an error in the modeling process. That is, the actual plant differs from the model to be used in the design of the control system. To ensure the controller designed based on a model will work satisfactorily when this controller is used with the actual plant, one reasonable approach is to assume from the start that there is an uncertainty or error between the actual plant and its mathematical model and

include such uncertainty or error in the design process of the control system. The control system designed based on this approach is called a robust control system (Paraskevopoulos 2017). Some of the works found in the literature that made use of robust control are presented below.

In the article (Sanjeeva and Parnichkun, 2019), mixed sensitivity H_∞ control was used to balance the rotary double inverted pendulum system. The controller was proposed to ensure the robust stability and enhance the time domain performance of the system under uncertainties and disturbances. Structure of the system dynamics and controller synthesis were presented. For performance evaluation, the proposed mixed sensitivity H_∞ controller was compared with LQR from both simulation and experiment on the rotary double inverted pendulum system. Even though the pendulum angles fluctuated around the upright position with small variation, both controllers could stabilize the nominal system. However, it was observed that transient response of the nominal system using LQR was better than the proposed controller, but the proposed mixed sensitivity H_∞ controller showed better performance than LQR in the presence of disturbances and uncertainties.

In (Patil and Kurode, 2018), stabilization of DRIP system was investigated using Higher Order Sliding Mode Control (HOSMC) technique. The controller was devised using Super Twisting Algorithm (STA). Performance of HOSMC was validated both in simulation and experimentation and found that, the controller yields stabilization in less than 3 second.

In (Aguilar-Avelar and Moreno-Valenzuela, 2015), a composite control scheme applied to the Furuta pendulum has been introduced. The proposed controller has two components, one derived from the feedback-linearization-based controller and the other is an energy-based compensation of the system. Analysis of the closed-loop system trajectories is given, showing that the proposed controller is able to ensure uniformly ultimately boundedness of the tracking error signal and the pendulum position. Real-time experiments and numerical

simulations were conducted, which show the practical viability of the proposed algorithm and confirm the obtained theoretical results.

Also, (Aribowo et al. 2007) developed a Linear Parameter Varying (LPV) controller for stabilization of upright position on DRIP. A robust gain scheduling approach was used for LPV controller synthesis. The designed LPV controller was compared with LQR Controller (simulation package). The response evaluation shows that LPV controller outperforms LQR, especially in terms of control performance and RMSE analysis. However, as expressed by the authors, some additional research is required to ensure stability of the DRIP system with larger range of deviations and uncertainty.

2.8 Research gap

Virtually all physical processes in the real world are nonlinear or complex in some other way. It is our abstraction of the real world that leads us to the use of linear systems in modeling these processes. The linear systems are simple and understandable, and, in many situations, they provide acceptable simulations of the actual processes that can be observe. Unfortunately, only the simplest of systems can be modeled with linear system theory and only a very small fraction of the nonlinear systems have verifiable solutions. Moreover, linearization is mostly not satisfactory for all nonlinear systems due to the different linearization points and high nonlinearity. In addition, the structure of the system or reference point or environmental conditions may be changed or some internal or external disturbances may be involved in the control loop which cause different linearization points (Cetin and Iplikci, 2015). The classical control techniques are generally based on the linearization of the process behavior regarding the operating points. However, for nonlinear systems, it is only nonlinear controller that can stabilize the system globally (Y. F. Chen, Huang, and Huang, 2014).

The shortcomings of conventional modern control in dealing with complex process dynamics, together with the abundance of such complexities in modern day processes, have motivated a significant and growing body of research work within the area of nonlinear process control over the past two decades, leading to the development of several practically implementable nonlinear control strategies that can deal effectively with a wide range of process control problems such as nonlinearities, constraints, uncertainties, and time delay (Mhaskar, El-farra, and Christofides, 2004).

Although modern control and hence optimal control appeared to be very attractive, it lacked a very important feature of robustness. That is, controllers designed based on LQR theory failed to be robust to measurement noise, external disturbances and unmodeled dynamics (Naidu, 2003).

The inspiration comes from the fact that each of the mentioned controllers has advantages and disadvantages that cannot be neglected; firstly, the LQR controller has a good control effect with an easy and effective way of obtaining optimal feedback gain for DRIP system stabilization. But, when it comes to the transient of particular output, LQR is not the best solution. In recent years, FLC has been applied successfully in the area of nonlinear process control (C.-L. Chen and Kuo, 1995; H. Li, Malki, and Chen, 1994). Unfortunately (W. Li 1998), defining membership functions of linguistic variables and formulating fuzzy rules by manual operation is time consuming work. Besides, a few of stability analysis for the real applied FLC were reported so that many people worry about their reliability.

This study proposes a hybrid combination of LQR controllers and fuzzy logic for the stabilization control of the DRIP system. This will be an attractive and powerful approach for designing robust control systems with high degrees of nonlinearities and uncertainties. The

control results on a manipulator and stoker-fired boilers show the effectiveness and robustness of the hybrid fuzzy logic plus conventional controllers (W. Li 1998).

2.9 General Fuzzy Systems

As largely found in (Passino and Yurkovich, 1998), fuzzy system is a static nonlinear mapping between its inputs and outputs (i.e., it is not a dynamic system). It is assumed that the fuzzy system has inputs $u_i \in \mathcal{U}_i$ where $i = 1, 2, \dots, n$ and outputs $y_i \in \mathcal{Y}_i$ where $i = 1, 2, \dots, m$. The inputs and outputs are “crisp” that is, they are real numbers, not fuzzy sets. The fuzzification block converts the crisp inputs to fuzzy sets, the inference mechanism uses the fuzzy rules in the rule-base to produce fuzzy conclusions (e.g., the implied fuzzy sets), and the defuzzification block converts these fuzzy conclusions into the crisp outputs.

2.10 Crisp set

The crisp set is defined in such a way as to dichotomize the individuals in some given universe of discourse into two groups: members and nonmembers of an element in a set (Klir and Yuan, 1997). In crisp sets, the transition for an element in the universe between membership and non-membership in a given set is abrupt and well defined.

$$\mu_A(X) = \begin{cases} 1, & X \in A \\ 0, & X \notin A \end{cases} \quad (2.7)$$

2.11 Fuzzy set

A fuzzy set can be defined mathematically by assigning to each possible individual in the universe of discourse a value representing its grade of membership in the fuzzy set. A fuzzy set, then, is a set containing elements that have varying degrees of membership in the set (Ross, 2004). A fuzzy set is an extension of a crisp set. Crisp sets only allow full membership or no membership at all, where fuzzy sets allow partial membership. In other words, an element may partially belong to a set. For an element in a universe that contains fuzzy sets,

this transition can be gradual. This transition among various degrees of membership can be thought of as conforming to the fact that the boundaries of the fuzzy sets are vague and ambiguous. Hence, membership of an element from the universe in this set is measured by a function that attempts to describe vagueness and ambiguity.

A fuzzy set, then, is a set containing elements that have varying degrees of membership in the set. When A is a fuzzy set and x is a relevant object, the proposition “ x is a member of A ” is not necessarily either true or false. It may be true only to some degree, the degree to which x is actually a member of A (Klir and Yuan, 1997). The fuzzy set also provides a way that is similar to a human being’s concepts and thought process. However, just the fuzzy set itself cannot lead to any useful and practical products until the fuzzy inference process is applied (Bai and Wang, 1982).

A notation convention for fuzzy sets when the universe of discourse, X , is discrete and finite, is as follows for a fuzzy set A

$$\mu_A(X) = \sum_i \frac{\mu_A(x_i)}{x_i} \quad (2.8)$$

When the universe, X , is continuous and infinite, the fuzzy set A is denoted by

$$\mu_A(X) = \int \frac{\mu_A(x)}{x} \quad (2.9)$$

In both notations, the horizontal bar is not a quotient but rather a delimiter. The numerator in each term is the membership value in set A associated with the element of the universe indicated in the denominator (Ross; 2004).

2.12 Propositional logic

Logic is the analysis of methods of reasoning. The propositional logic is a logic, which deals with propositions. A proposition is a sentence, which is either true or false. The "true " and "false" are called the truth-values. We denote these values by 1 and 0, respectively. Then to any sentence, propositional logic deals with finding the truth values of formulas containing atomic propositions, whose truth value is either zero or one, connected by "and" (\wedge), "or" (\vee), implication (\rightarrow), etc. (Buckley and Eslami, 1992)

The propositional logic based on this presumption is said to be the two-valued or classical propositional logic. Simple sentences or atomic propositions are denoted by p, q, \dots or p_1, p_2, \dots

2.13 Fuzzy logic

As indicated in (Siddique and Widrow, 2014), logic is the study of reasoning processes, where reasoning involves receiving new ideas from existing propositions. In classical logic, a proposition, p , is either true or false, that is, either 1 or 0 is the true value of a proposal. For more than a century, the classical two-valued logic dominated the scientific world. But there are many real world situations where, due to the fact of absolute truth principles, the standard two-valued reasoning did not work well or failed to be true. Fuzzy logic is a transformation from absolute truth to partial truth that generalizes classical two-value logic by making the partial truth values of a proposition expressed by a number in the interval of $[0, 1]$

2.14 Fuzzy logic control

The real world is complex; complexity in the world generally arises from uncertainty in the form of ambiguity. Our understanding of most physical processes is based largely on imprecise human reasoning. This imprecision (when compared to the precise quantities

required by computers) is nonetheless a form of information that can be quite useful to humans (Ross, 2004).

Fuzzy logic was introduced by LotfiZadeh in 1965, it has had many successful applications mostly in control (Reznik, 1997).

Fuzzy logic, as its name suggests, is the logic underlying modes of reasoning which are approximate rather than exact. Fuzzy logic is a method to formalize the human capacity of imprecise reasoning. Such reasoning represents the human ability to reason approximately and judge under uncertainty. The importance of fuzzy logic derives from the fact that most modes of human reasoning-and especially commonsense reasoning-are approximate in nature(Zadeh, 1992).

Fuzzy control provides a formal methodology for representing, manipulating, and implementing a human’s heuristic knowledge about how to control a system (Passino and Yurkovich, 1998). FLC can be viewed as an artificial decision maker that operates in a closed-loop system in real time. The ability to embed such reasoning in hitherto intractable and complex problems is the criterion by which the efficacy of fuzzy logic is judged.

As shown in Figure 2.2, it gathers plant output data $y(t)$, compares it to the reference input $r(t)$, and then decides what the plant input $u(t)$ should be to ensure that the performance objectives will be met (Passino and Yurkovich, 1998).

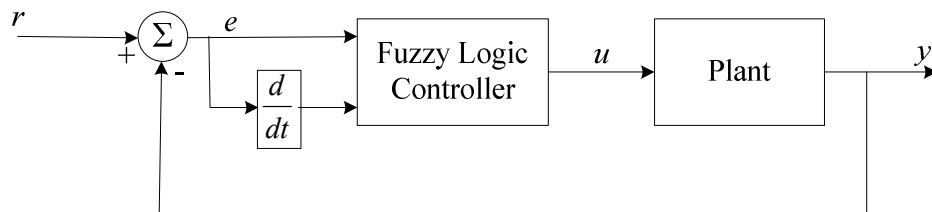


Figure 2.1.Fuzzy Logic Controller

2.15 Component of fuzzy logic controller

Fuzzy controller has four main components:

- I. The “rule-base”
- II. The inference mechanism
- III. The fuzzification interface
- IV. The defuzzification interface

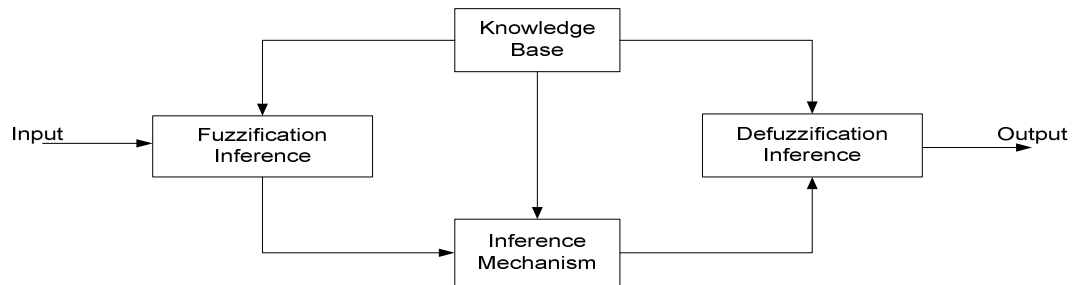


Figure 2.2 Fuzzy controller block diagram

2.16 Fuzzy rule base (FRBS)

In a broad sense, an FRBS is a rule-based system where fuzzy sets and FL are used as tools for representing different forms of knowledge about the problem at hand, as well as for modeling the interactions and relationships existing between its variables (Kumbasar and Hagraas 2015a)

Fuzzy control rule as described in (Bai and Wang 1982), can be considered as the knowledge of an expert in any related field of application. The FRBS system is most useful in modeling some complex systems that can be observed by humans because it makes use of linguistic variables as its antecedents and consequents; as described here these linguistic variables can be naturally represented by fuzzy sets and logical connectives of these sets. The fuzzy rule is represented by a sequence of the form IF THEN, leading to algorithms describing what action or output should be taken in terms of the currently observed information, which includes both input and feedback if a closed-loop control system is

applied. The law to design or build a set of fuzzy rules is based on a human being's knowledge or experience, which is dependent on each different actual application. The "rule-base" holds the knowledge, in the form of a set of rules, of how best to control the system.

A fuzzy IF-THEN rule associates a condition described using linguistic variables and fuzzy sets to an output or a conclusion. The IF part is mainly used to capture knowledge by using the elastic conditions, and the THEN part can be utilized to give the conclusion or output in linguistic variable form. This IF-THEN rule is widely used by the fuzzy inference system to compute the degree to which the input data matches the condition of a rule. A fuzzy relation below is used to represent a fuzzy rule:

R: If x is A then y is B., which is sometimes abbreviated as

R: $A \rightarrow B$ (or $R=A \rightarrow B$).

R can be viewed as a fuzzy set with a two-dimensional membership function

$$\mu_R(x, y) = f(\mu_A(x), \mu_B(y)) \quad (2.10)$$

where the function f , called the fuzzy implication function, performs the task of transforming the membership degrees of x in A and y in B into those of (x, y) in $A \times B$.

2.17 Inference mechanism

The inference system is the component that derives the fuzzy outputs from the input fuzzy sets according to the relation defined through the fuzzy rules. Inference is the process of formulating a nonlinear mapping from a given input space to output space. The mapping then provides a basis from which decisions can be made. The process of fuzzy inference involves all input-output membership functions, fuzzy logic operators and if-then rules (Siddique and

Widrow 2013). The inference mechanism evaluates which control rules are relevant at the current time and then decides what the input to the plant should be.

2.18 Fuzzification

Fuzzification is the process of making a crisp input quantity fuzzy. Fuzzification is the first step to apply a fuzzy inference system. Most variables existing in the real world are crisp or classical variables. One needs to convert those crisp variables (both input and output) to fuzzy variables and before applying fuzzy inference to process those data to obtain the desired output.

2.19 Defuzzification

The defuzzification interface converts the conclusions reached by the inference mechanism into the inputs to the plant (crisp quantity). Defuzzification is the conversion of a fuzzy quantity to a precise quantity (Ross, 2010). Three defuzzification techniques are commonly used, which are: Mean of Maximum method, Center of Gravity method and the Height method.

2.15.1 Mean of maximum method (MOM)

The MOM strategy generates a quantity, which represents the mean value of all outputs (Siddique and Widrow, 2013), whose membership functions reach the maximum as shown in Figure 2.5. This defuzzification can be expressed as:

$$X_o = \sum_{j=1}^k \frac{X_j}{k} \quad (2.11)$$

X_j : action whose membership functions reach the maximum.

k : number of such actions.

A shortcoming of the MOM method is that it does not consider the entire shape of the output membership function, and it only takes care of the points that have the highest degrees in that function. For those membership functions that have different shapes but the same highest degrees, this method will produce the same result.

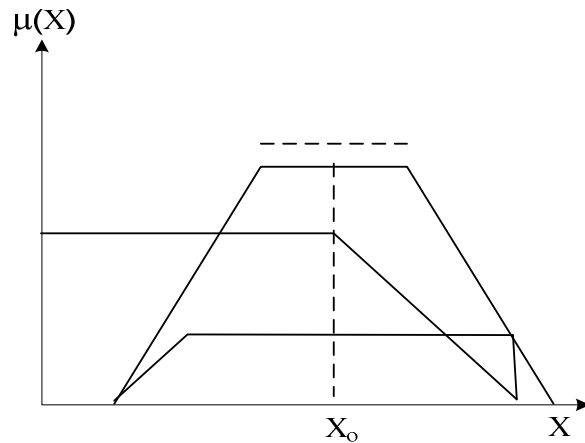


Figure 2.2 MOM Method

2.15.2 Center of gravity method (COG)

The widely used COG strategy generates the center of gravity of the possibility distribution of a fuzzy set A . This method is similar to the formula for calculating the center of gravity in physics. The weighted average of the membership function or the center of the gravity of the area bounded by the membership function curve is computed to be the most crisp value of the fuzzy quantity (Ross 2010).

$$X_0 = \frac{\sum_{j=1}^n \mu_A(x_j) \cdot z_j}{\sum_{j=1}^n \mu_A(x_j)} \quad (2.12)$$

n : the number of quantization levels of the output

A : a fuzzy set defined on the output dimension (z)

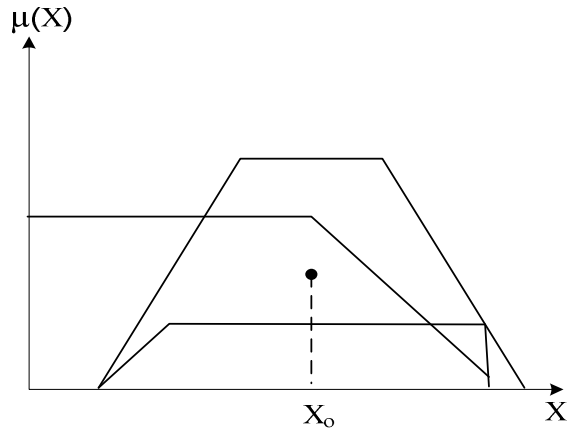


Figure 2.3 COG Method

2.15.3 Bisector of area (BOA)

As shown in Figure 2.7, the BOA generates the action (X_0) which partitions the area into two regions with the same area (Passino and Yurkovich, 1998).

$$\int_{\alpha}^{X_0} \mu_A(X) dx = \int_{X_0}^{\beta} \mu_A(X) dx \quad (2.13)$$

$$\alpha = \min\{x \mid x \in W\}$$

$$\beta = \max\{x \mid x \in W\}$$

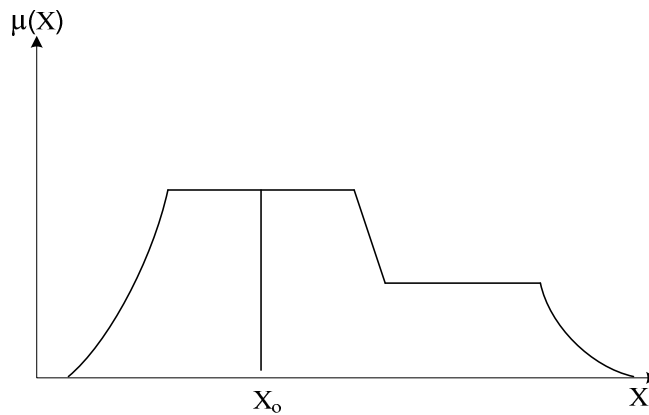


Figure 2.4 BOA Method

2.15.4 The height method (HM)

This defuzzification method is valid only for the case where the output membership function is an aggregated union result of symmetrical functions. This method can be divided into two steps. First, the consequent membership function F_i can be converted into a crisp consequent $X = f_i$ where f_i is the center of gravity of F_i . Then the COG method is applied to the rules with crisp consequents, which can be expressed as

$$X = \frac{\sum_{i=1}^M w_i f_i}{\sum_{i=1}^M w_i} \quad (2.14)$$

Where w_i is the degree to which the i^{th} rule matches the input data. The advantage of this method is its simplicity. Therefore, many neuro-fuzzy models use this defuzzification method to reduce the complex of calculations.

2.20 Membership functions (MFs)

A membership function (μ) for a fuzzy set A on the universe of discourse X is a mapping from the universe of discourse X to the unit interval, i.e., $\mu_A: X \rightarrow [0,1]$, where each element of X is mapped to a value between 0 and 1. This value, called membership value or degree of membership, quantifies the grade of membership of the element in X to the fuzzy set A .

Membership functions allow us to graphically represent a fuzzy set. The x axis represents the universe of discourse, whereas the y axis represents the degrees of membership in the $[0,1]$ interval. Different type of fuzzy membership functions has been used in fuzzy logic control. Most often, four types are most common (Berenji, 1992)

2.16.1 Triangular membership function

Triangular function is defined by a lower limit a , an upper limit b , and a value m , where $a < m < b$.

$$\mu_A(X) = \begin{cases} 0, & x \leq a \\ \frac{x-a}{m-a}, & a < x < m \\ \frac{b-x}{b-m}, & m < x < b \\ 0, & x \geq b \end{cases} \quad (2.40)$$

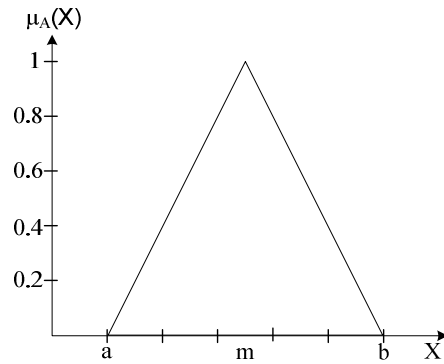


Figure 2.5 Triangular Membership Function

2.16.2 Trapezoidal membership function

Trapezoidal membership function defined by a lower limit a , an upper limit d , a lower support limit b , and an upper support limit c , where $a < b < c < d$.

$$\mu_A(X) = \begin{cases} 0, & (x < a) \text{ or } (x > d) \\ \frac{x-a}{b-a}, & a \leq x \leq b \\ 1, & b \leq x \leq c \\ \frac{d-x}{d-c}, & c \leq x \leq d \\ 0, & x \geq d \end{cases} \quad (2.15)$$

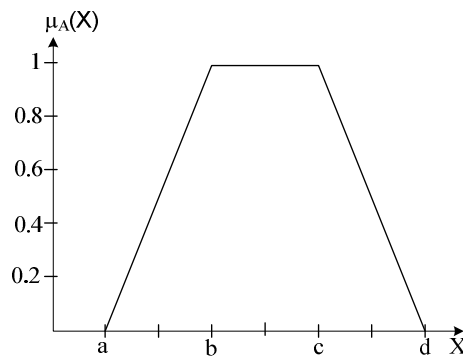


Figure 2.6 Trapezoidal Membership Function

2.16.3 Gaussian membership function

Gaussian membership function defined by a central value m and a standard deviation $k > 0$. A Gaussian MF is determined complete by m and k ; m represents the MFs center and k determines the MFs width.

$$\mu_A(X) = e^{-\frac{1}{2}\left(\frac{x-m}{k}\right)^2} \quad (2.16)$$

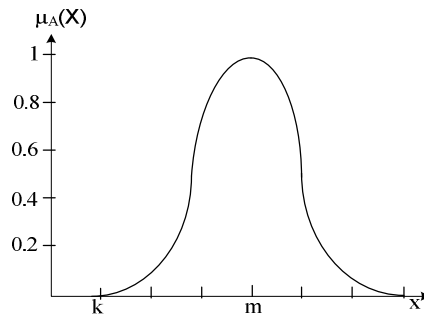


Figure 2.7 Gaussian Membership Function

2.16.4 Universe of discourse

The universe of discourse is the universe of all available information on a given problem. Once this universe is defined, we are able to define certain events on this information space. In practical applications, most often the universes of discourse are simply the set of real numbers or some interval or subset of real numbers. Sometimes for convenience it is refer to an “effective” universe of discourse $[\alpha, \beta]$ where α and β are the points at which the outermost membership functions saturate for input universes of discourse, or the points beyond which the outputs will not move for the output universe of discourse.

2.16.5 Membership function selection

A fuzzy control system connects input membership functions, functions representing the input to the controller, e , to output membership functions that represent the control action, u . It has been pointed out in (Bai and Wang, 1982) that, for those systems that need significant

dynamic variation in a short period of time, a triangular or trapezoidal waveform should be utilized. Figure 3.7 and 3.8 shows the input and output membership functions respectively.

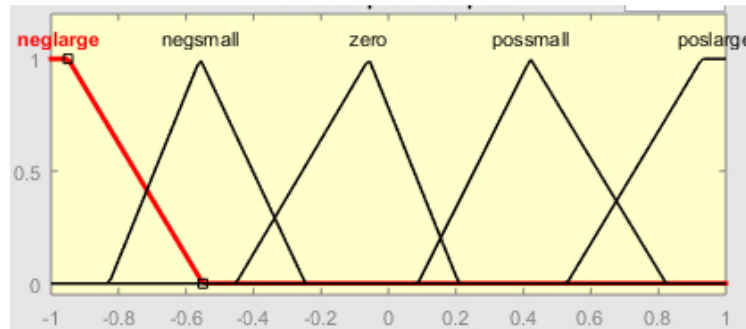


Figure 2.8 Input Membership Function

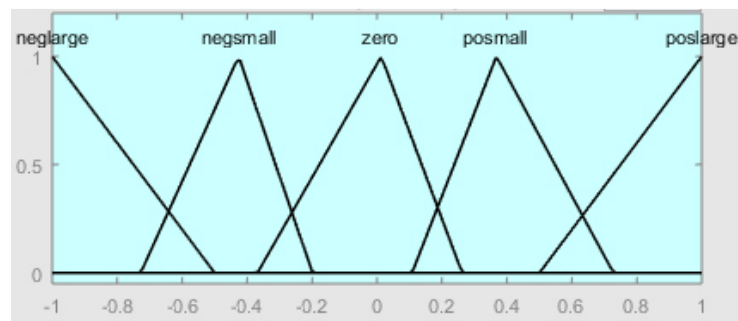


Figure 2.9 Output Membership Function

2.21 Setting up the control knowledge base

There are two main tasks in designing the control knowledge base (Berenji, 1992). First, a set of linguistic variables must be selected which describe the values of the main control parameters of the process. Both the main input parameters and the main output parameters must be linguistically defined in this stage using proper term sets. The selection of the level of granularity of a term set for an input variable or an output variable plays an important role in the smoothness of control. Secondly, a control knowledge base must be developed which uses the above linguistic description of the main parameters.

2.22 Linguistic descriptions

Sugeno(Sugeno, 1985)has suggested four methods for linguistic description:

- I. Expert's Experience and Knowledge
- II. Modeling the Operator's Control Actions
- III. Modeling a process
- IV. Self-Organization

Among the above methods, the first method is the most widely used (Mamdani and Assilian, 1975). Operator's knowledge, fuzzy control rules for single-input, single-output system is of the form:

IF premise THEN consequent

A typical example of a rule for a multiple-input, single-output system is as follows:

IF *premise1* and *premise2* THEN *consequence*

The premises (which are sometimes called “antecedents”) are associated with the fuzzy controller inputs and are on the left-hand-side of the rules. The consequents (sometimes called “actions”) are associated with the fuzzy controller outputs and are on the right-hand-side of the rules. Each premise (or consequent) can be composed of the conjunction of several “terms” The number of fuzzy controller inputs and outputs places an upper limit on the number of elements in the premises and consequents. Note that there does not need to be a premise (consequent) term for each input (output) in each rule, although often there is (Passino and Yurkovich 1997).

2.23 Linguistic value

This is one of the linguistic qualifiers, determined for the proper variable: error, change-of-error or control signal, for example: high, low, medium, etc.

2.24 Overlapping membership functions

This conditioning will be the first step in the process that establishes a compact mapping of the input space to the output space (Passino and Yurkovich, 1998). One reason why overlapping membership functions, where $\sum x_i \mu = 1.0, \forall x_i \text{ in } X$, is important is because this allows for a good interpolation of the input values. In other words, the entire input space is accommodated.

2.25 Fuzzy-PID controller structure (FPID)

In the fuzzy control literature, FPID are often mentioned as an alternative to the conventional PID controllers since they are analogous to the conventional PID controllers from the input–output relationship point of view (Galichet and Foulloy, 1995). The FPID controllers can be classified into three major categories as direct action type, fuzzy gain scheduling type, and hybrid type FPID controllers (Hu et al., 2001). The direct action type can also be classified into three categories according to the number of inputs as single input, double input, and triple input direct action FPID controllers (Hu et al., 2001). In the literature, researchers mainly focused on and analyzed double input direct action FPID controllers (Hu et al., 2001). In this study, double input direct action type and hybrid type FPID controllers are considered.

2.26 Double input FPID controllers

Structure of the two input direct action type FPID controllers formed using a FPID controller with an integrator and a summation unit at the output (Zhi, Qiao and Mizumoto, 1996).

As described in (Kumbasar and Hagnas, 2015), the standard FPID controller is constructed by choosing the inputs to be error (e) and derivative of error (Δe) as shown in Figure 2.10 and the output is the control signal (u).

The output of the FPID is defined as:

$$u = \alpha U + \beta \int U dt \quad (2.17)$$

Where U is the output of the fuzzy inference system.

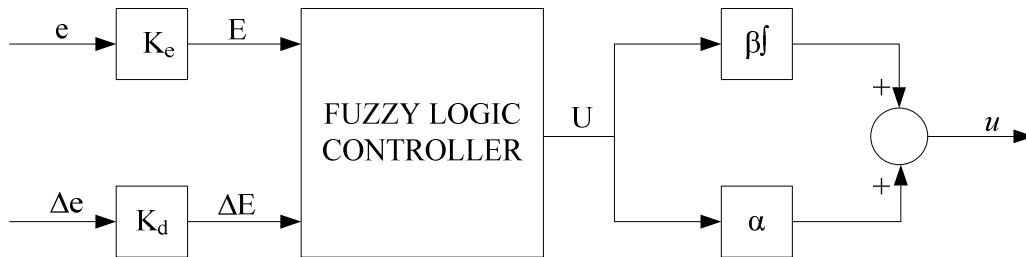


Figure 2.10 Double input direct action type FPID controller structure

The design parameters of the FPID controller structure can be summarized within two groups, structural parameters and tuning parameters (Hu et al., 2001).

The structural parameters include input/output variables to fuzzy inference, fuzzy linguistic sets, type of membership functions, fuzzy rules, and the inference mechanism, i. e., the fuzzy logic controller. In the handled FPID structure, the FLC is constructed as a set of heuristic control rules, and the control signal is directly deduced from the knowledge base and the fuzzy inference as done in diagonal rule base generation approaches (Kumbasar and Hagrass, 2015). Usually the structural parameters of the FPID controller structure are determined during an off-line design.

The tuning parameters include input/output scaling factors (SFs) and parameters of membership functions (MFs) (Kumbasar and Hagrass, 2015). As can be seen from Figure 2.10., the handled FPID controller structure has two input and two output scaling factors. The input SFs K_e (for error (e)) and K_d (for the change of error (Δe)) normalize the inputs to the common interval $[-1, 1]$ in which the membership functions of the inputs are defined (thus

$e(t)$ and $\Delta e(t)$ are converted after normalization into E and ΔE . While the FLC output (U) is mapped onto the respective actual output (u) domain by output SFs α and β (Magdalena,2015). Usually, the tuning parameters can be calculated during offline design process as well as online adjustments of the controller to enhance the process performance (Duan, Li, and Deng, 2008).

2.27 Hybrid FPID controller

The hybrid FPID controller as shown in Figure 2.11 is constructed by the combination of a two-input direct action FPID controller and a conventional PID controller(Birkan, Ibrahim, and Engin, 2005).

The output of the hybrid FPID is defined as:

$$u = \alpha U + \beta \int U dt + K \tag{2.18}$$

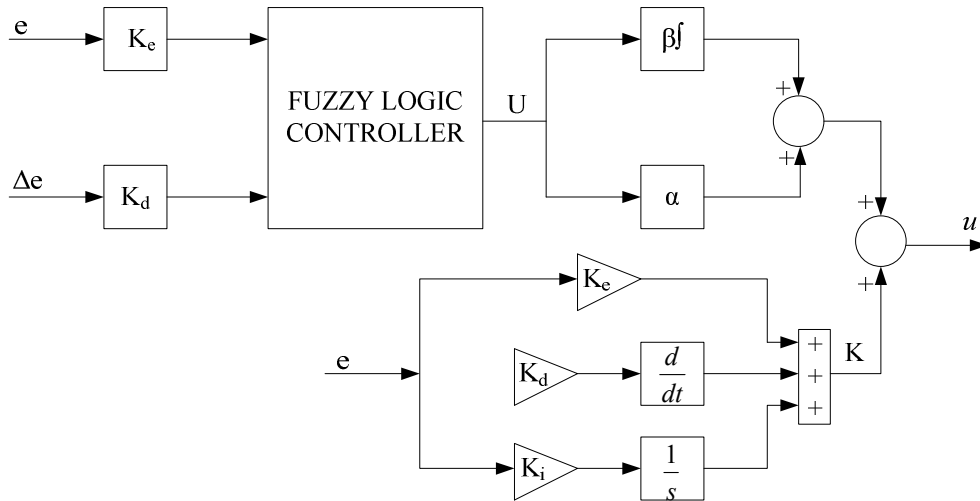


Figure 2.11 Hybrid FPID controller

Some of the advanced controllers that were used in hybrid strategy in previous works are; Full State Feedback controller, FLC and Double-PID with LQR controller.

In (Bagheri et al., 2016) LQR together with PID controller working together to provide robust stability and step reference tracking for the nonlinear dynamics of SmartFly Unmanned Aerial Vehicle (UAV) was considered. Functionality of this method was verified through computer simulation in MATLAB/SIMULINK for a nonlinear model of SmartFly UAV. Closed-loop system performance was evaluated in terms of robustness and step reference tracking. According to their results, the controller performance and robustness is acceptable.

A combination of PID and LQR controller with a fuzzy-based switching system is investigated in (Mohammadi et al., 2018) and the results of applying this controller to the balancing control of the unicycle robot, which is under a disturbance. The proposed controller has advantages of both LQR and PID controllers. The controller is designed in a way that when system's error is small, LQR controller is applied, and when the error is big, PID controller is chosen. To avoid on-off switching, a fuzzy logic-based switching system is applied to change between control signals and for calculating the controlling signal as a combination of the output signals of PID and LQR controllers. The results prove that the proposed controller can maintain the stability of the system precisely.

2.28 Cascade control method

The structure of the proposed cascade control is shown in Figure 2.13. Numerous researchers implemented a different kind of control of RIP system based on cascade method. Some used the two similar controllers in cascade form as in literature (Casanova et al. 2016; Stelian-Emilian Oltean, 2014;) while others used different controllers in cascade form as in literature (Y. F. Chen, Huang, and Huang 2014; Muske et al. 2012)

In this context, the system to be controlled is represented by three sub-systems, that is sub-system1, sub-system2 and sub-system3. The structure of cascade control method consists of

three control loops with a controller in each loop. The input to the outer (third) controller is the error between the desired input signal y_{ref} and the output of the sub-system3 y_3 . The input to the inner (second) controller is the difference between the output of the outer controller (r_3) and the output of sub-system2 (y_2). The input to the innermost (first) controller is the difference between the output of the inner (second) controller (r_2) and the output of sub-system1 (y_1). The output signal from innermost controller (r_1) serve as the control input to the sub-system1, while the output of sub-system 1 (y_2) serve as the control input to sub-system2, likewise the output of sub-system2 (y_2) serve as the control input to sub-system3. The tuning of the control parameters in cascade control strategy can be done individually as done in reference (Kumbasar and Hagra, 2015), i.e. to design the inner loop controller based on the propose objective function firstly. Subsequently, the outer loop controller can be design after the tuning of the inner controller. However, the tuning can be done simultaneously since the three controller must be keep in touch to each other as done in literature (Oh, Jang, and Pedrycz, 2011).

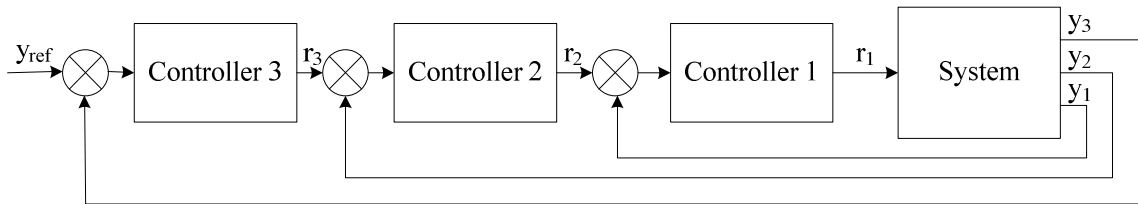


Figure 2.12 General Cascade Control Structure

2.29 Controllability

Controllability deals with the possibility of forcing the system to a particular state by application of a control input. If a state is uncontrollable then no input will be able to control that state. In order to be able to do whatever we want with the given dynamic system under control input, the system must be controllable. For general realization, the necessary and

sufficient condition for controllability is that the composite matrix has full rank (Naidu 2003; Ogata, 2010).

2.30 Observability

On the other hand, whether or not the initial states can be observed from the output is determined using observability property. Thus, if a state is not observable then the controller will not be able to determine its behavior from the system output and hence not be able to use that state to stabilize the system. For general realization, the necessary and sufficient condition for observability is that the composite matrix has full rank (Naidu 2003; Ogata, 2010).

CHAPTER THREE:Methodology

3.15 Introduction

The study of system dynamics resides in modeling its behaviour. The DRIP consists of a series of two pendulums attached to a rotary arm that rotate around motor shaft axis. It has three DOF, which are the rotary arm angle θ , the lower pendulum angle α , and the upper pendulum angle γ . The free body diagram of DRIP is shown in Figure 3.1.

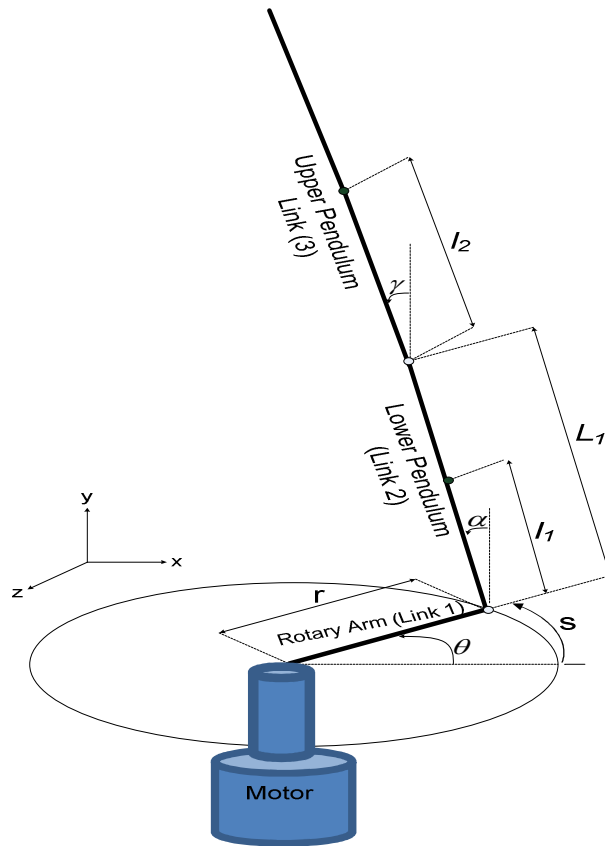


Figure 3.1 Schematic Diagram of DRIP

Derivation of mathematical equation describing dynamics of the DRIP system is based on Euler-Lagrange equation of motion (Sukontanakarn and Parnichkun, 2009). The complete mathematical equation describing the dynamics of the DRIP is found in (Aranda-Escolástico et al., 2016; V. Casanova et al., 2012; B. Li, 2013) as shown in the following equations.

$$\tau_a = [J_a + r^2(m_1 + m_2)\ddot{\theta}] + r(m_1l_1 + m_2L_1) \cos \alpha \ddot{\alpha} + m_2l_2r\dot{\gamma} \cos \gamma + b_a\dot{\theta} - r(m_1l_1 + m_2L_1) \sin \alpha \dot{\alpha}^2 - m_2l_2r \sin \gamma \dot{\gamma}^2 \quad (3.1)$$

$$\mathbf{0} = r(m_1l_1 + m_2L_1) \cos \alpha \ddot{\theta} + (J_1 + m_1l_1^2 + m_2L_1^2)\ddot{\alpha} + m_2L_1l_2 \cos(\alpha - \gamma) \ddot{\gamma} - b_1\dot{\alpha} + m_2L_1l_2 \sin(\alpha - \gamma) \dot{\gamma}^2 - g(m_1l_1 + m_2L_1) \sin \alpha \quad (3.2)$$

$$0 = m_2l_2r \cos \gamma \ddot{\theta} + m_2L_1l_2 \cos(\alpha - \gamma) \ddot{\alpha} + (J_2 + m_2l_2^2)\ddot{\gamma} + b_2\dot{\gamma} - m_2L_1l_2 \sin(\alpha - \gamma) \dot{\alpha}^2 - gm_2l_2 \sin \gamma \quad (3.3)$$

Equations (3.1), (3.2) and (3.3) are the three nonlinear, coupled, second order differential equations of motion describing the dynamics of the double inverted rotary pendulum system.

Where,

$\theta, \dot{\theta}, \ddot{\theta}$: Angular position, velocity and acceleration of the motor shaft, around the vertical axis.

$\alpha, \dot{\alpha}, \ddot{\alpha}$: Angular position, velocity and acceleration of the lower pendulum, around the motor shaft axis.

$\gamma, \dot{\gamma}, \ddot{\gamma}$: Angular position, velocity and acceleration of the upper pendulum, around the motor shaft axis.

X_i : Horizontal position for link i

Y_i Vertical position for link i

J_a : Moment of inertia around the center of rotation of the motor arm.

J_1 : Moment of inertia around the center of rotation of the first rod of the pendulum.

J_2 : Moment of inertia around the center of the second rod of the pendulum.

r : Length of the rotary arm from pivot to tip

L_1 : Length of lower pendulum from pivot to tip.

l_1 : Length between the centers of rotation and gravity of the lower pendulum.

l_2 : Length between the centers of rotation and gravity of the upper pendulum.

m_a : Mass of the rotary arm.

m_1 : Mass of the lower pendulum.

m_2 : Mass of the upper pendulum

b_a : Viscous friction in the joint of the motor arm.

b_1 : Viscous friction in the joint of the lower pendulum.

b_2 : Viscous friction in the joint of the upper pendulum.

g : Acceleration due to gravity.

If the equations are parameterized, they reduce to a more manageable form. Define $z_1, z_2,$

z_3, z_4, z_5, z_6, z_7 and z_8 as

$$z_1 = J_a + r^2(m_1 + m_2) \quad (3.4)$$

$$z_2 = r(m_1 l_1 + m_2 L_1) \quad (3.5)$$

$$z_3 = m_2 l_2 \quad (3.6)$$

$$z_4 = J_1 + m_1 l_1^2 + m_2 L_1^2 \quad (3.7)$$

$$z_5 = L_1 l_2 m_2 \quad (3.8)$$

$$z_6 = J_2 + m_2 l_2^2 \quad (3.9)$$

$$z_7 = g(m_1 l_1 + m_2 L_1) \quad (3.10)$$

$$z_8 = g m_2 l_2 \quad (3.11)$$

The dynamic equations (3.1), (3.2) and (3.3) are reduced into the form

$$\tau_a = z_1 \ddot{\theta} + z_2 \cos \alpha \ddot{\alpha} + z_3 \ddot{\gamma} \cos \gamma + b_a \dot{\theta} - z_2 \sin \alpha \dot{\alpha}^2 - z_3 \sin \gamma \dot{\gamma}^2 \quad (3.12)$$

$$0 = z_2 \cos \alpha \ddot{\theta} + z_4 \ddot{\alpha} + z_5 \cos(\alpha - \gamma) \ddot{\gamma} + b_1 \dot{\alpha} + z_5 \sin(\alpha - \gamma) \dot{\gamma}^2 - z_7 \sin \alpha \quad (3.13)$$

$$0 = z_3 \cos \gamma \ddot{\theta} + z_5 \cos(\alpha - \gamma) \ddot{\alpha} + z_6 \ddot{\gamma} + b_2 \dot{\gamma} - z_5 \sin(\alpha - \gamma) \dot{\alpha}^2 - z_8 \sin \gamma \quad (3.14)$$

The above parameters can be calculated using the specifications of Table 3.1.

3.16 System specifications

Table 3.1 lists and characterizes the main parameters (whose values are provided by the manufacturer) associated with the SRV02 DRIP module. They are used in the mathematical model.

Table 3.1 SRV02 DRIP Specifications

Symbol	Description	Value	Unit
J_a	Rotary arm moment of inertia about its center of mass	0.0041	kg.m ²
J_1	First Pendulum moment of inertia about center of mass	0.00032	kg.m ²
J_2	Second Pendulum moment of inertia about center of mass	0.0012	kg.m ²
R	Rotary arm length from pivot to tip	0.2159	M
L_1	Lower pendulum length from pivot to tip	0.2	M
l_1	Lower pendulum length from pivot to center of mass	0.097	M
l_2	Upper pendulum length from pivot to center of mass	0.156	M
b_a	Viscous damping coefficient of the motor arm.	0.0024	N.m/(rad/s)
b_1	Upper Pendulum viscous damping coefficient as seen at the pivot axis	0.0024	N.m/(rad/s)
b_2	Lower Pendulum viscous damping coefficient as seen at the pivot axis	0.0024	N.m/(rad/s)
V_{nom}	Motor nominal input voltage	6.0	V
R_m	Motor armature resistance	2.6	Ω
η_m	Motor efficiency	0.63	
η_g	Gear efficiency	0.9	
K_g	Total gear ratio	70	
K_m	Back-emf constant	0.00768	V/(rad/s)
K_t	Motor torque constant	0.00768	N.m

$$z_1 = J_a + r^2(m_1 + m_2) = 0.0041 + 0.2159^2 \times (0.097 + 0.127) = 0.0145$$

$$z_2 = r(m_1l_1 + m_2L_1) = 0.2159 \times ((0.097 \times 0.1635) + (0.127 \times 0.2)) = 0.0089$$

$$z_3 = m_2l_2r = 0.2159 \times 0.127 \times 0.156 = 0.0043$$

$$z_4 = J_1 + m_1l_1^2 + m_2L_1^2 = 0.00032 + ((0.097 \times 0.1635^2) + (0.127 \times 0.2^2)) = 0.0079$$

$$z_5 = L_1l_2m_2 = 0.127 \times 0.156 \times 0.2 = 0.0039$$

$$z_6 = J_2 + m_2l_2^2 = 0.0012 + (0.127 \times 0.156^2) = 0.0043$$

$$z_7 = g(m_1l_1 + m_2L_1) = 9.81 \times ((0.097 \times 0.1635) + (0.127 \times 0.2)) = 0.4048$$

$$z_8 = gm_2l_2 = 9.81 \times 0.127 \times 0.156 = 0.1944$$

3.17 Torque (τ)

Torque is a measure of how much force acting on an object causes that object to rotate. The object rotates about an axis called a pivot point. The servomotor as described by the equation (3.15) generates the torque, which serve as the input to the DRIP.

$$\tau_m(t) = \frac{\eta_g K_g \eta_m k_t (V_m(t) - K_g k_m \dot{\theta}(t))}{R_m} \quad (3.15)$$

The value of the torque for the system under consideration can be calculated using equation (3.63) below.

$$\begin{aligned} \tau_a &= \frac{0.9 \times 0.63 \times 70 \times 7.68 \times 10^{-3} (v - 70 \times 7.68 \times 10^{-3} \dot{\theta})}{2.6} \\ &= 0.117238v - 0.063\dot{\theta} \text{ Nm} \end{aligned}$$

$$\tau_a = 0.117238v - 0.063\dot{\theta} \text{ Nm} \quad (3.16)$$

Substituting the values of the z_i and (3.15) into equations (3.1), (3.2) and (3.3) now becomes

$$0.117238v = 0.0145\ddot{\theta} + 0.0089 \cos \alpha \ddot{\alpha} + 0.0043\dot{\gamma} \cos \gamma + 0.0654\dot{\theta} - 0.0089 \sin \alpha \dot{\alpha}^2 - 0.0043 \sin \gamma \dot{\gamma}^2 \quad (3.17)$$

$$0 = 0.0089 \cos \alpha \ddot{\theta} + 0.0079\ddot{\alpha} + 0.0039 \cos(\alpha - \gamma) \ddot{\gamma} + 0.0024\dot{\alpha} + 0.0039 \sin(\alpha - \gamma) \dot{\gamma}^2 - 0.4048 \sin \alpha \quad (3.18)$$

$$0 = 0.0043 \cos \gamma \ddot{\theta} + 0.0039 \cos(\alpha - \gamma) \ddot{\alpha} + 0.0043\ddot{\gamma} + 0.0024\dot{\gamma} - 0.0039 \sin(\alpha - \gamma) \dot{\alpha}^2 - 0.1944 \sin \gamma \quad (3.19)$$

3.18 Matlab modeling

For the purpose of controller design and evaluation, the DRIP Simulink model was developed in Matlab/Simulink using the nonlinear, parameterized mathematical model as shown in Figure 4. This is done by first rearranging the nonlinear-coupled equations of motion (3.17), (3.18) and (3.19) to obtain an explicit form of the acceleration for each of the three links into equations (3.20), (3.21) and (3.22) respectively.

$$\ddot{\theta} = 0.8085v - 0.6138 \cos \alpha \ddot{\alpha} - 0.2966 \cos \gamma \ddot{\gamma} - 4.5103\dot{\theta} + 0.6138 \sin \alpha \dot{\alpha}^2 + 0.2966 \sin \gamma \quad (3.20)$$

$$\ddot{\alpha} = -1.1266 \cos \alpha \ddot{\theta} - 0.4937 \cos(\alpha - \gamma) \ddot{\gamma} - 0.3038\dot{\alpha} - 0.4937 \sin(\alpha - \gamma) \dot{\gamma}^2 + 51.2405 \sin \alpha \quad (3.21)$$

$$\ddot{\gamma} = -\cos \gamma \ddot{\theta} - 0.9096 \cos(\alpha - \gamma) \ddot{\alpha} - 0.5581\dot{\gamma} + 0.9096 \sin(\alpha - \gamma) \dot{\alpha}^2 + 45.2093 \sin \gamma \quad (3.22)$$

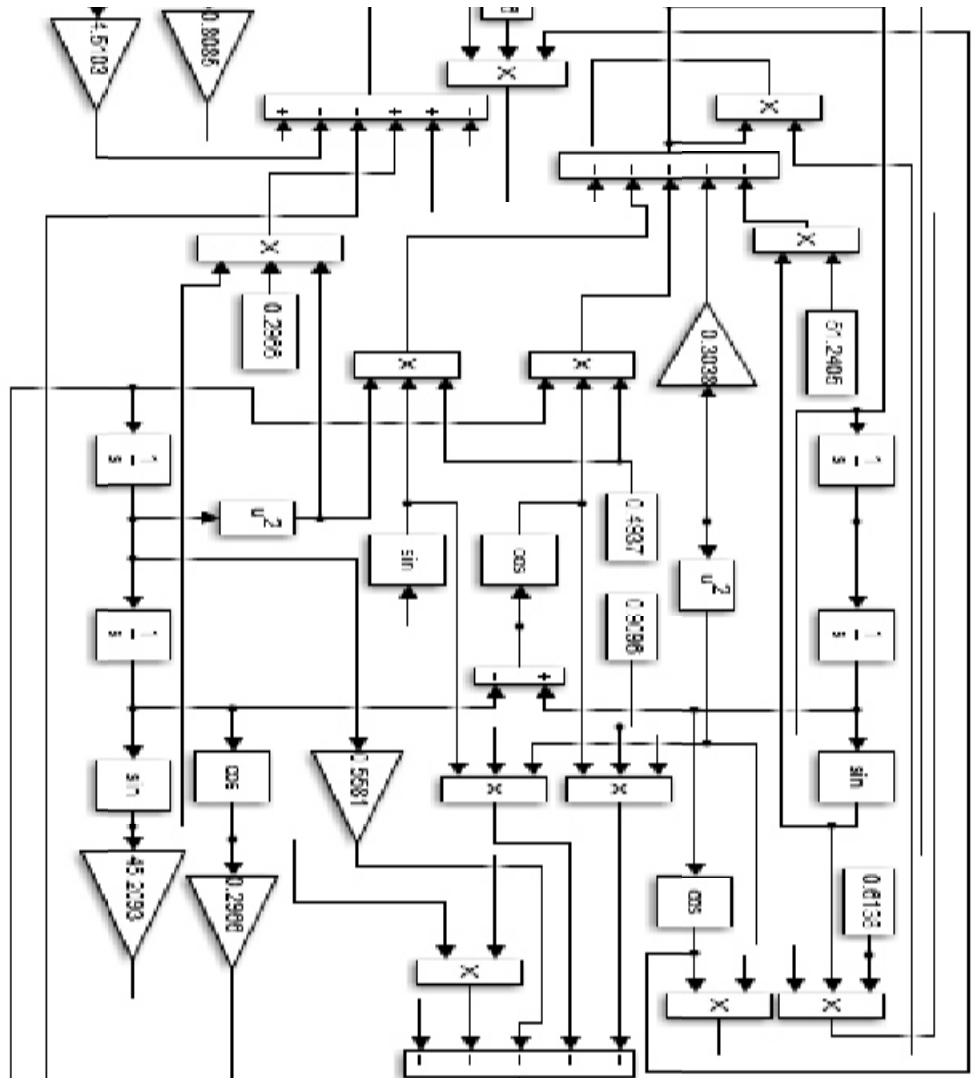


Figure 3.2 Simulink Model of DRIP

3.5 Model validation

In order to verify the validity of the derived model, a visual simulation was carried out in matlab/Simulink environment. The simulation was performed with the parameters given in Table 3.1. As we have mentioned before, the upward position is an unstable equilibrium for the system. A little disturbance will lead the open-loop system to leave from the unstable equilibrium and fall to the downward position, which is the stable equilibrium of the system. This characteristic (open loop responses) can be seen by the MATLAB simulation result in Figures 4.1, 4.2 and 4.3.

3.6 Tests for controllability and observability

Controllability and observability are two important properties of state models which are to be studied prior to designing a controller. The controllability and observability matrix can be obtained by first finding the state space representation of the system after linearizing the nonlinear equations of motion of the system.

In most situations where we seek a linearized model, the nominal state is an equilibrium point. This term refers to an initial state where the system remains unless perturbed (Fadali and Visioli, 2013). Therefore, to linearize the model (Stelian-Emilian Oltean, 2014), the following approximations are applied: $\cos \theta \approx 1$, $\cos \alpha \approx 1$, $\cos \gamma \approx 1$, $\sin \theta = \theta$, $\sin \alpha = \alpha$, $\sin \gamma = \gamma$, $\dot{\theta}^2 = \dot{\alpha}^2 = \dot{\gamma}^2 \approx 0$.

The linearized model of the nonlinear equations of motion (3.17), (3.18) and (3.19), thus, becomes:

$$z_1 \ddot{\theta} + z_2 \ddot{\alpha} + z_3 \ddot{\gamma} + b_a \dot{\theta} = \tau_a \quad (3.23)$$

$$z_2 \ddot{\theta} + z_4 \ddot{\alpha} + z_5 \ddot{\gamma} + b_1 \dot{\alpha} - z_7 \alpha = 0 \quad (3.24)$$

$$z_3 \ddot{\theta} + z_5 \ddot{\alpha} + z_6 \ddot{\gamma} + b_2 \dot{\gamma} - z_8 \gamma = 0 \quad (3.25)$$

In matrix form, the linearized model thus becomes:

$$\begin{bmatrix} z_1 & z_2 & z_3 \\ z_2 & z_4 & z_5 \\ z_3 & z_5 & z_6 \end{bmatrix} \begin{bmatrix} \ddot{\theta} \\ \ddot{\alpha} \\ \ddot{\gamma} \end{bmatrix} + \begin{bmatrix} b_a & 0 & 0 \\ 0 & b_1 & 0 \\ 0 & 0 & b_2 \end{bmatrix} \begin{bmatrix} \dot{\theta} \\ \dot{\alpha} \\ \dot{\gamma} \end{bmatrix} + \begin{bmatrix} 0 & 0 & 0 \\ 0 & -\alpha z_7 & 0 \\ 0 & 0 & -\gamma z_8 \end{bmatrix} = \begin{bmatrix} \tau_a \\ 0 \\ 0 \end{bmatrix} \quad (3.26)$$

Substituting values of z_i s as calculated in section 3.4.

$$\begin{bmatrix} 0.0145 & 0.0089 & 0.0043 \\ 0.0089 & 0.0079 & 0.0039 \\ 0.0043 & 0.0039 & 0.0043 \end{bmatrix} \begin{bmatrix} \ddot{\theta} \\ \ddot{\alpha} \\ \ddot{\gamma} \end{bmatrix} + \begin{bmatrix} 0.0024 & 0 & 0 \\ 0 & 0.0024 & 0 \\ 0 & 0 & 0.0024 \end{bmatrix} \begin{bmatrix} \dot{\theta} \\ \dot{\alpha} \\ \dot{\gamma} \end{bmatrix} + \begin{bmatrix} 0 & 0 & 0 \\ 0 & -0.4048\alpha & 0 \\ 0 & 0 & -0.1944\gamma \end{bmatrix} = \begin{bmatrix} 0.1172V - 0.063\dot{\theta} \\ 0 \\ 0 \end{bmatrix}$$

To obtain the state space representation of the system, the matrix multiplying the link accelerations was inverted and the equation multiplied by the result to get the expression in terms of the link accelerations independently. This was then rewritten in terms of the six states. The resulting equations are as follows:

$$\begin{bmatrix} \ddot{\theta} \\ \ddot{\alpha} \\ \ddot{\gamma} \end{bmatrix} = \begin{bmatrix} 0.0145 & 0.0089 & 0.0043 \\ 0.0089 & 0.0079 & 0.0039 \\ 0.0043 & 0.0039 & 0.0043 \end{bmatrix}^{-1} \left(- \begin{bmatrix} 0.0024\dot{\theta} \\ 0.0024\dot{\alpha} \\ 0.0024\dot{\gamma} \end{bmatrix} - \begin{bmatrix} 0 \\ -0.4048\alpha \\ -0.1944\gamma \end{bmatrix} + \begin{bmatrix} 0.1172V - 0.063\dot{\theta} \\ 0 \\ 0 \end{bmatrix} \right)$$

$$\begin{bmatrix} \ddot{\theta} \\ \ddot{\alpha} \\ \ddot{\gamma} \end{bmatrix} = \begin{bmatrix} 223.7275 & -256.4041 & 8.8251 \\ -256.4041 & 523.0644 & -218.0031 \\ 8.8251 & -218.0031 & 421.4569 \end{bmatrix} \begin{bmatrix} -0.0654\dot{\theta} + 0.1172V \\ -0.0024\dot{\alpha} + 0.4048\alpha \\ -0.0024\dot{\gamma} + 0.1944\gamma \end{bmatrix}$$

$$\begin{bmatrix} \ddot{\theta} \\ \ddot{\alpha} \\ \ddot{\gamma} \end{bmatrix} = \begin{bmatrix} -14.6318\dot{\theta} + 0.6154\dot{\alpha} - 0.0212\dot{\gamma} - 103.7924\alpha + 1.7156\gamma + 26.2209V \\ 16.7688\dot{\theta} - 1.2554\dot{\alpha} + 0.5232\dot{\gamma} + 211.7365\alpha - 42.3798\gamma - 30.0506V \\ -0.5772\dot{\theta} + 0.5232\dot{\alpha} - 1.0115\dot{\gamma} - 88.2477\alpha + 81.9312\gamma + 1.0343V \end{bmatrix}$$

$$\ddot{\theta} = -14.6318\dot{\theta} + 0.6154\dot{\alpha} - 0.0212\dot{\gamma} - 103.7924\alpha + 1.7156\gamma + 26.2209 \quad (3.27)$$

$$\ddot{\alpha} = 16.7688\dot{\theta} - 1.2554\dot{\alpha} + 0.5232\dot{\gamma} + 211.7365\alpha - 42.3798\gamma - 30.0506 \quad (3.28)$$

$$\ddot{\gamma} = -0.5772\dot{\theta} + 0.5232\dot{\alpha} - 1.0115\dot{\gamma} - 88.2477\alpha + 81.9312\gamma + 1.0343V \quad (3.29)$$

The general form of the state space equations for linear systems is

$$\dot{x}(t) = Ax(t) + Bu(t) \quad (3.30)$$

$$y(t) = Cx(t) + Du(t) \quad (3.31)$$

Where $x(t)$ is an $n \times 1$ real vector, $u(t)$ is an $m \times 1$ real vector, and $y(t)$ is an $l \times 1$ real vector.

A = $n \times n$ state matrix

B = $n \times m$ input or control matrix

C = $l \times n$ output matrix

D = $l \times m$ direct transmission matrix

By defining the state variables as: $x_1 = \theta$ $x_2 = \alpha$ $x_3 = \gamma$ $x_4 = \dot{\theta}$ $x_5 = \dot{\alpha}$ $x_6 = \dot{\gamma}$

A linear state space system can thus be represented by

$$\begin{bmatrix} \dot{x}_1 \\ \dot{x}_2 \\ \dot{x}_3 \\ \dot{x}_4 \\ \dot{x}_5 \\ \dot{x}_6 \end{bmatrix} = \begin{bmatrix} 0 & 0 & 0 & 1 & 0 & 0 \\ 0 & 0 & 0 & 0 & 1 & 0 \\ 0 & 0 & 0 & 0 & 0 & 1 \\ 0 & -103.7924 & 1.7156 & -14.6318 & 0.6154 & -0.0212 \\ 0 & 211.7365 & -42.3798 & 16.7688 & -1.2554 & 0.5232 \\ 0 & -88.2477 & 81.9312 & -0.5772 & 0.5232 & -1.0115 \end{bmatrix} \begin{bmatrix} x_1 \\ x_2 \\ x_3 \\ x_4 \\ x_5 \\ x_6 \end{bmatrix} + \begin{bmatrix} 0 \\ 0 \\ 0 \\ 26.2209 \\ -30.0506 \\ 1.0343 \end{bmatrix} \quad (3.32)$$

$$y = \begin{bmatrix} 1 & 0 & 0 & 0 & 0 & 0 \\ 0 & 1 & 0 & 0 & 0 & 0 \\ 0 & 0 & 1 & 0 & 0 & 0 \end{bmatrix} \begin{bmatrix} \theta \\ \alpha \\ \gamma \\ \dot{\theta} \\ \dot{\alpha} \\ \dot{\gamma} \end{bmatrix} + \begin{bmatrix} 0 \\ 0 \\ 0 \end{bmatrix} V \quad (3.33)$$

$$A = \begin{bmatrix} 0 & 0 & 0 & 1 & 0 & 0 \\ 0 & 0 & 0 & 0 & 1 & 0 \\ 0 & 0 & 0 & 0 & 0 & 1 \\ 0 & -103.7924 & 1.7156 & -14.6318 & 0.6154 & -0.0212 \\ 0 & 211.7365 & -42.3798 & 16.7688 & -1.2554 & 0.5232 \\ 0 & -88.2477 & 81.9312 & -0.5772 & 0.5232 & -1.0115 \end{bmatrix} \quad (3.34)$$

$$B = \begin{bmatrix} 0 \\ 0 \\ 0 \\ 26.2209 \\ -30.0506 \\ 1.0343 \end{bmatrix} \quad (3.35)$$

$$C = \begin{bmatrix} 1 & 0 & 0 & 0 & 0 & 0 \\ 0 & 1 & 0 & 0 & 0 & 0 \\ 0 & 0 & 1 & 0 & 0 & 0 \end{bmatrix} \quad (3.36)$$

3.7 The controllability matrix (C_0)

The system of equations (3.30) and (3.31) with the pair ($A: nxn, B: nxm$) is given in equation (3.37).

$$C_0 = [B \ BA \ BA^2 \ \dots \ \dots \ BA^{n-1}] \quad (3.37)$$

With the linear state matrices A and B (with $n=6$), the controllability of the system has been figured out to be

$$C_0 = [B \ BA \ BA^2 \ BA^3 \ BA^4 \ BA^5]$$

$$C_0 = \begin{bmatrix} 0 & 26.2209 & -402.1740 & 9300.1194 & -194280.0801 & 4449166.3650 \\ 0 & -30.0506 & 447.9596 & -13766.8168 & 277458.8830 & 6690531.6270 \\ 0 & 1.0343 & -30.9034 & 3250.0999 & -60569.0916 & 1799745.0900 \\ 26.2209 & -402.1740 & 9300.1194 & -194280.0801 & 4449166.3650 & -98156855.8800 \\ -30.0506 & 477.9596 & -13766.8168 & 277456.8830 & -6690531.6270 & 145263179.4000 \\ 1.0343 & -30.9034 & 3250.0999 & -60569.0916 & 1799745.0900 & -37336593.7600 \end{bmatrix} \quad (3.38)$$

The determinant of the controllability matrix $C_0=7$

The rank of the controllability matrix C_0 as found using matlab is six (6), which implies that, the matrix has full rank. For that reason, the system is controllable.

3.8 The observability matrix (O)

The system of equations (3.30) and (3.31) with the pair ($A: nxn, C: lxn$) is given in equation (3.83).

$$O = [C \ CA \ CA^2 \ \dots \ \dots \ CA^{n-1}]^T \quad (3.39)$$

With the linear state matrices A and C (with $n=6$), the observability matrix of the system has been figured out to be

$$O = [C \ CA \ CA^2 \ CA^3 \ CA^4 \ CA^5]^T$$

$$\begin{pmatrix} 1 & 0 & 0 & 0 & 0 & 0 \\ 0 & 1 & 0 & 0 & 0 & 0 \\ 0 & 0 & 1 & 0 & 0 & 0 \\ 0 & 0 & 0 & 1 & 0 & 0 \\ 0 & 0 & 0 & 0 & 1 & 0 \\ 0 & 0 & 0 & 0 & 0 & 1 \\ 0 & -103.7924 & 1.7156 & -14.6318 & 0.6154 & -0.0212 \\ 0 & 211.7365 & -42.3798 & 16.7688 & -1.2554 & 0.5232 \\ 0 & -88.2477 & 81.9312 & -0.5772 & 0.5232 & -1.0115 \\ 0 & 1650.0843 & -52.9198 & 224.4213 & -113.5805 & 2.3692 \\ 0 & -2052.4592 & 124.8386 & -266.7113 & 223.9058 & -43.9213 \\ 0 & 259.9521 & -106.0368 & 17.8027 & -89.7890 & 83.2403 \\ 0 & -47551.4382 & 5392.6477 & -5189.6638 & 1932.7805 & -119.4993 \\ 0 & 78967.5878 & -13545.1805 & 7682.4487 & -2520.6643 & 292.0668 \\ 0 & -28205.1539 & 10655.7584 & -1814.1855 & 427.1802 & -237.5893 \\ 0 & 958433.3753 & -100604.9587 & 108413.5070 & -53234.0919 & 6634.7728 \\ 0 & -1356870.6453 & 143934.6390 & -154845.1494 & 87012.6180 & -15322.2855 \\ 0 & 299715.0327 & -40682.2093 & 33845.2365 & -29982.1925 & 11158.0415 \end{pmatrix}$$

Here, there exist a 6x6 sub-matrix, which is in a Row Reduce Echelon form. This means the matrix has full rank, which fulfill the condition of observability. Therefore, the system is observable.

3.9 Test for stability

As pointed out in (Mandal, 2017), the necessary and sufficient condition for stability of a system is that all the roots of the characteristic equation (λ , also referred to as eigenvalues) should have negative real parts. If any of the roots has positive real part, the contribution from the corresponding exponential term will grow with time, the output response will be unbounded, and the entire system will be regarded as unstable.

This can be determined by finding the eigenvalues (λ). The characteristic equation (P) is given as:

$$P(\lambda) = \det(\lambda I - A) \quad (3.40)$$

Where, I is an identity matrix

$$P(\lambda) = \det \left[\lambda \begin{pmatrix} 1 & 0 & 0 & 0 & 0 & 0 \\ 0 & 1 & 0 & 0 & 0 & 0 \\ 0 & 0 & 1 & 0 & 0 & 0 \\ 0 & 0 & 0 & 1 & 0 & 0 \\ 0 & 0 & 0 & 0 & 1 & 0 \\ 0 & 0 & 0 & 0 & 0 & 1 \end{pmatrix} - \begin{pmatrix} 0 & 0 & 0 & 1 & 0 & 0 \\ 0 & 0 & 0 & 0 & 1 & 0 \\ 0 & 0 & 0 & 0 & 0 & 1 \\ 0 & -103.7924 & 1.7156 & -14.6318 & 0.6154 & -0.0212 \\ 0 & 211.7365 & -42.3798 & 16.7688 & -1.2554 & 0.5232 \\ 0 & -88.2477 & 81.9312 & -0.5772 & 0.5232 & -1.0115 \end{pmatrix} \right] \quad (3.41)$$

$$\mathbf{P}(\lambda) = \begin{vmatrix} \lambda_1 & 0 & 0 & -1 & 0 & 0 \\ 0 & \lambda_2 & 0 & 0 & -1 & 0 \\ 0 & 0 & \lambda_3 & 0 & 0 & -1 \\ 0 & 103.7924 & -1.7156 & \lambda_4 + 14.6318 & 0.0212 & 0 \\ 0 & -211.7365 & 42.3798 & -16.7688 & \lambda_5 + 1.2554 & -0.5232 \\ 0 & 88.2477 & -81.9312 & 0.5772 & -0.5232 & \lambda_6 + 1.0115 \end{vmatrix}$$

$$\begin{aligned}\lambda_1 &= 0 \\ \lambda_2 &= -22.5049 \\ \lambda_3 &= 12.8716 \\ \lambda_4 &= 6.2333 \\ \lambda_5 &= -3.3489 \\ \lambda_6 &= -10.1498\end{aligned}$$

From the eigenvalues (λ_i) obtained, it is found that two of the poles are in positive real part of s-plane. Hence, the system is confirmed to be unstable.

3.10 Hybrid PID/LQR controller design

The hybrid PID/LQR controller in the present study is constructed by the combination of conventional PID and LQR controllers. This structure is shown in Figure 3.3.

To design a PID controller for nonlinear systems, the PID parameters are usually tuned for local points using a linearization method. The PID controller can control the linear model of DRIP balance but it vibrates larger in the vicinity of balance point and subsequently turns to instability within a very short time, thus, the static performance is poor. To enhance the stability of the system an LQR controller is used to support the proposed PID controller.

For the LQR controller, it has a good control effect in small-angle scope, but, for larger disturbance, then the angle beyond the linearization constraint conditions, the LQR controller do not have good control effect to be robust to measurement noise, external disturbances and unmodeled dynamics (Naidu, 2003). Moreover, most work in conventional control to date has focused only on the linear model of the plant. A further point of note is that the resulting LQR regulates only about zero equilibrium. Since the equations of motion are not zero about the desired operating point and that in general the upright equilibrium can be described by an

infinite number of coordinates some kind of conditioning of the signal passed to the constant gain controller is needed(Driver and Thorpe, 2004).

3.11 PID controller design

The conventional PID can only control one output. However, the system under consideration has three outputs to be control; arm angular position, lower pendulum angle and upper pendulum angle. Therefore, three PID controllers in cascade are designed with each controlling one output.

The parameters of the PID for each of the links are obtained by manual tuning in this study. Manual tuning of the PID is done by increasing the proportional term until the system oscillates around the set point while the integral and derivative terms kept at zero. Keeping the proportional term at this new value and the integral term at zero the derivative term is then increased until the overshoot is deemed reasonable. Lastly keeping the proportional and derivative terms at their new values gradually increase the integral term until any steady-state error is reduced to an acceptable error margin.

After iterative manual tuning, the values of PID gains for each of the three links of DRIP are found as follows:

Arm

$$K_P=0.97 \quad K_I=0.37 \quad K_D=0.29$$

Lower Pendulum

$$K_P=0.96 \quad K_I=0.0002202 \quad K_D=0.009$$

Upper Pendulum

$$K_P=1.019 \quad K_I=0.0001 \quad K_D=0.09$$

3.12 LQR controller design

The LQR is an optimal controller that requires a state-space linear approximation of the nonlinear system but generally has superior performance. LQR measures all states and stabilizes the system using full state feedback (Akgül, 2011).

To design a state feedback control $u = -kx$ to stabilize the system, the design of K is a tradeoff between the transient response and control effort. The optimal control approach to this design tradeoff is to define the performance index (cost function) of equation (2.5) and search for the control (equation 2.5) that minimizes the index.

The weighting matrices Q and R are important components of an LQR optimization process. The designer is free to select the matrices Q and R, but the selection of matrices Q and R is normally based on an iterative procedure using experience and physical understanding of the problems involved (E and Jerome, 2013) to get the desired response.

The key problem in the design of optimal controller using LQR is the choice of Q and R matrices. The compositions of Q and R elements have great influences on system performance. The number of elements of Q and R matrices depend on the number of state variable (n) and the number of input variable (m), respectively.

LQR function in matlab m-file is in this research used to determine the value of the vector K that determines the feedback control law (equation 2.4) as follows:

$$K = [0.3162 \quad -46.4165 \quad 61.2213 \quad 0.2169 \quad -0.8726 \quad 6.6182]$$

3.13 Cascade control structure for DRIP

The DRIP is a single input multiple output (SIMO) system. In SIMO systems, a change of one of the outputs by some disturbances affects the control of the other outputs (Aguilar-Avelar and Moreno-Valenzuela, 2015). Thus, considering nonlinear behavior of DRIP system, it is difficult to achieve a desired settling time. In addition, it has high level of disturbances and large time constant. Therefore, the best control strategy is the cascade control one (Figure 3.6), since it has the advantage of attenuating the effect of disturbances and improving the dynamics of entire control loop (Fatihu et al., 2019). The output of the first controller is the control voltage to the servomotor $v_m(t)$.

However, since PID has the limitation of controlling only one output (Emre Akgul 2011), as depicted in figure 3.6, three PID controllers in cascade topology combined with LQR controller for stabilization control of DRIP system are chosen in the present research.

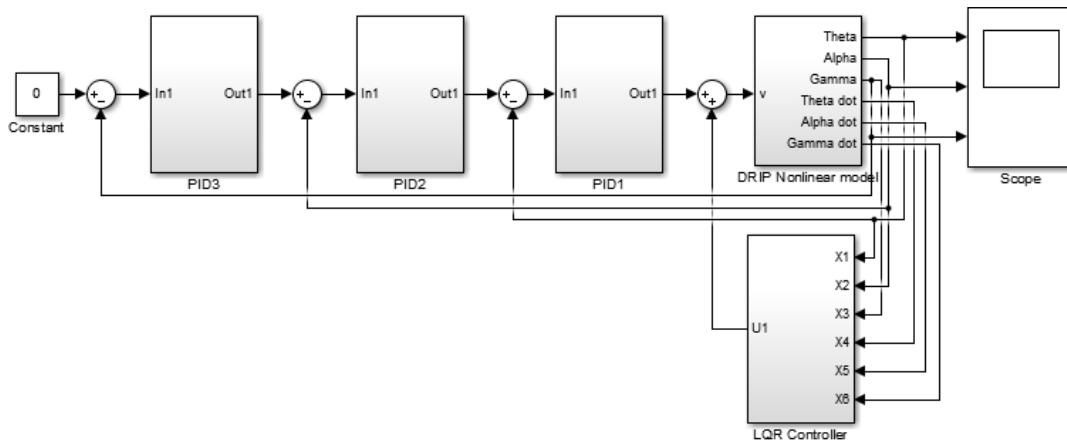


Figure 3.3 Hybrid Cascade PID/LQR Controller Structure for Double Rotary Inverted Pendulum

3.14 Hybrid FPID /LQR controller design

In recent years, FLC has been applied successfully in the area of nonlinear process control (C.-L. Chen and Kuo, 1995; H. Li, Malki, and Chen, 1994). Unfortunately (W. Li 1998), defining membership functions of linguistic variables and formulating fuzzy rules by

manual operation is time consuming work. Besides, a few of stability analysis for the real applied FLC were reported so that many people worry about their reliability. A hybrid combination of conventional controllers and fuzzy logic is an attractive and powerful approach for designing robust control systems with high degrees of nonlinearities and uncertainties. The control results on a manipulator and stoker-fired boilers show the effectiveness and robustness of the hybrid fuzzy logic plus conventional controllers (W. Li 1998). Figure 3.10 presents the schematic diagram of the proposed hybrid FPID/LQR cascade control topology.

3.15 Design of fuzzy control rules

A set of rules on how to control the DRIP for all possible cases is written down as shown in Table 3.2. For the pendulum problem under consideration, with two inputs and seven linguistic values for each of these, there are at most $7^2 = 49$ possible rules.

Table 3.2 Fuzzy Rules for the stabilization control of DRIP

		Change-In-Error						
		NB	NM	NS	Z	PS	PM	PB
Error	NB	NB	NB	NB	NB	NM	NS	Z
	NM	NB	NB	NB	NM	NS	Z	PS
	NS	NB	NB	NM	NS	Z	PS	PM
	Z	NB	NM	NS	Z	PS	PM	PB
	PS	NM	NS	Z	PS	PM	PB	PB
	PM	NS	Z	PS	PM	PB	PB	PB
	PB	Z	PS	PM	PB	PB	PB	PB

Where the acronyms contained in the table means;

NB: negative big

NM: negative medium

NS: negative small

Z: zero

PB: positive big

PM: positive medium

PS: positive small

3.16FPID structure

The standard FPID controller is constructed by choosing the inputs to be error (e) and derivative of error (Δe) as shown and the output is the control signal (u). As indicated in (Birkan, Ibrahim, and Engin 2005), among the three categories of FPID structure, double input type is the most robust structure for unstable pole systems. As can be seen from Figure 3.9, the handled FPID controller structure has two input and two output scaling factors (Kumbasar and Hagnas 2015b). The input SFs K_e (for error (e)) and K_d (for the change of error (Δe)). While the FLC output (U) is mapped onto the respective actual output (u) domain by output scaling factors β and α .

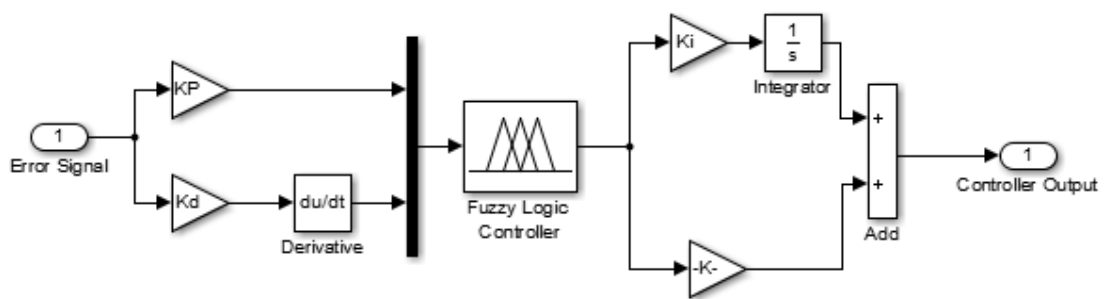


Figure3.4Internal Structure of FPID Controller

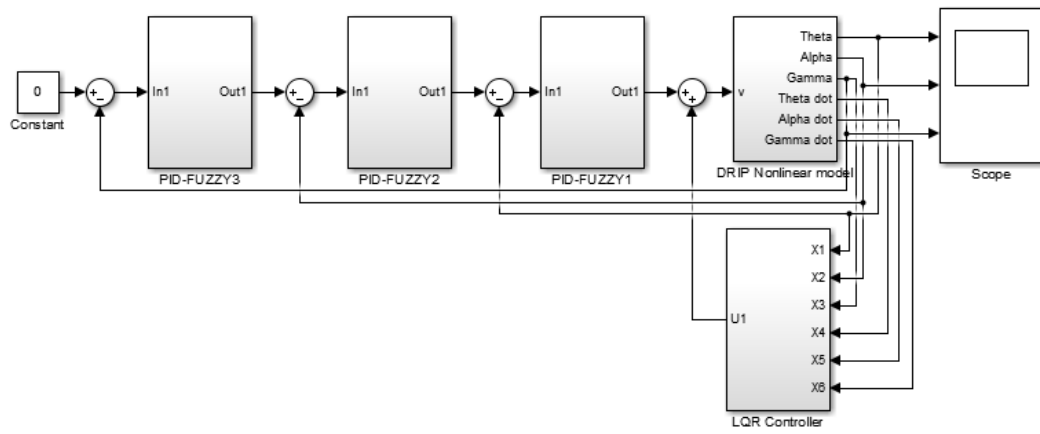


Figure 3.4 Hybrid Cascade PID-Fuzzy/LQR Controllers for Double Rotary Inverted Pendulum

CHAPTER FOUR: Results and Discussion

4.1 Introduction

The simulation results are presented in this chapter. The results include open loop response for the derived dynamic model, the stabilization control and disturbance rejection analysis. At the end of the chapter the comparisons between the proposed controllers will be presented.

4.2 Open loop responses

Visual matlab simulations of open loop responses for the DRIP are represented in this section. As expected from the behavior of the system under consideration, which is unstable, a little disturbance will lead the open-loop system to move from the unstable equilibrium and fall to the inverted position, which is the stable equilibrium of the system. The performance of the DRIP model, at the point when there is no control contribution to the system, as can be seen in Figures 4.1 to 4.3.

In Figure 4.2, the open loop response of the DRIP due to a unit step input is portrayed. The obtained result indicates that without control, the motor carrying the arm rotates continuously. It simply means bounded input produces unbounded (infinite) output which clearly reflects the behavior of an unstable system.

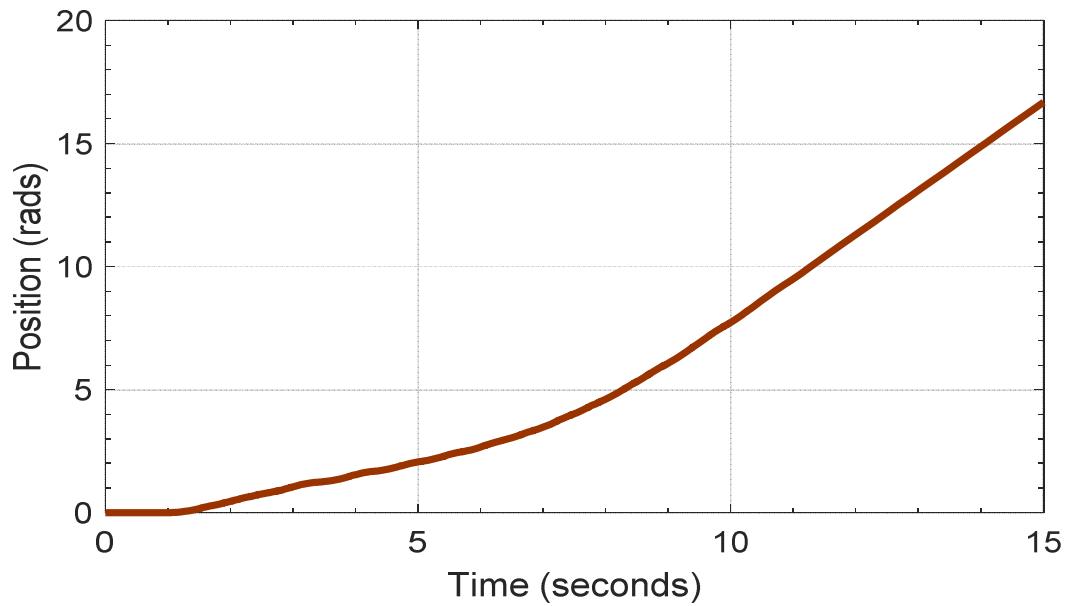


Figure 4.1 Rotary arm open loop response

The open loop step response of the lower and upper pendulums obtained by the MATLAB function is presented in Figure 4.2 and 4.3 respectively. In the dynamic modeling initially, the pendulum is considered in the inverted upward position and represented by 0 radian (Gupta and Dewan 2019). As there is no any control acting on the DRIP, the injection of the step signal moves the arms from an arbitrary position and brings the pendulum down from its vertically upward inverted position to a position around 3.142 radian away which is the stable equilibrium of the DRIP. As can be seen the natural response of the two pendulums departs to zero as time approaches around 11 second.

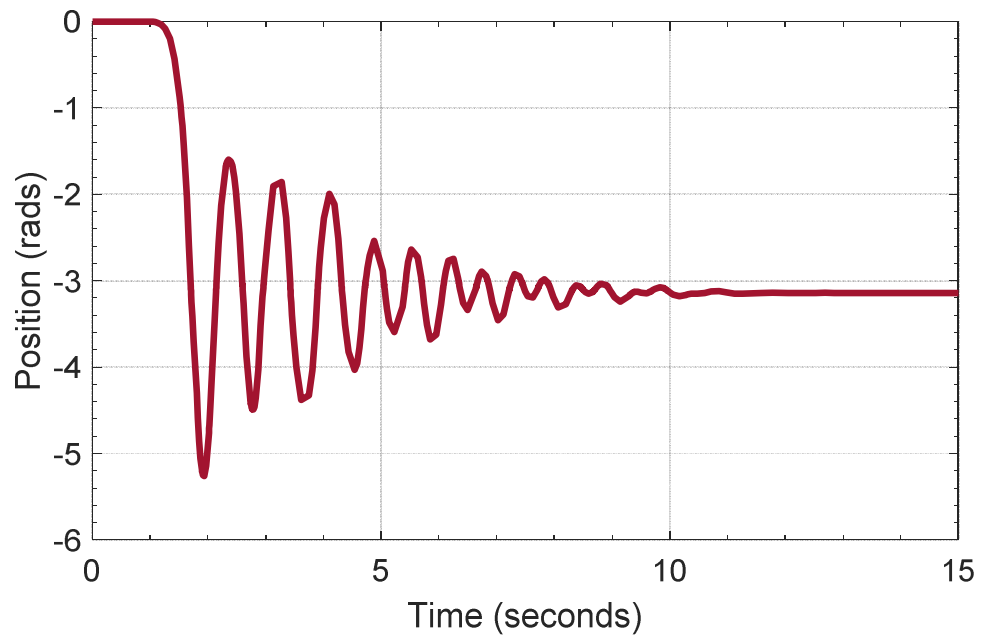


Figure 4.1 Lower pendulum open loop response

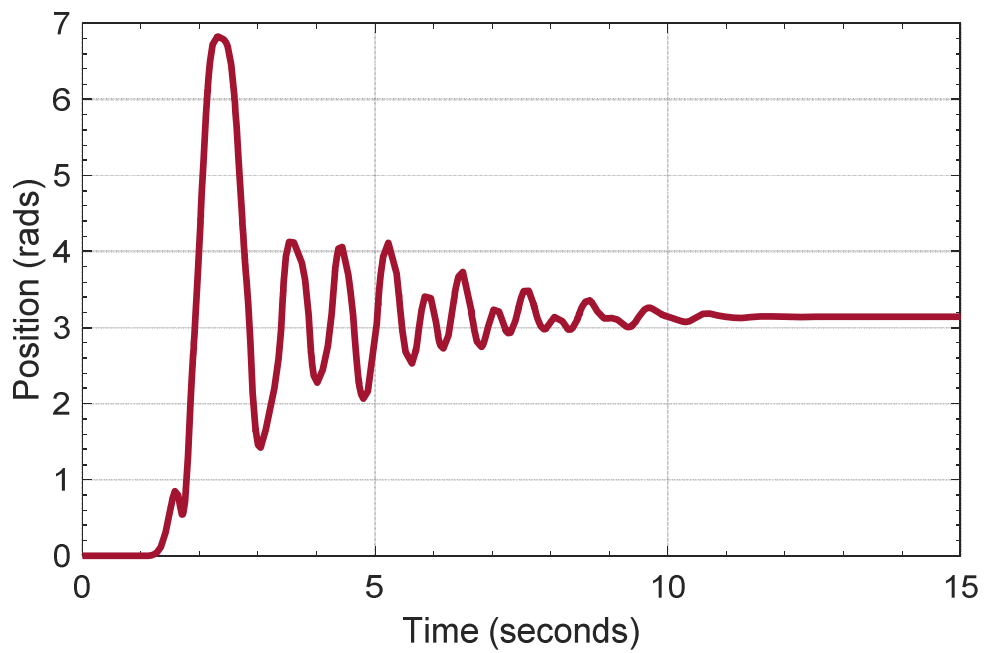


Figure 4.2 Upper pendulum open loop response

4.3 Stabilization control using cascade FPID and LQR

In this segment, stabilization control of DRIP using cascade FPID and LQR controllers has been analyzed.

Figure 4.4 to 4.6 show the simulation results of the arm angle, lower pendulum angle and upper pendulum angle when only FPID and LQR controllers are acting independently.

From Figure 4.4, the two controllers try to stabilize the arm of the DRIP. The LQR controller was able to stabilize the arm in 25.3 seconds with higher overshoot of 9.549% compared to FPID controller as shown with dotted line of the Figure. However, the FPID controller was able to stabilize the rotary arm in 34.7 seconds with overshoot of 1.030%. Impliedly, the controllers were not robust enough for the DRIP.

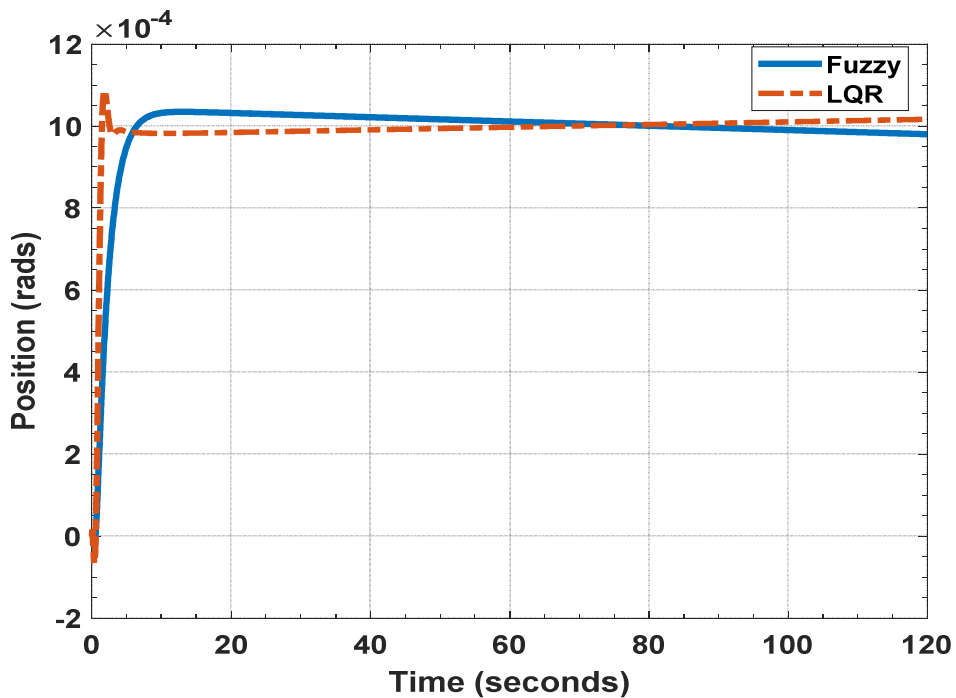


Figure 4.4 Arm angular position

As appeared in Figure 4.5, the simulation outcome for the lower pendulum's angle revealed that the two methodologies give a good performance to control the system. The pendulum's angle converge to the desired zero position. The controllers stabilize the system at nearly the same time. But the FPID controller performs better with smaller overshoot of 1.890% than the LQR controller having overshoot of 36.301%. In this way, the FPID has performed better than the LQR controller.

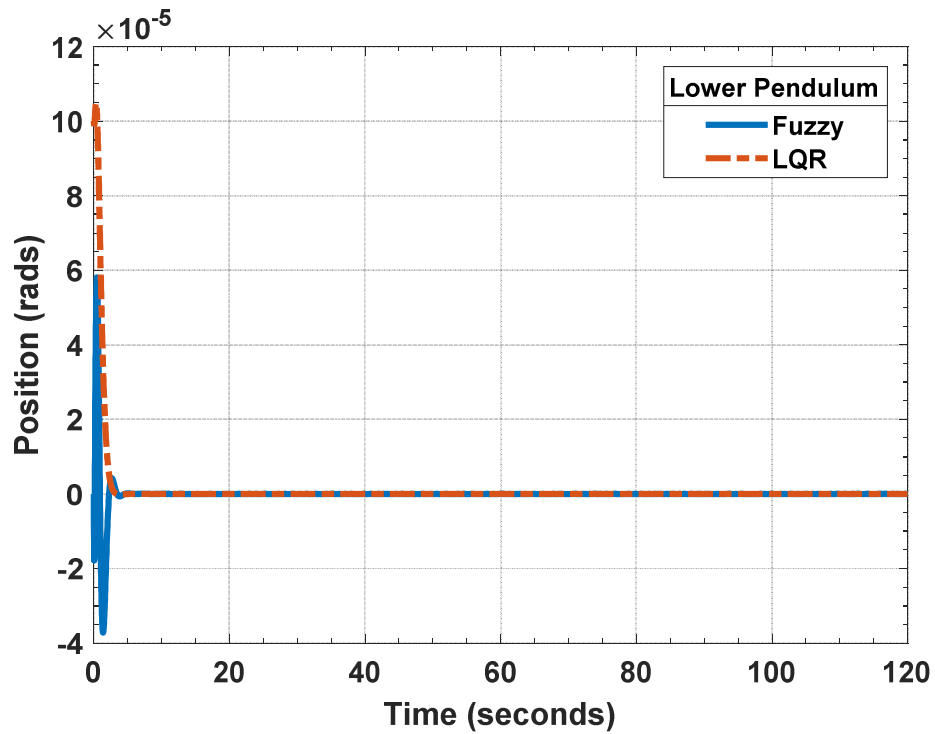


Figure 4.5 Lower Pendulum Angular Position

From Figure 4.5, the simulation outcome for the upper pendulum's angle revealed that the two methodologies give a good performance in controlling the system. The pendulum's angle converge to the desired zero position. The FPID controllers stabilize the system faster than the LQR controller. More so, the FPID controller performs better with smaller overshoot of 2% than the LQR controller having overshoot of 42.143%. Therefore, the FPID has performed better than the LQR controller.

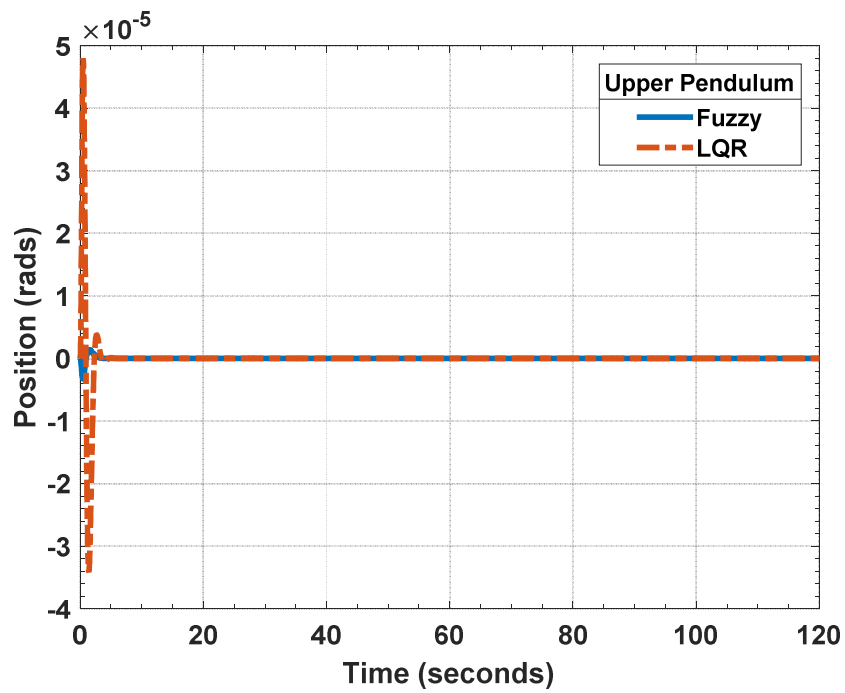


Figure 4.6 Upper pendulum angular position

The results obtained from the implementation of each controller are illustrated in Figures 4.7 and 4.8.

Figure 4.7 presents the control signal of the FPID controller. The magnitude of the signals is small and practically realize.

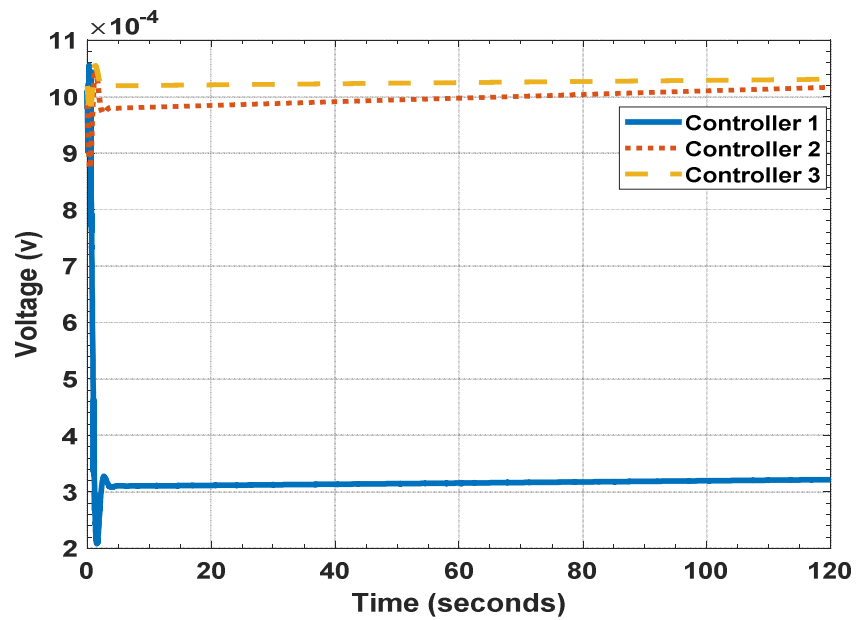


Figure 4.7 Fuzzy controller output signal

In Figure 4.8 the output signal of the LQR controller is presented. The magnitude of the signals is smaller than that of the FPID controller. Hence, in terms of control efforts, LQR control is better than the FPID controller.

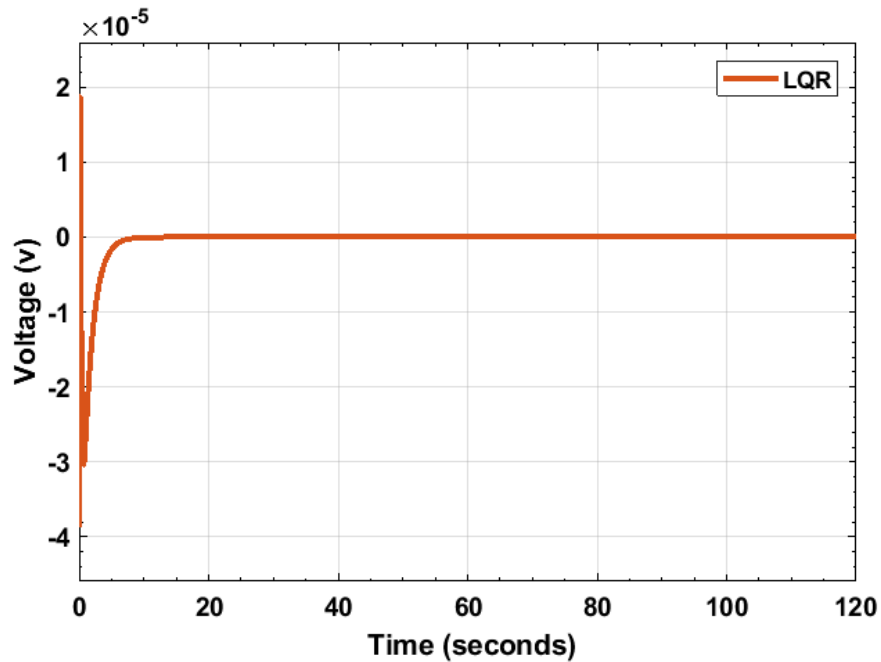


Figure 4.8 LQR controller output signal

4.4 Performance indices

The output characteristic obtained from the implementation of FPID and LQR controllers are illustrated in Table 4.1. From the table, it is evident that based on the performance indices considered, FPID controller perform better than the LQR controller. However, the general performance is not robust enough; hence a more enhanced control strategy is required. This is portrayed in the following section.

Table 4.1 Performance Indices for FPID and LQR controller

Controllers	System Output Characteristics				
	Rise Time (s)	Settling Time (s)	Overshoot (%)	Undershoot (%)	Steady State Error
Arm LQR	0.688	25.300	9.549	1.469	-0.201
Arm Fuzzy	3.700	34.700	1.030	2.195	0.001
Lower Pendulum LQR	0.747	6.200	36.301	-0.766	-0.010
Lower Pendulum Fuzzy	0.331	5.210	1.890	2.577	0.002
Upper Pendulum LQR	1.327	7.901	42.143	-0.354	-0.020
Upper Pendulum Fuzzy	0.333	5.940	2.010	2.078	0.2002

4.5 Stabilization control using cascade hybrid FPID/LQR and hybrid PID/LQR

This section elaborates the details of the verdicts which have been yields through the employment of the proposed hybrid control strategy. A cascade hybrid FPID/LQR and hybrid PID/LQR is considered for the stabilization control of DRIP in this study. Several simulations are performed to investigate and compare controllers' convergence characteristics. As it can be seen in simulations in Figures 4.9 to 4.11, though all controllers can stabilize the DRIP, FPID/LQR controller has better performance characteristics, showing that the proposed FPID/LQR model has a superior robust performance. The performance characteristics considered are; the rise time, settling time, overshoot, undershoot and steady state error.

Simultaneously, we can also find from Figures 4.12to4.15 control efforts of the proposed controllers.

The sequences of verdicts are organized as follows:

As can be seen from Figure 4.9, the two proposed control strategy were able to control the rotary arm. Hybrid PID/LQR controller has higher overshoot of 0.538% as shown with dotted

line. In terms of all the performance indices considered, the proposed hybrid FPID/LQR controller performs better than the hybrid PID/LQR.

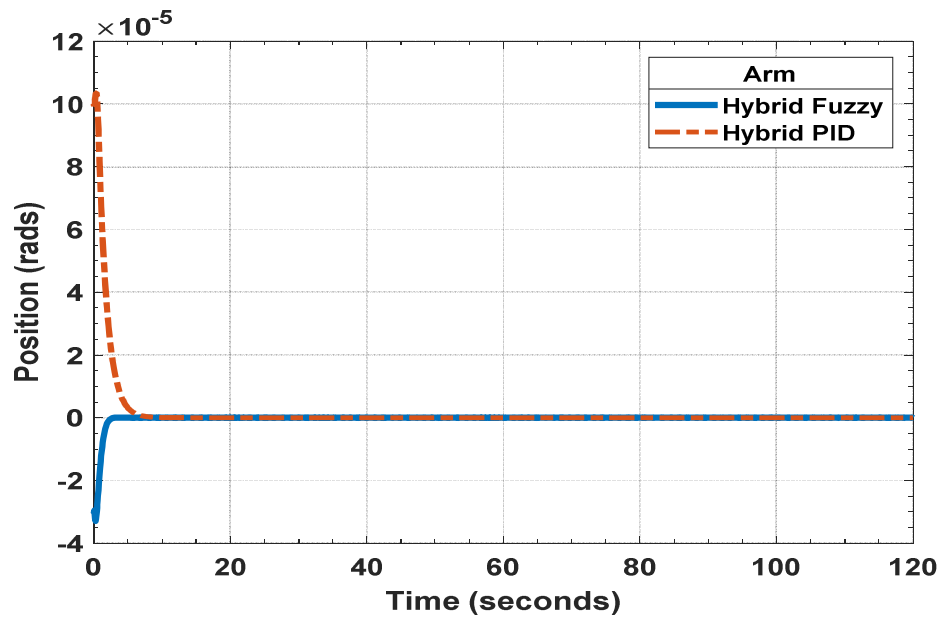


Figure 4.9 Hybrid controlled arm angle

Figure 4.10 shows the simulation result for the performance of the proposed controllers in controlling the angular position of the lower pendulum of the DRIP. The both controllers were capable to maintain the pendulum in an inverted upward position. However, the proposed hybrid FPID/LQR performed better than hybrid PID/LQR in relations to all the performance characteristics considered.

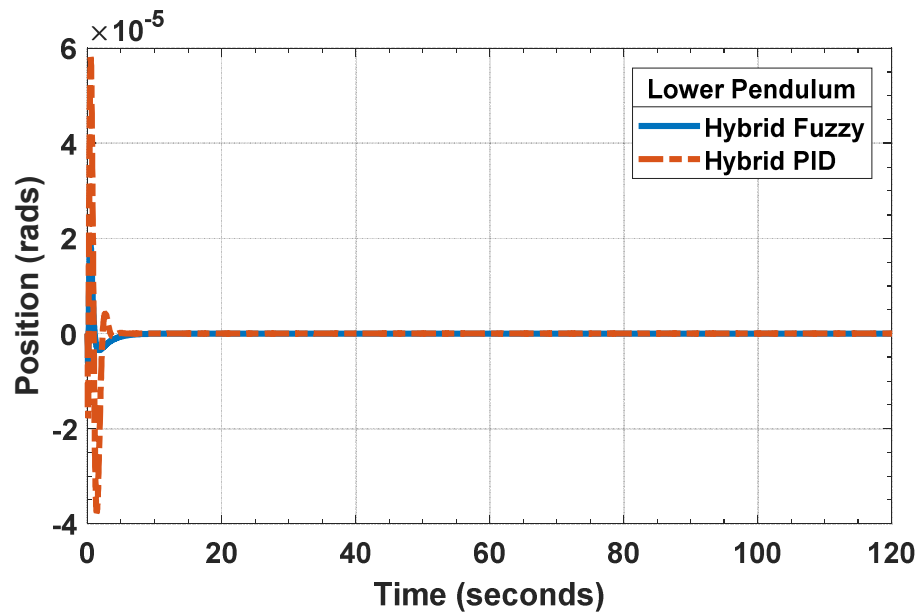


Figure 4.10 Hybrid controlled lower pendulum angle

Figure 4.11 shows the simulation result for the performance of the proposed controllers in controlling the angular position of the upper pendulum of the DRIP. The both controllers were capable to maintain the pendulum in an inverted upward position. We can see that both approaches deliver overwhelming results in controlling the system. All links converges at the set reference (0 rad). However, the proposed hybrid FPID/LQR performed better than hybrid PID/LQR in relations to all the performance characteristics considered.

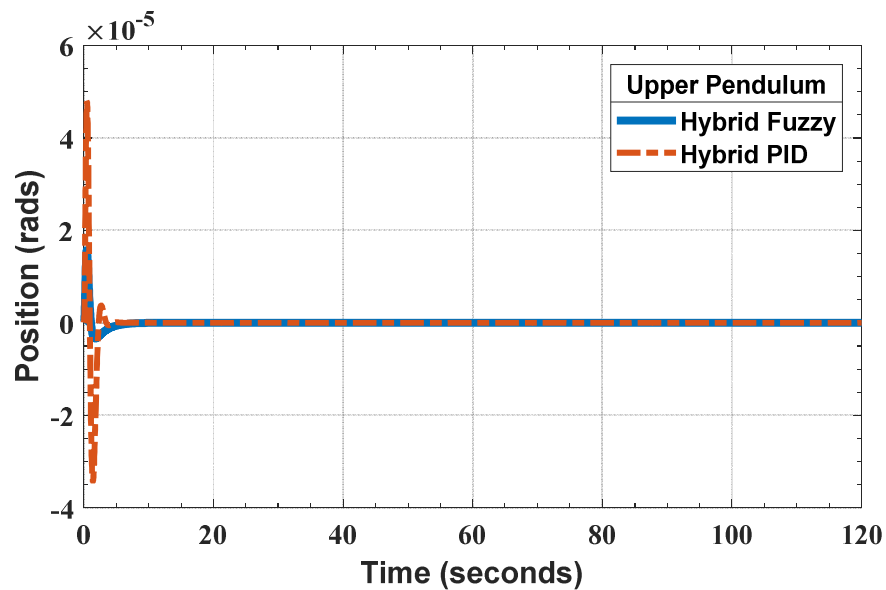


Figure 4.11 Hybrid controlled upper pendulum angle

Figure 4.12 to 4.15 describes the individual controller output (control signals) and that of the hybrid controller output. It can be observed that, the overall control effort has been comparatively improved with the one obtained in the prior section of this chapter.

The findings obviously indicate that by mixing the two in hybrid topology, the quality of the FPID and LQR controllers outlined in the prior chapter is enhanced. However, hybrid PID/LQR has less control effort than the proposed hybrid FPID/LQR controller.

In Figure 4.12, the output of the first controllers is presented. This is the signal that is serving as the input to the hybrid controllers. Each of these controllers is showing a very small control effort requirement to stabilize the DRIP system.

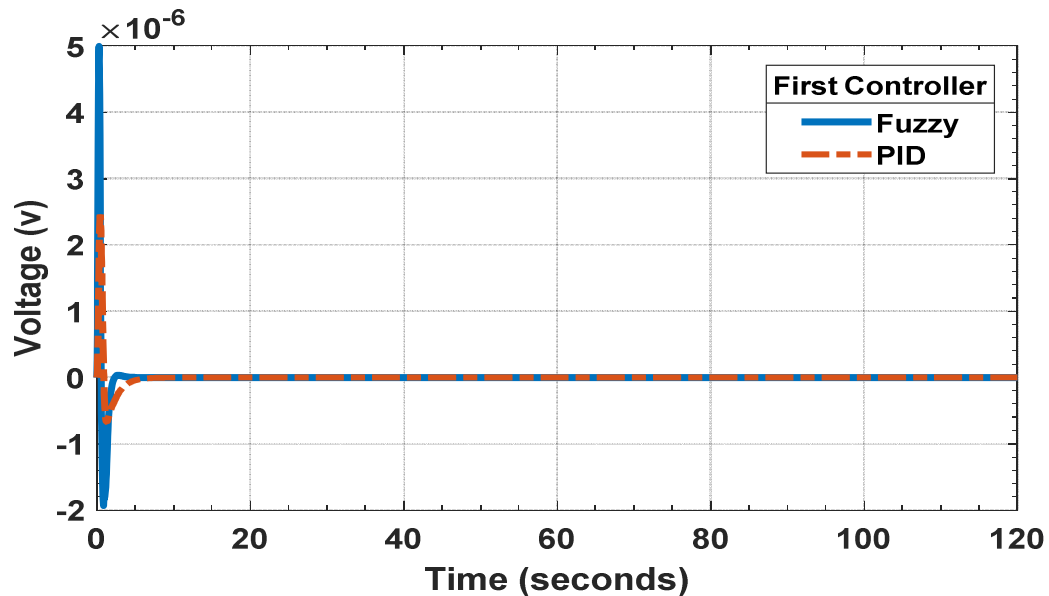


Figure 4.12 Outputs of the first controller

In Figure 4.13, the output of the second controllers is presented. This is the signal that is serving as the input to the first controllers. Each of these controllers is showing a very small control effort requirement to stabilize the DRIP system.

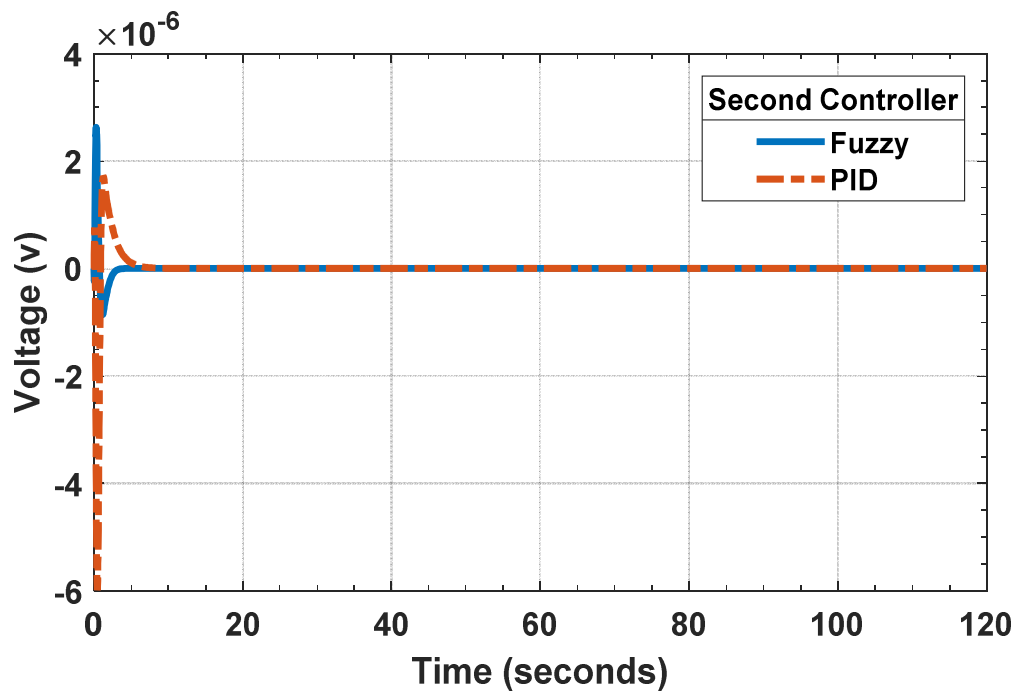


Figure 4.13 Outputs of the second controller

In Figure 4.14, the output of the third controllers is presented. This is the controller that reference signal is fed into. Its output is the input to the second controllers. Each of these controllers is showing a very small control effort requirement to stabilize the DRIP system.

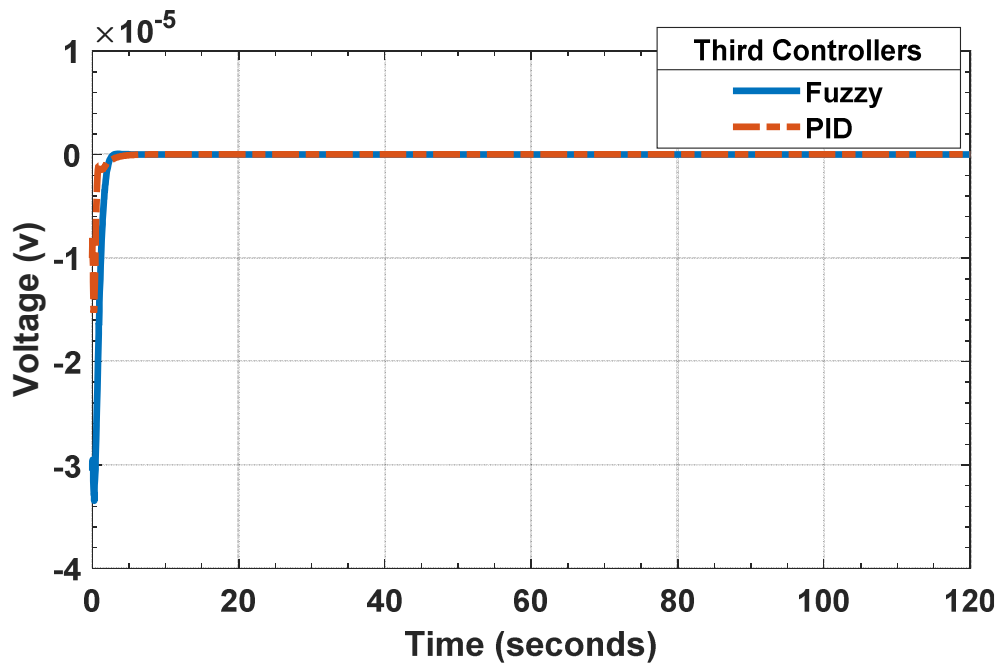


Figure 4.14 Outputs of the third controllers

In Figure 4.15, the output of the hybrid controllers is presented. This is the signal that is serving as the input to the system. Each of these controllers is showing a very small control effort requirement to stabilize the DRIP system.

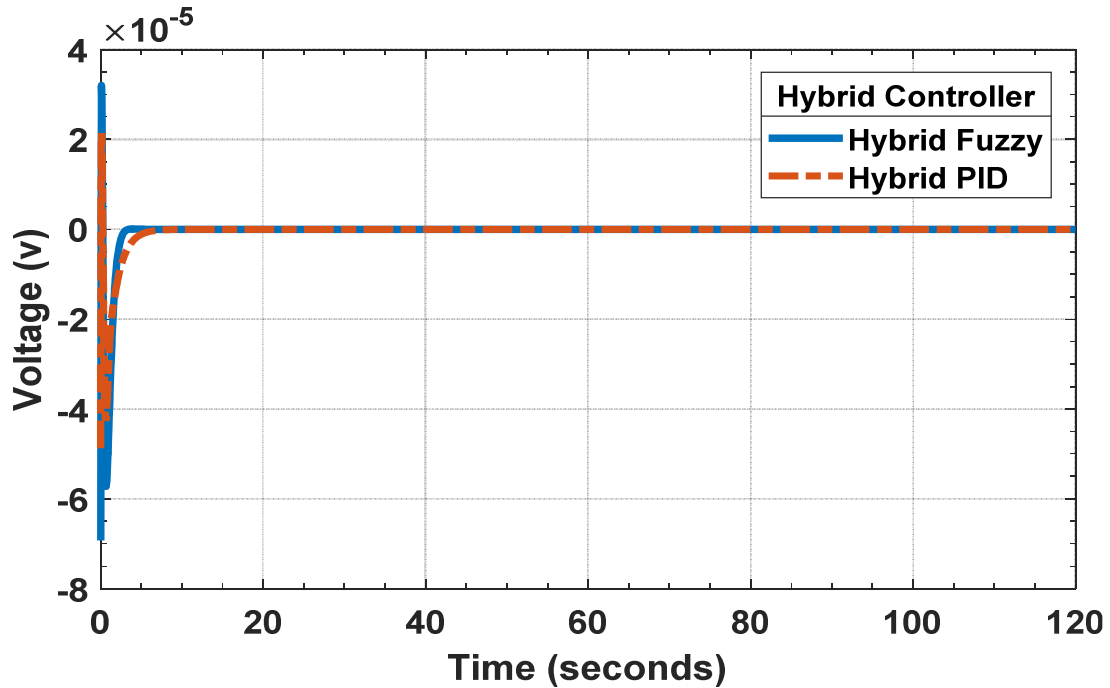


Figure 4.15 Outputs of the hybrid controller

4.6 System output characteristics

The response parameters, including rise time (rt), settling time (st), overshoot (os) and steady state error (ss) for this study are shown in Table 4.2 to 4.4. It is pretty straightforward to read from table that from the performance indices considered, both approaches deliver overwhelming results in controlling the system. However, the proposed hybrid FPID/LQR has exhibited a better performance.

Table 4.2 Arm Control Performance Indices

Controllers	System Output Characteristics				
	Rise Time (s)	Settling Time (s)	Overshoot (%)	Undershoot (%)	Steady State Error
Arm Hybrid PID-LQR	0.263	5.142	0.538	1.302	0.00012
Arm Hybrid Fuzzy-LQR	0.201	2.321	0.000	-0.00023	0.000

Table 4.3 Lower Pendulum Control Performance Indices

Controllers	System Output Characteristics				
	Rise Time (s)	Settling Time (s)	Overshoot (%)	Undershoot (%)	Steady State Error
Lower Pendulum Hybrid PID-LQR	0.193	3.921	0.557	2.083	-0.000033
Lower Pendulum Hybrid Fuzzy-LQR	0.300	2.893	0.0074	0.00000101	0.000

Table 4.4 Upper Pendulum Control Performance Indices

Controllers	System Output Characteristics				
	Rise Time (s)	Settling Time (s)	Overshoot (%)	Undershoot (%)	Steady State Error
Upper Pendulum Hybrid PID-LQR	0.200	3.443	0.194	0.714	-0.00015
Upper Pendulum Hybrid Fuzzy-LQR	0.311	3.028	0.0012	0.00000107	0.000

Figure 4.17 to 4.19 shows the performance of the hybrid FPID/LQR controller when an impulse disturbance is applied to the DRIP. As can be viewed from these figures, hybrid FPID/LQR was able to reject the disturbance and maintain the positions of all the three links within the specified set points (0 rad)

4.7 Test for robustness

The results of both pendulums and arm under disturbance using hybrid FPID/LQR and PID/LQR controllers are presented in this section. In order to evaluate robustness of the

proposed controllers, a pulse disturbance is added to the process at the 30th second. Figure 4.17 to 4.22 displayed the performance of the proposed controllers.

In Figure 4.17 the result of the rotary arm using the proposed hybrid FPID/LQR controller under disturbance. From the result, the rotary arm oscillates due to the applied disturbance; yet the controller is able to bring the arm to the stable position within short period of time.

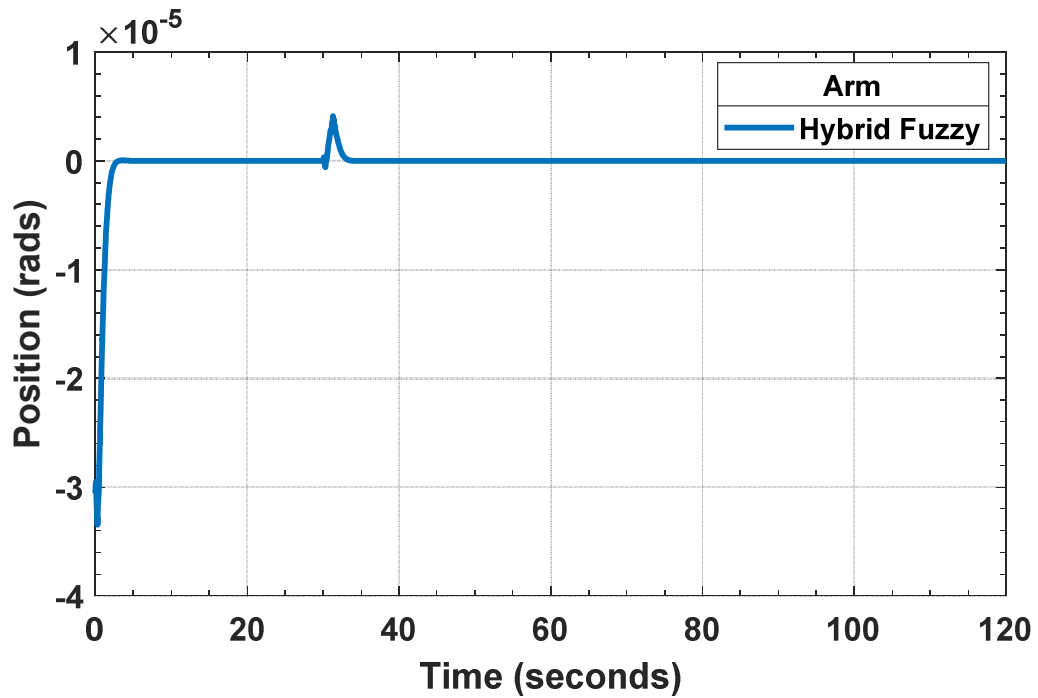


Figure 4.16 Hybrid FPID robustness: Arm response

As the impulse disturbance is injected into the DRIP, the disturbance force makes the lower pendulum to deviate from the stabilized position as shown in Figure 4.18. However, the proposed hybrid FPID/LQR controller is able to re-stabilize pendulum to the upright position within short period of time.

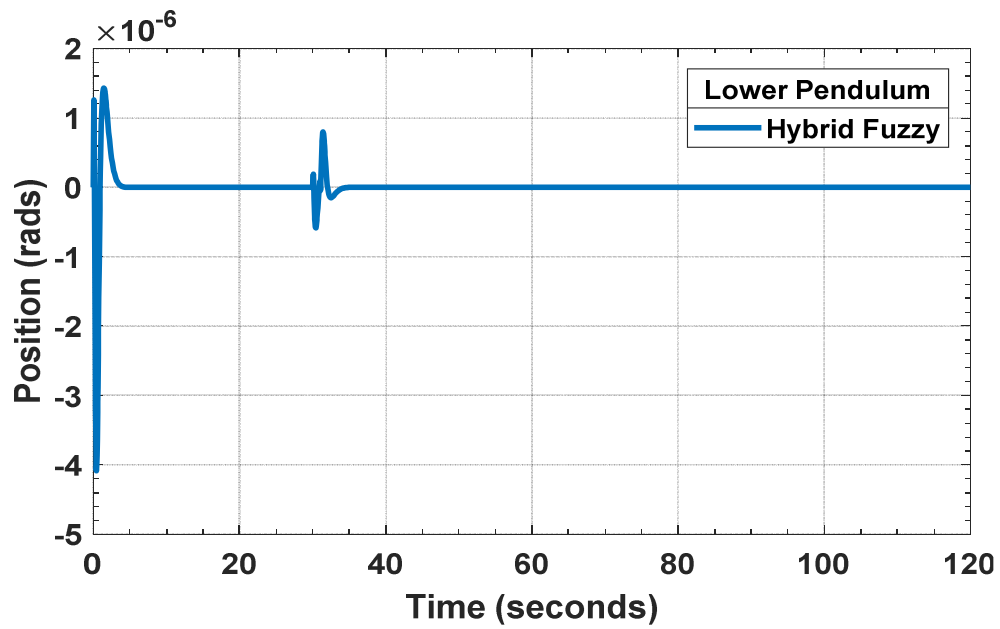


Figure 4.17 Hybrid FPID test for robustness: Lower pendulum

As can be seen in Figure 4.19, the upper pendulum angle change position as the impulse disturbance is injected into the system. But, the proposed hybrid FPID/LQR controller is able to bring back the pendulum to the stabilized upright position within short period of time.

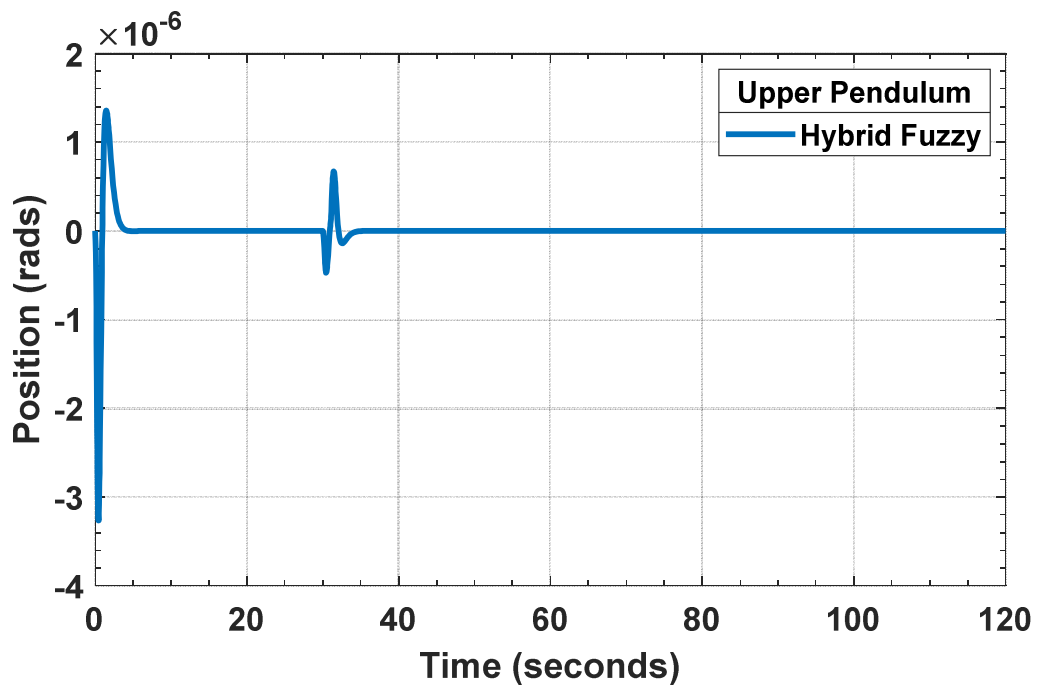


Figure 4.18 Hybrid FPID test for robustness: Upper pendulum angle

Figure 4.19 shows the result of the rotary arm using the hybrid PID/LQR controller under disturbance. From the result, the rotary arm rotates continuously due to the applied disturbance; the rotary arm now produced unbounded output. From the result it is evident that the hybrid PID/LQR cannot stabilize the system under the disturbance.

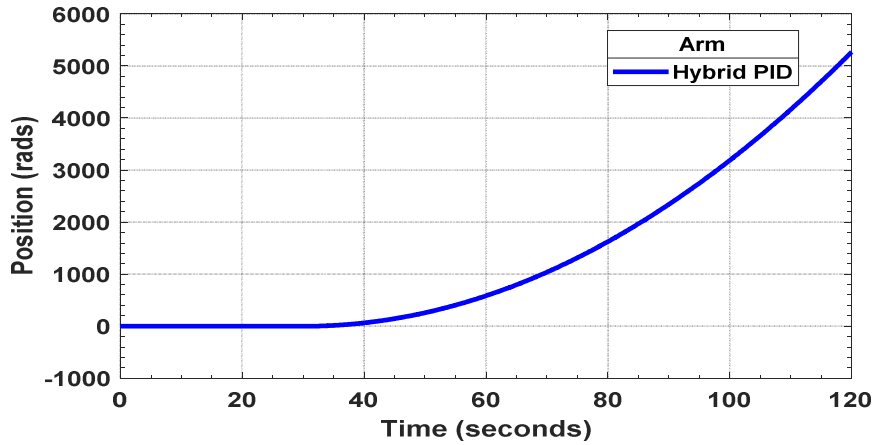


Figure 4.19 Hybrid PID test for robustness: Arm angle

As the impulse disturbance is injected into the DRIP, the disturbance force makes the lower pendulum to move from the 0 radian (inverted position) tilt angular position to a position 3.142 radian away as shown in Figure 4.21. It shows that the pendulum falls to the stable equilibrium. From the result, the hybrid PID/LQR fails to maintain the stabilize system under disturbance.

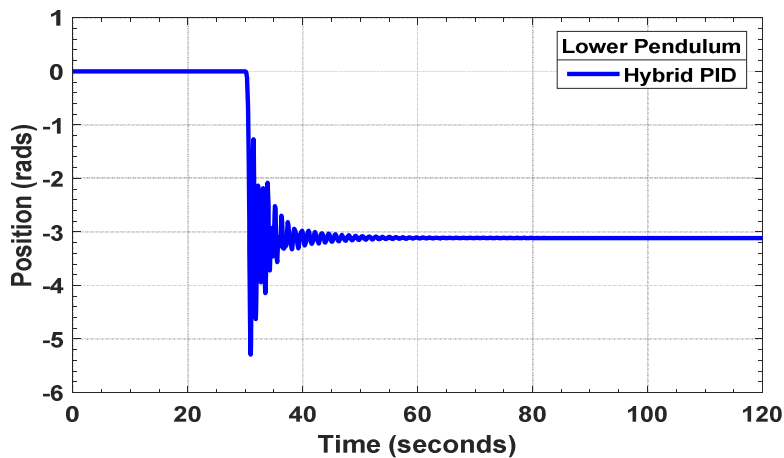


Figure 4.20 Hybrid PID test for robustness: Lower pendulum

As shown in Figure 4.22, the upper pendulum departs from the inverted position and fall to its downward stable equilibrium as soon as the impulse disturbance is injected into the system. Obviously, the hybrid PID/LQR fails to maintain the stabilize system in the present of disturbance.

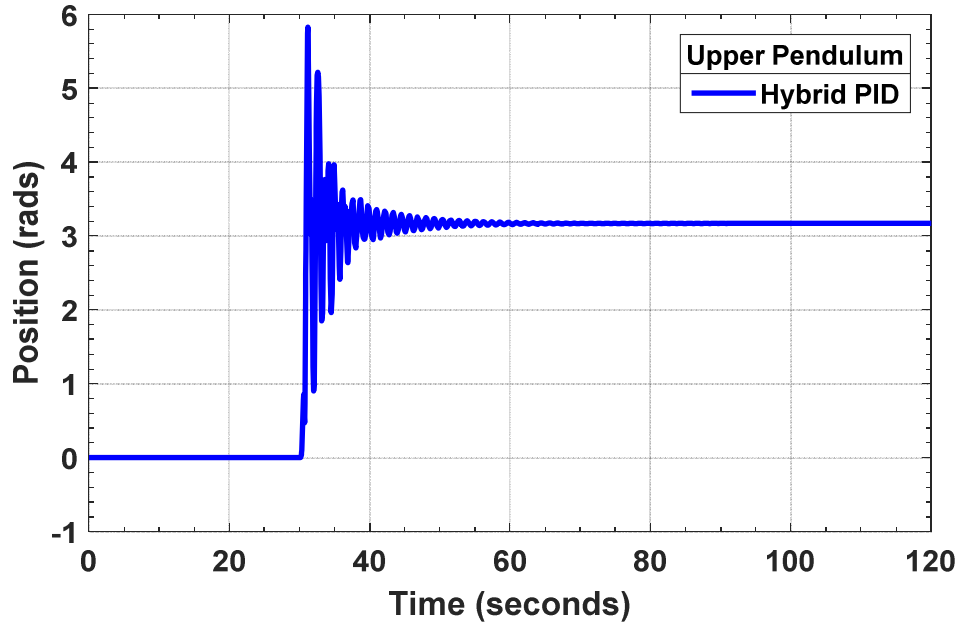


Figure 4.21 Hybrid PID test for robustness: Upper pendulum

So far, the above results indicate the effectiveness and robustness of the hybrid FPID/LQR controllers in rejecting the disturbance.

Besides, the Figures below describe the individual controller output (control signals) and that of the hybrid controller output when disturbance is applied to the system. The results obtained shows that, for the proposed hybrid FPID/LQR, the control signal is still within the supply capacity. Simulation results shown in Figures 4.23 to 4.26 illustrate the robustness and effectiveness of the proposed hybrid FPID/LQR controller subject to the disturbance. The results motivate the consideration of the proposed hybrid FPID/LQR procedure as a suitable algorithm for the stabilization control of DRIP and other unstable, nonlinear and underactuated mechanical system. Contrariwise, from Figures 4.27 to 4.30, the outputs of the hybrid PID/LQR controller overshoot beyond the supply capacity to the value that

is practically unrealizable. Therefore, hybrid FPID/LQR algorithm cannot stabilize the system under the disturbance.

The system control input fluctuates due to the applied impulse disturbance is shown in Figure 4.22. Still, it is within the supplied capacity. It means the system stability can be maintained with the proposed hybrid FPID/LQR control algorithm when subjected to disturbance.

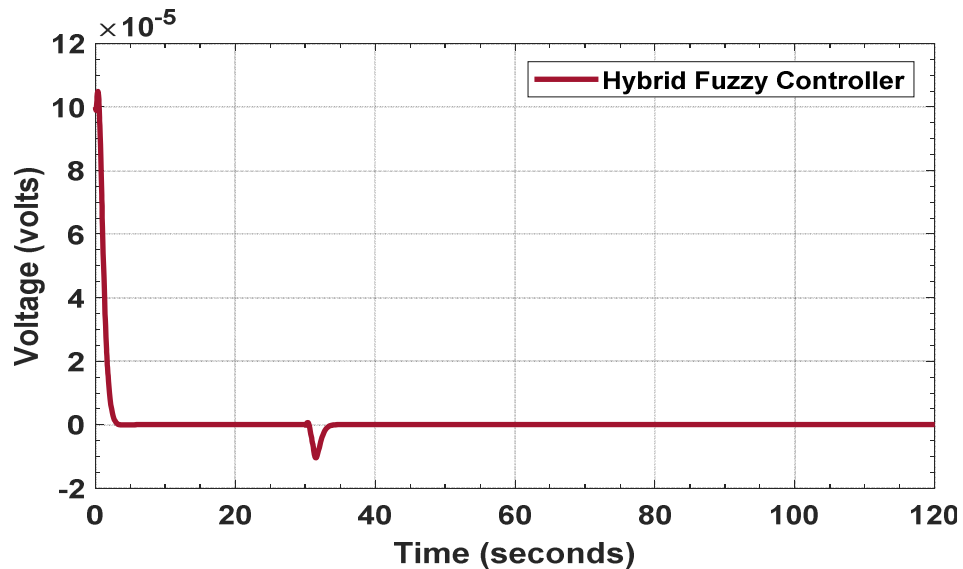


Figure 4.22 Output of the hybrid fuzzy controller under disturbance

Figure 4.23 shows the output of the first controller fluctuates due to the applied impulse disturbance. Using the proposed hybrid FPID/LQR method, the control signal deviation is quickly driven back to within the supplied capacity boundary.

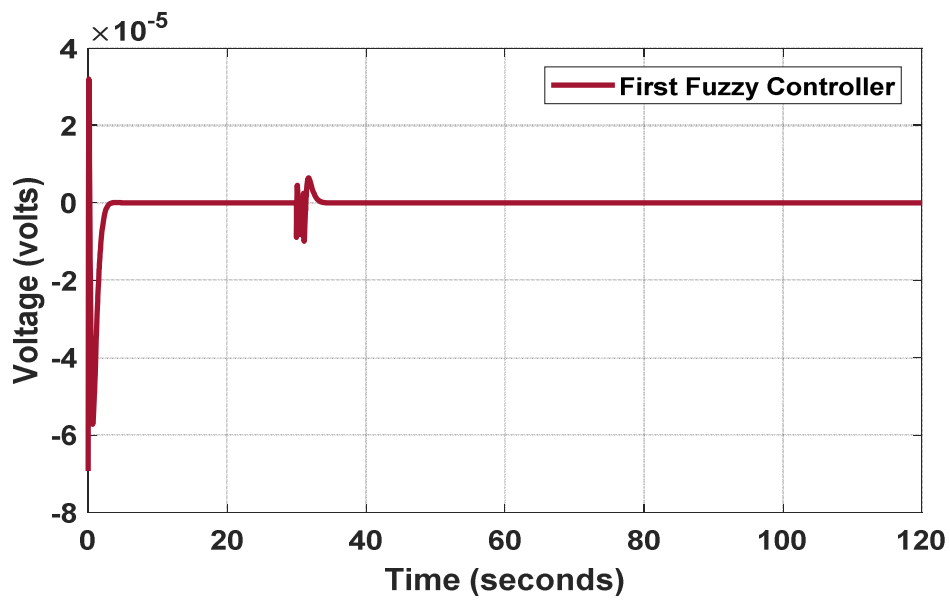


Figure 4.23 Output of the first fuzzy controller under disturbance

From Figure 4.25 the output of the second controller fluctuates due to the applied impulse disturbance. The control signal deviation is quickly driven back to within the supplied capacity boundary by the action of the proposed hybrid FPID/LQR control strategy.

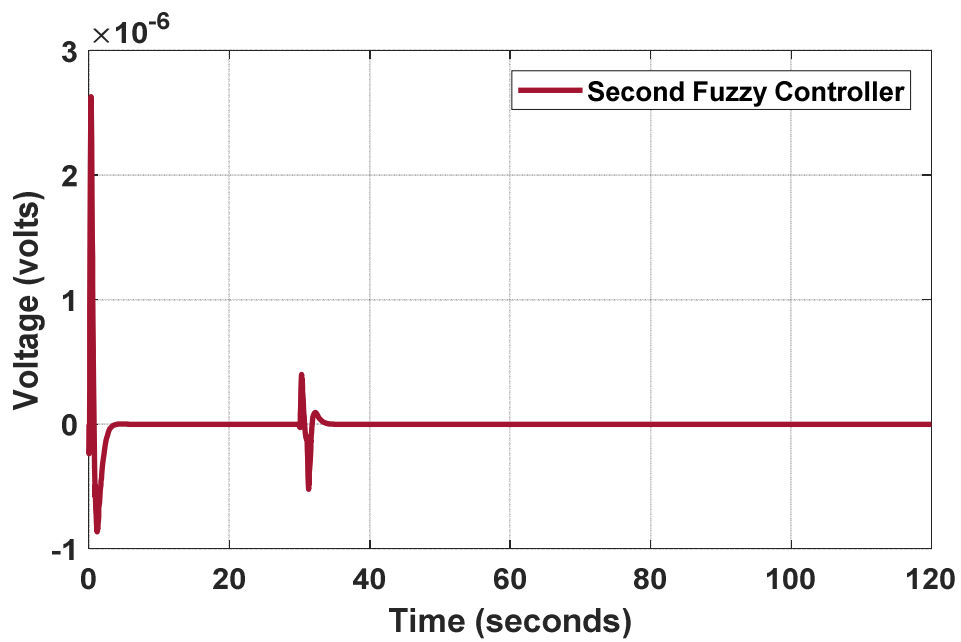


Figure 4.24 Output of the second fuzzy controller under disturbance

Also Figure 4.26 presents the output of the third controller fluctuation due to the applied impulse disturbance. The control signal deviation is quickly driven back to within the supplied capacity boundary by the action of the proposed hybrid FPID/LQR control strategy.

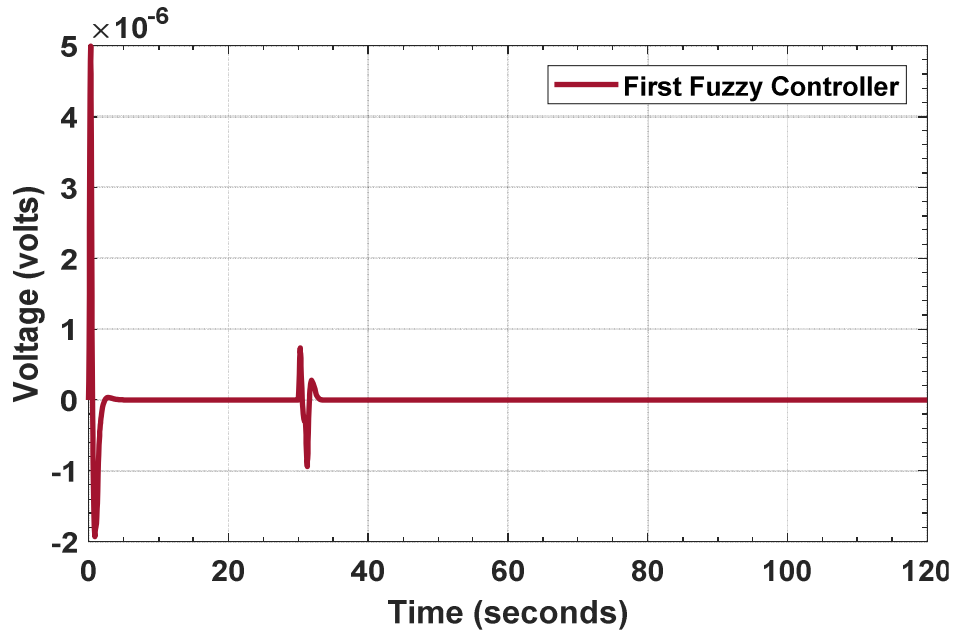
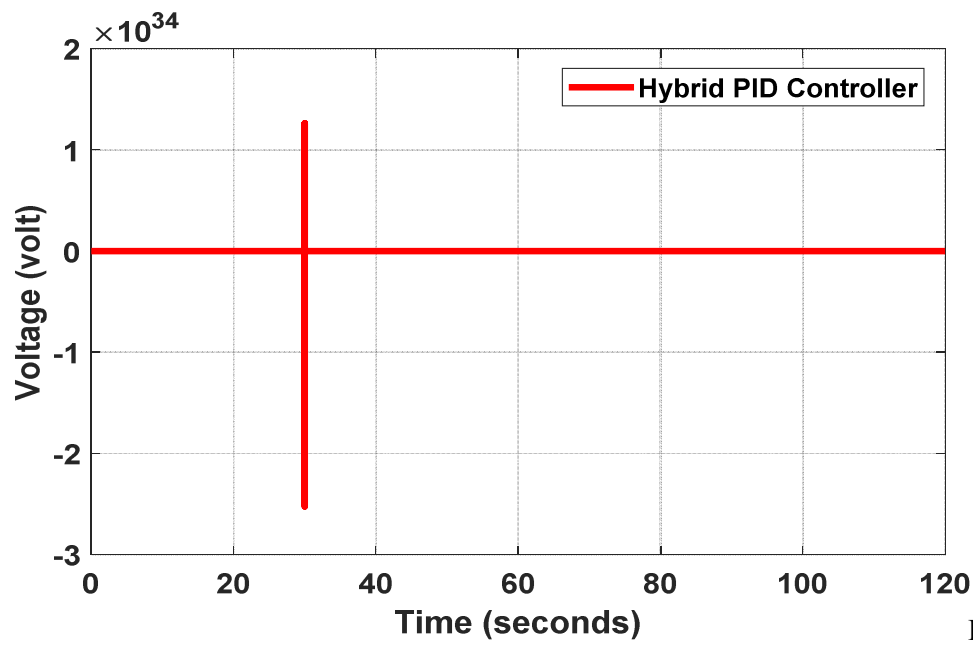


Figure 4.25 Output of the third fuzzy controller under disturbance

Figure 4.27 shows the control signal deviation of the hybrid PID/LQR controller. It overshoots to thousands of voltage beyond the supply capacity which is practically unrealizable. Therefore, hybrid FPID/LQR algorithm cannot be regarded as the control method for stabilization control of DRIP system in the presence of disturbance.



Figure

4.26 Output of the hybridPID controller under disturbance

Figure 4.28 also shows the control signal deviation of the first controller of the hybrid PID/LQR control algorithm. It overshoots too to thousands of voltage beyond the supply capacity which is practically unrealizable.

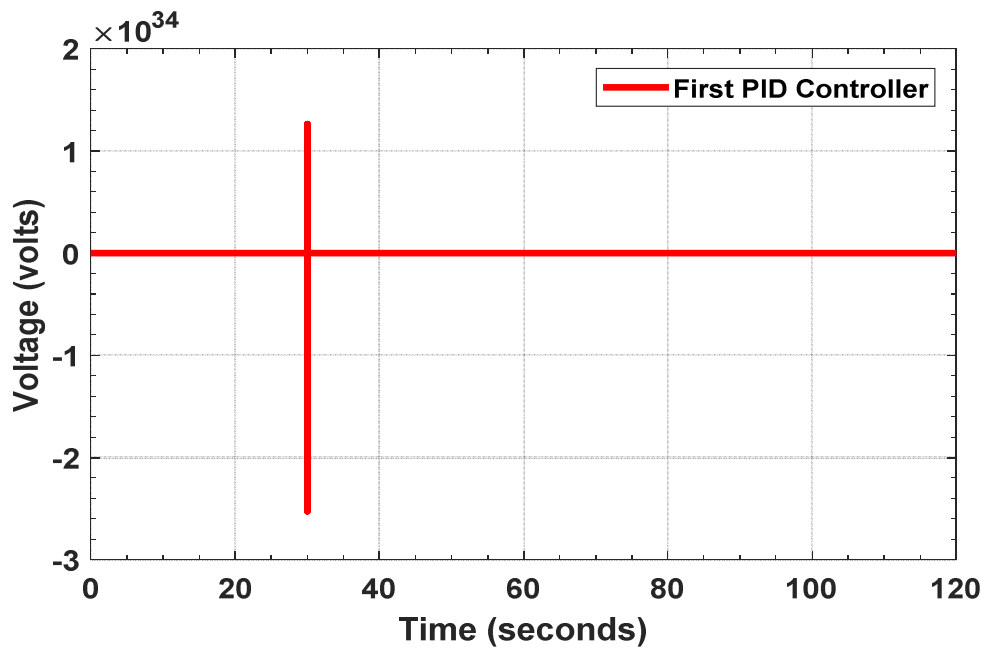


Figure 4.27 Output of the firstPID controller under disturbance

Similarly, Figure 4.29 also shows the control signal deviation of the second controller of the hybrid PID/LQR control algorithm. It overshoots too to thousands of voltage beyond the supply capacity which is practically unrealizable.

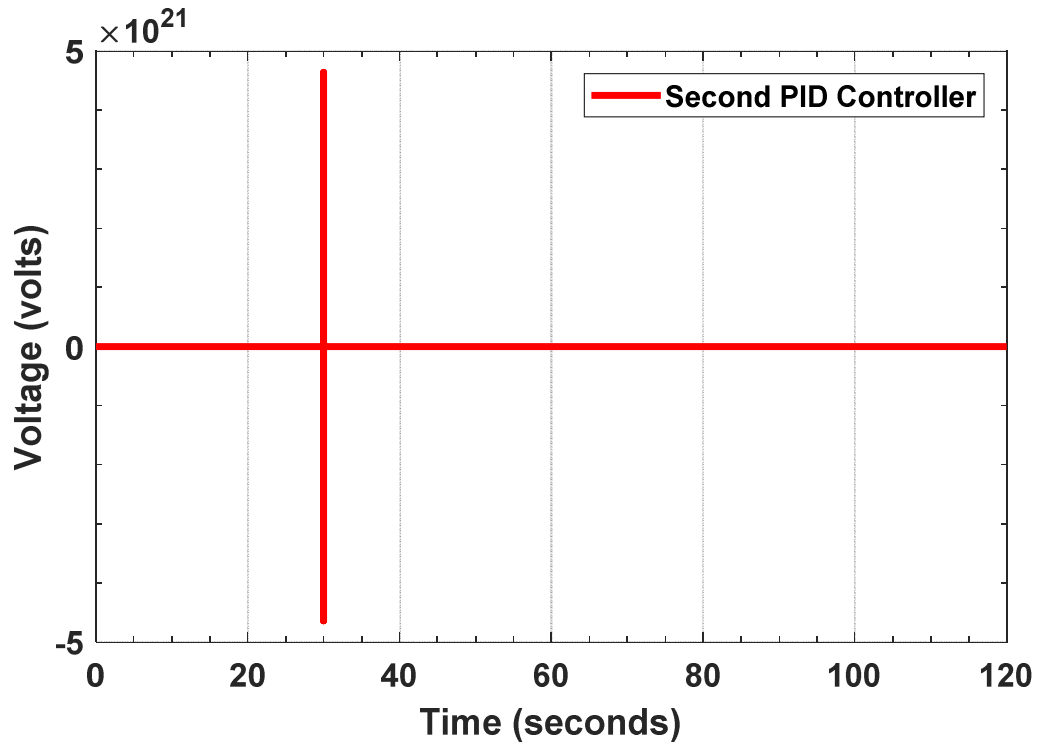


Figure 4.28 Output of the secondPID controller under disturbance

Likewise, in Figure 4.30 the control signal deviation of the third controller of the hybrid PID/LQR control algorithm is presented. As well, it overshoots to thousands of voltage beyond the supply capacity which is practically unrealizable.

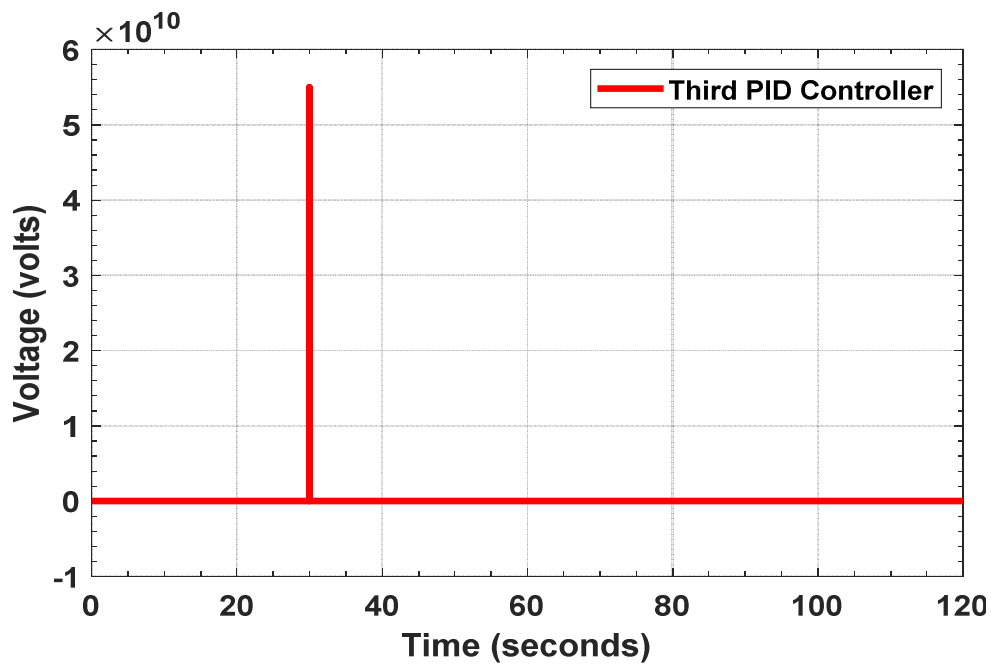


Figure 4.29 Output of the third PID controller under disturbance

.However, taking into account the output of the hybrid PID controllers contained in b part of Figures 4.21 to 4.24, the energy needed to control the DRIP in the presence of disturbance is reasonably high and the controller cannot be realized implicitly.

4.8 Validation of Results

The results found were compared with the published work for the purpose of validation. The proposed publication by (Aranda-Escolástico et al. 2016) considered. (Aranda-Escolástico et al., 2016) compare the performances of LQR and Fuzzy controllers.

Table 4.5 Result Validation Using Performance Indices

Performance Indices	Present Study (Hybrid Fuzzy-LQR)			Escolastico et.al (Fuzzy controller)		
	Arm	Lower Pendulum	Upper Pendulum	Arm	Lower Pendulum	Upper Pendulum
Overshoot (%)	0.000	0.0074	0.0012	2.110	2.390	3.001
Undershoot (%)	-0.00023	0.00000101	0.000001073	2.523	3.067	2.718
Rise time (s)	0.201	0.300	0.311	2.990	1.531	1.883
Settling time (s)	2.321	2.893	3.028	13.78	3.010	4.430
Steady state error	0.000	0.000	0.000	0.009	0.056	0.01

It can be seen from Table 4.5 that, both proposed Hybrid FPID-LQR controller and Hybrid PID-LQR controller have outperformed the published controllers based on the performance indices considered in this research.

CHAPTER FIVE: Conclusion

5.1 Introduction

A hybrid controller for stabilization control of DRIP is proposed in this study by combining the cascade FPID control method with the LQR control technique. The proposed controller aims to control the arm, lower pendulum and upper pendulum compare and its performance with hybrid of cascade PID control scheme and LQR control strategy in the absence and presence of disturbance.

The same disturbance of 0.01 was tested in the two approaches. From the results presented in chapter four, numerous findings emerge. It has been demonstrated that in the absence of disturbance, both the controllers were able to stabilize the DRIP. Though, hybrid FPID performs better than the hybrid PID controllers. 63

Simulation results demonstrate that as compared to existing controllers, the proposed hybrid control strategy offers superior transient and steady state performances. Consequently, the hybrid FPID control strategy can be regarded as a promising strategy for controlling highly nonlinear, unstable, non-minimum phase and under-actuated mechanical systems especially in the presence of noise and disturbances. The research findings from this study show consistency with regard to the objectives identified. This strategy is conceived.

5.2 Contribution of the Research

A design of hybrid FPID/LQR for nonlinear stabilization control of DRIP.

Secondly, the design of three controllers in cascade topology.

References

- Aguilar-Avelar, Carlos, and Javier Moreno-Valenzuela. 2015. "A Composite Controller for Trajectory Tracking Applied to the Furuta Pendulum." *ISA Transactions* 57: 286–94. <http://dx.doi.org/10.1016/j.isatra.2015.02.009>.
- Ajami, A., and N. Taheri. 2012. "A Hybrid Fuzzy/LQR Based Oscillation Damping Controller Using 3-Level STATCOM." *International Journal of Computer and Electrical Engineering* 3(2): 184–89.
- Al-Hadithi, B. M., Javier Barragan, A., Manuel Andujar, J., & Jimenez, A. (2012). *Fuzzy optimal control for double inverted pendulum. 2012 7th IEEE Conference on Industrial Electronics and Applications (ICIEA)*. doi:10.1109/iciea.2012.6360687
- Andújar, J. M., Irigoyen, E., & Becerra, V. M. (2018). Intelligent Control Approaches for Modeling and Control of Complex Systems. *Complexity*, 2018, 3. <https://doi.org/10.1155/2018/2090715> Editorial
- Aranda-Escolástico, Ernesto, María Guinaldo, Matilde Santos, and Sebastián Dormido. 2016. "Control of a Chain Pendulum: A Fuzzy Logic Approach." *International Journal of Computational Intelligence Systems* 9(2): 281–95.
- Aribowo, A. G., Y. Y. Nazaruddin, E. Joelianto, and H. Y. Sutarto. 2007. "Stabilization of Rotary Double Inverted Pendulum Using Robust Gain-Scheduling Control." *Proceedings of the SICE Annual Conference* (2): 507–14.
- Awtar, S., King, N., Allen, T., Bang, I., Hagan, M., Skidmore, D., & Craig, K. (2002). *Inverted pendulum systems: rotary and arm-driven - a mechatronic system design case study. Mechatronics*, 12(2), 357–370. doi:10.1016/s0957-4158(01)00075-7
- Babu, Jithin, and Elizabeth Varghese. 2015. "Stabilization of Rotary Arm Inverted Pendulum Using State Feedback Techniques." *International Journal of Engineering Research & Technology (IJERT)* 4(07): 563–68.
- Bagheri, S., Jafarov, T., Freidovich, L., & Sepehri, N. 2016. *Beneficially combining LQR and PID to control longitudinal dynamics of a SmartFly UAV. 2016 IEEE 7th Annual Information Technology, Electronics and Mobile Communication Conference (IEMCON)*. doi:10.1109/iemcon.2016.7746309
- Bai, Y., & Wang, D. (2007). Fundamentals of Fuzzy Logic Control — Fuzzy Sets, Fuzzy Rules and Defuzzifications. *Advanced Fuzzy Logic Technologies in Industrial Applications*, 17–36. doi:10.1007/978-1-84628-469-4_2
- Bao-Gang Hu, Mann, G. K. I., & Gosine, R. G. 2001. *A systematic study of fuzzy PID controllers-function-based evaluation approach. IEEE Transactions on Fuzzy Systems*, 9(5), 699–712. doi:10.1109/91.963756
- Barton, T. W. (2010). *Stabilizing the dual inverted pendulum. IFAC Proceedings Volumes*, 42(24), 113–118. doi:10.3182/20091021-3-jp-2009.00022

- Berenji, H. R. 1992. *Fuzzy Logic Controllers. An Introduction to Fuzzy Logic Applications in Intelligent Systems*, 69–96. doi:10.1007/978-1-4615-3640-6_4
- Bhargal, Narinder Singh. 2013. “Design and Performance of LQR and LQR Based Fuzzy Controller for Double Inverted Pendulum System.” *Journal of Image and Graphics* 1(3): 143–46.
<https://pdfs.semanticscholar.org/e056/4171da5581309d483589a0f5dc6504a4c3af.pdf>.
- Birkan, Akbıyık, Eksin Ibrahim, and Yesil Engin. 2005. “Evaluation of the Performance of Various Fuzzy PID Controller Structures on Benchmark Systems.” In ReaearchGate, 7.
- Boubaker, Olfa. 2013. “The Inverted Pendulum Benchmark in Nonlinear Control Theory : A Survey.” *International Journal of Advanced Robotic Systems* 10(15 Mar 2012): 9.
<https://www.semanticscholar.org/paper/The-Inverted-Pendulum-Benchmark-in-Nonlinear-A-Boubaker/52c32c18f75144d3865883c593f56bb48a5efc6d>.
- Boubaker, Olfa. 2017. “The Inverted Pendulum : History and Survey of Open and Current Problems in Control Theory and Robotics.”10.1049/PBCE111E_ch1.
- Buckley, James J., and Esfandiar Eslami. 1992. An Introduction to Fuzzy Logic and Fuzzy Sets *Advances in Soft Computing*. 1st ed. ed. Prof. Janusz Kacprzyk. Birmingham, USA: Springer US.
- Casanova, V., J. Salt, R. Piza, and A. Cuenca. 2012. “Controlling the Double Rotary Inverted Pendulum with Multiple Feedback Delays.” *International Journal of Computers, Communications and Control* 7(1): 20–38.
- Casanova, Vicente et al. 2016. “Control of the Rotary Inverted Pendulum through Threshold-Based Communication.” *ISA Transactions*: 1–10.
<http://dx.doi.org/10.1016/j.isatra.2016.01.009>.
- Cetin, Meric, and Serdar Iplikci. 2015. “A Novel Auto-Tuning PID Control Mechanism for Nonlinear Systems.” *ISA Transactions*: 1–17.
<http://dx.doi.org/10.1016/j.isatra.2015.05.017>.
- Chen, Cheng-Liang, and Fong-Chih Kuo. 1995. “Design and Analysis of a Fuzzy Logic Controller.” *International Journal of Systems Science* 26(5): 1223–48.
- Chen, Yung Feng, An Chyau Huang, and Yung-feng Chen An-chyau Huang. 2014. “Adaptive Control of Rotary Inverted Pendulum System with Time-Varying Uncertainties.” *Nonlinear Dynamics* 76(1): 95–102.
- Choukchou-Braham, Amal, Brahim Cherki, Mohamed Djemaï, and Krishna Busawon. 2014. Springer *Analysis and Control of Underactuated Mechanical Systems*. New York: Springer International Publishing Switzerland 2014.
- Driver, James, and Mr. Dylan Thorpe. 2004. “Design, Build and Control of a Single / Double Rotational Inverted Pendulum.” The University of Adelaide, Australia.
<http://data.mecheng.adelaide.edu.au/robotics/projects/2004/Pendulum/pendulum.pdf>.

- Duan, X.-G., Li, H.-X., & Deng, H. 2008. *Effective Tuning Method for Fuzzy PID with Internal Model Control. Industrial & Engineering Chemistry Research*, 47(21), 8317–8323. doi:10.1021/ie800485j
- E, Vinodh Kumar, and Jovitha Jerome. 2013. “Robust LQR Controller Design for Stabilizing and Trajectory Tracking of Inverted Pendulum.” *Procedia Engineering* 64: 169–78. <http://dx.doi.org/10.1016/j.proeng.2013.09.088>.
- Emre Akgul. 2011. “PID and LQR Control of a Planar Head Stabilization Platform.” Middle East Technical University. <http://etd.lib.metu.edu.tr/upload/12613713/index.pdf>.
- Fadali, M. Sami, and Antonio Visioli. 2013. *Digital Control Engineering Analysis and Design*. Second. Elsevier. <http://www.ece.mtu.edu/faculty/shiyan/EE4262Spring17/DigitalControlTextBook.pdf>.
- Fantoni, Isabelle, and Rogelio Lozano. 2002. *Communications and Control Engineering*. second.
- Furuta, K., M. Yamakita, and S. Kobayashi. 1992. “Swing-up Control of Inverted Pendulum Using Pseudo-Sate Feedback.” *Journal of Systems and Control Engineering* 206(4): 263–69.
- Gaing, Zwe Lee. 2004. “A Particle Swarm Optimization Approach for Optimum Design of PID Controller in AVR System.” *IEEE Transactions on Energy Conversion* 19(2): 384–91. https://www.researchgate.net/publication/3270304_A_Particle_Swarm_Optimization_Approach_for_Optimum_Design_of_PID_Controller_in_AVR_System.
- Galichet, S., & Foulloy, L. (1995). *Fuzzy controllers: synthesis and equivalences. IEEE Transactions on Fuzzy Systems*, 3(2), 140–148. doi:10.1109/91.388169
- Ghorbani, Farhad, Mahdi Aliyari Shooredeli, and Mohammad Teshnehlab. 2013. “Fault Tolerant Improvement with Chaos Synchronization Using Fuzzy-PID Control.” *13th Iranian Conference on Fuzzy Systems, IFSC 2013* (2000).
- Gupta, Neha, and Lillie Dewan. 2019. “Modeling and Simulation of Rotary-Rotary Planer Inverted Pendulum.” *Journal of Physics: Conference Series* 1240(1): 9. <https://iopscience.iop.org/article/10.1088/1742-6596/1240/1/012089/pdf>.
- Hamza M. F., Yap H. J., Choudhury I. A., Isa A. I., Zimit A. Y. 2016. “Simulation Studies for Stabilization Control of Furuta Pendulum System Using Cascade Fuzzy PD Controller.” : 1–9.
- Hamza M. F., Yap H. J., Choudhury I. A., Isa A. I., Zimit A. Y. 2015. “Genetic Algorithm and Particle Swarm Optimization Based Cascade Interval Type 2 Fuzzy PD Controller for Rotary Inverted Pendulum System.” 2015.
- Hamza, M. F., Yap, H. J., Choudhury, I. A., Isa, A. I., Zimit, A. Y., & Kumbasar, T. 2019. *Current development on using Rotary Inverted Pendulum as a benchmark for testing linear and nonlinear control algorithms. Mechanical Systems and Signal Processing*,

- Hamza, Mukhtar Fatihu, Yap Hwa Jen. 2016. “Application of Kane ’ s Method for Dynamic Modeling of Rotary Inverted Pendulum System.” In *2016 First International Conference on Micro and Nano Technologies, Modelling and Simulation*, , 27–32.
- Hassanzadeh, I., & Mobayen, S. 2011. *Controller Design for Rotary Inverted Pendulum System Using Evolutionary Algorithms. Mathematical Problems in Engineering*, 2011, 1–17.
- Jabbar, A., Malik, F. M., & Sheikh, S. A. 2016. *Nonlinear stabilizing control of a rotary double inverted pendulum: a modified backstepping approach. Transactions of the Institute of Measurement and Control*, 39(11), 1721–1734. doi:10.1177/0142331216645174
- Jaiwat, Pathompong, and Toshiyuki Ohtsuka. 2014. “Real-Time Swing-up of Double Inverted Pendulum by Nonlinear Model Predictive Control.” *5th International Symposium on Advanced Control of Industrial Processes*: 290–95.
- Jose, A. , Augustine, C. , Malola, S. and Chacko, K. 2015 Performance Study of PID Controller and LQR Technique for Inverted Pendulum. *World Journal of Engineering and Technology*, 3, 76-81. doi:10.4236/wjet.2015.32008.
- Kafetzis, Ioannis, and Lazaros Moysis. 2017. “Inverted Pendulum : A System with Innumerable Applications Inverted Pendulum.” In *9th International Week Dedicated to Maths. Thessaloniki, Greece, March 2017.*, ReearchGate, 13.
- Klir, George J., and Bo Yuan. 1997. 14 Neurocomputing *Fuzzy Sets and Fuzzy Logic: Theory and Applications*. First. eds. Patti Guerrieri, Paul Becker, and Maureen Diana. New Jersey: Prentice Hall P T R Upper Saddle River, New Jersey 07458.
- Krohling, Renato A., Joost P. Rey, R. A. Krohling, and J. P. Rey. 2001. “Design of Optimal Disturbance Rejection PID Controllers Using Genetic Algorithms.” *IEEE Transactions on Evolutionary Computation* 5(1):78–82. http://inf.ufes.br/~rkrohling/papers/paper_citado1.pdf.pdf.
- Kumare, Vinodh, and Jovitha Jerome. 2016. “Algebraic Riccati Equation Based Q and R Matrices Selection Algorithm for Optimal LQR Applied to Tracking Control of 3rd Order Magnetic Levitation System.” *Archives of Electrical Engineering* 65(1): 151–68. <https://www.degruyter.com/view/j/aee.2016.65.issue-1/aee-2016-0012/aee-2016-0012.xml>.
- Kumbasar, T., & Hagrass, H. 2014. *Big Bang–Big Crunch optimization based interval type-2 fuzzy PID cascade controller design strategy. Information Sciences*, 282, 277–295. doi:10.1016/j.ins.2014.06.005
- Kumbasar, T., & Hagrass, H. 2015. *Interval Type-2 Fuzzy PID Controllers. Springer Handbook of Computational Intelligence*, 285–294. doi:10.1007/978-3-662-43505-2_18
- Li, Bo. 2013. “Rotational Double Inverted Pendulum.” University of Dayton.

https://etd.ohiolink.edu/!etd.send_file?accession=dayton1375188910&disposition=inline

- Li, Huaidong, Heidar Malki, and Guanrong Chen. 1994. "Performance Analysis of Fuzzy Proportional-Derivative Control Systems." *Proceedings of the ACM Symposium on Applied Computing Part F1294*(January): 115–19.
https://www.researchgate.net/publication/221001610_Performance_analysis_of_fuzzy_proportional-derivative_control_systems/link/0c9605395cc560d6f6000000/download.
- Mamdani, E. H., & Assilian, S. 1999. *An Experiment in Linguistic Synthesis with a Fuzzy Logic Controller. International Journal of Human-Computer Studies*, 51(2), 135–147. doi:10.1006/ijhc.1973.0303
- Mamma-Graham, Adamantia S. 2014. "An Intermittent Predictive Control Approach to Modelling Sustained Human Motor Control." College of Science and Engineering, University of Glasgow. <http://theses.gla.ac.uk/5425/>.
- Mandal, Ajit K. 2017. *Introduction to Control Engineering Modeling, Analysis and Design*. Third. Kolkata, India: New Academic Science Limited. www.newacademicscience.co.uk.
- Mathew, N. J., Rao, K. K., & Sivakumaran, N. 2013. *Swing Up and Stabilization Control of a Rotary Inverted Pendulum. IFAC Proceedings Volumes*, 46(32), 654–659. doi:10.3182/20131218-3-in-2045.00128
- Mhaskar, P., El-Farra, N. H., & Christofides, P. D. (2004). *A method for PID controller tuning using nonlinear control techniques. Proceedings of the 2004 American Control Conference*. doi:10.23919/acc.2004.1384356
- Mohammadi Asl, R., Mahdoudi, A., Pourabdollah, E., & Klančar, G. (2018). *Combined PID and LQR controller using optimized fuzzy rules. Soft Computing*. doi:10.1007/s00500-018-3180-3
- Moreno-Valenzuela, J., & Aguilar-Avelar, C. (2018). *Motion Control of Underactuated Mechanical Systems. Intelligent Systems, Control and Automation: Science and Engineering*. doi:10.1007/978-3-319-58319-8
- Moysis, Lazaros. (2016). Balancing a double inverted pendulum using optimal control and Laguerre functions. 10.13140/RG.2.1.2948.6486.
- Muske, Kenneth R., Hashem Ashrafiuon, Sergey Nersesov, and Mehdi Nikkhah. 2012. "Optimal Sliding Mode Cascade Control for Stabilization of Underactuated Nonlinear Systems." *Journal of Dynamic Systems, Measurement and Control, Transactions of the ASME* 134(2): 11.
https://www.researchgate.net/profile/H_Ashrafiuon/publication/270752688_Optimal_Sliding_Mode_Cascade_Control_for_Stabilization_of_Underactuated_Nonlinear_Systems/links/54b91e260cf2c27adc4915a9.pdf.
- Naidu, D. S. (2002). *Optimal control systems*. (Electrical engineering textbook series). Boca Raton, Fla: CRC Press

- Nath, Vishwa, and R. Mitra. 2014. "Swing-up and Control of Rotary Inverted Pendulum Using Pole Placement with Integrator." *2014 Recent Advances in Engineering and Computational Sciences, RAECS 2014* (1): 6–8.
- Nikolov, S. (2012). Complex Behavior of Double Inverted Pendulum with a Vertically Oscillating Suspension Point. *Mechanics Transport Communications: Academic Journal*, 1, 2012, 1–7. <http://www.mtc-aj.com>
- Ogata, Katsuhiko. 2010. *Modern Control Engineering*. Fifth. Pearson Education, Inc.
- Oh, Sung-kwun, Han-jong Jang, and Witold Pedrycz. 2011. "Simulation Modelling Practice and Theory Optimized Fuzzy PD Cascade Controller: A Comparative Analysis and Design." *Simulation Modelling Practice and Theory* 19(1): 181–95.
- Oh, Sung-kwun, Wook-dong Kim, and Witold Pedrycz. 2012. "Engineering Applications of Artificial Intelligence Design of Optimized Cascade Fuzzy Controller Based on Differential Evolution: Simulation Studies and Practical Insights." *Engineering Applications of Artificial Intelligence* 25(3): 520–32. <http://dx.doi.org/10.1016/j.engappai.2012.01.002>.
- Passino, K. M., & Yurkovich, S. (1997). *Fuzzy Control* (L. Cheu & R. Tonomura (eds.); 1st ed.). Addison Wesley Publishing Company. <http://www2.ece.ohio-state.edu/~passino/FCbook.pdf>
- Patil, Madhura, and Shailaja Kurode. 2018. "Stabilization of Rotary Double Inverted Pendulum Using Higher Order Sliding Modes." *2017 Asian Control Conference, ASCC 2017* 2018-Janua: 1818–23.
- Reznik, Leonid 1997. *Fuzzy controllers*. Newnes, Oxford ; Boston
- Ross, Timothy J. 2010. *Fuzzy Logic With Engineering Application*. Third. Washington: A John Wiley and Sons, Ltd., Publication.
- Ross, Timothy. 2009. *Fuzzy Logic With Engineering Applications*. Fuzzy Logic with Engineering Applications: Third Edition. 10.1002/9781119994374.
- Sanjeewa, Sondarangallage D.A., and Manukid Parnichkun. 2019. "Control of Rotary Double Inverted Pendulum System Using Mixed Sensitivity H_∞ Controller." *International Journal of Advanced Robotic Systems* 16(2): 1–17.
- Siddique, Nazmul, and Bernard Widrow. 2013. *Intelligent Control: A Hybrid Approach Based on Fuzzy Logic, Neural Networks and Genetic Algorithms*. ed. Poland J. Kacprzyk, Warsaw. London: Springer International Publishing Switzerland 2014.
- Singh, Narinder, and Sk Yadav. 2012. "Comparison of LQR and PD Controller for Stabilizing Double Inverted Pendulum System." *International Journal of Engineering Research and Development* 1(12): 69–74. https://www.idc-online.com/technical_references/pdfs/instrumentation/Comparison_of_LQR.pdf.

- Sooraj, M S. 2016. "Comparison of Linear and Nonlinear Control Strategies for the Stabilization of Rotary Pendulum." *International Journal of Advanced Information in Engineering Technology (IJAIET)* 3(May 2016): 527–31. <http://www.ijaiet.com/comparison-of-linear-and-nonlinear-control-strategies-for-the-stabilization-of-rotary-pendulum/>.
- Stelian-Emilian Oltean. 2014. "Swing-up and Stabilization of the Rotational Inverted Pendulum Using PD and Fuzzy-PD Controllers." In *The 7th International Conference Interdisciplinarity in Engineering (INTER-ENG 2013)*, Elsevier, 57–64. www.sciencedirect.com.
- Sugeno, Michio. 1985. "An Introductory Survey of Fuzzy Control." *Information Sciences* 36,59-83 (1985) 83: 59–83.
- Sukontanakarn, Viroch, and Manukid Parnichkun. 2009. "Real-Time Optimal Control for Rotary Inverted Pendulum Viroch Sukontanakarn and Manukid Parnichkun Mechatronics , School of Engineering and Technology , Asian Institute of Technology , Pathumthani , Thailand." *American Journal of Applied Sciences* 6(6): 1106–15.
- Sukontanakarn, V., & Parnichkun, M. 2011. *Hybrid NN predictive-based LQR controller for rotary double inverted pendulum systems: an analytical study. International Journal of Automation and Control*, 5(4), 337. doi:10.1504/ijaac.2011.043611
- Tang, Y., Zhou, D., & Jiang, W. 2016. *A New Fuzzy-Evidential Controller for Stabilization of the Planar Inverted Pendulum System. PLOS ONE*, 11(8), e0160416. doi:10.1371/journal.pone.0160416
- Tinkir, M., Onen, U., Kalyoncu, M., & Botsali, F. M. 2010. *Pid and interval type-2 fuzzy logic control of double inverted pendulum system. 2010 The 2nd International Conference on Computer and Automation Engineering (ICCAE)*. doi:10.1109/iccae.2010.5451988
- Visioli, A. 2001. *Tuning of PID controllers with fuzzy logic. IEE Proceedings - Control Theory and Applications*, 148(1), 1–8. doi:10.1049/ip-cta:20010232
- Wei Li. 1998. *Design of a hybrid fuzzy logic proportional plus conventional integral-derivative controller. IEEE Transactions on Fuzzy Systems*, 6(4), 449–463. doi:10.1109/91.728430
- Wu Zhi Qiao, & Mizumoto, M. 1996. *PID type fuzzy controller and parameters adaptive method. Fuzzy Sets and Systems*, 78(1), 23–35. doi:10.1016/0165-0114(95)00115-8
- Yadav, Sandeep Kumar, Sachin Sharma, and Mr. Narinder Singh. 2012. "Optimal Control of Double Inverted Pendulum Using LQR Controller." *International Journal of Advanced Research in Computer Science and Software Engineering* 2(2): 189–92.
- Yang, Xuebo, and Xiaolong Zheng. 2018. "Swing-Up and Stabilization Control Design for an Underactuated Rotary Inverted Pendulum System: Theory and Experiments." *IEEE Transactions on Industrial Electronics* 65(9): 7229–38.

- Yi, J., & Yubazaki, N. 2000. *Stabilization fuzzy control of inverted pendulum systems. Artificial Intelligence in Engineering*, 14(2), 153–163. doi:10.1016/s0954-1810(00)00007-8
- Yu, W. 2009. *Recent Advances in Intelligent Control Systems* (1st ed.). Springer. <https://doi.org/10.1007/978-1-978-1-84882-548-2>
- Zhong, Wei, and R Helmut. 2001. “Energy and Passivity Based Control of the Double Inverted Pendulum on a Cart.” In *Proceedings of the 2001 IEEE International Conference on Control Applications*, Mexico: Chair for Automation and Control Engineering, Christian-Albrechts-University of KielKaiserstr. 2, Kiel, D - 24143, Germany, 896–901.
- Zhou, G., & Birdwell, J. D. 1994. Fuzzy logic-based PID autotuner design using simulated annealing. *Proceedings of IEEE Symposium on Computer-Aided Control Systems Design (CACSD)*. doi:10.1109/cacsd.1994.288947